

Prey availability and snake fungal disease as drivers of timber rattlesnake habitat  
selection across multiple spatial scales

Thesis

Presented in Partial Fulfillment of the Requirements for the Degree Master of  
Environment and Natural Resources in the Graduate School of The Ohio State University

By

Annalee McCulloh Tutterow

Graduate Program in Environment and Natural Resources

The Ohio State University

2020

Thesis Committee

William E. Peterman, Advisor

Risa R. Pesapane

Stephen N. Matthews

Copyrighted by  
Annalee McCulloh Tutterow  
2020

## Abstract

Habitat selection can be multi-scale and hierarchical, suggesting that varied environmental or resource gradients can influence habitat use patterns across different spatial scales. Snake habitat selection is influenced by microhabitat features that affect an individual's ability to forage, avoid predation, and thermoregulate. However, it is unclear and debated whether snakes prioritize thermoregulatory needs over prey availability when foraging (i.e. opportunistically forage) or selectively forage to maximize potential prey encounters (i.e. prey-mediated habitat selection). Additionally, snakes infected with an emerging mycosis, snake fungal disease (SFD), may alter their behavior and site use to optimize physiological performance. The collective physiological and behavioral shifts associated with SFD may scale to differences in site selection patterns and home range characteristics, but these predictions on habitat use have not been robustly examined.

Understanding habitat use for individuals in various physiological and behavioral states is essential for developing comprehensive management strategies for imperiled wildlife. Rattlesnake natural history characteristics, including their stereotyped behaviors, make them ideal subjects to test hypotheses about habitat selection. My research seeks to address how distinct behaviors or physiological states, such as foraging or infection status, shape timber rattlesnake (*Crotalus horridus*; hereafter, TRS) space use. I used a multi-year radio-telemetry dataset to differentiate among behavior/physiology-specific

site use and account for individual variation in habitat selection. The primary goals of this study were to (1) assess the influence of landscape-scale prey availability on TRS ambush site selection and to (2) quantitatively assess the effects of SFD infection on individual behavior, site selection, and space use metrics.

(1) I found that the cumulative prey landscape (i.e. the combined spatial distributions of *Peromyscus* spp., *Tamias striatus*, and *Sciurus* spp.) was highly predictive of snake ambush site selection. Although the spatial distributions of individual prey species did not overlap well, TRS responded to overall prey availability. My findings suggest that TRS can detect fine-scale differences in prey availability and selectively forage in prey-rich areas, making the prey landscape an important driver of habitat selection.

(2) I compared behavior, movement patterns, habitat use, and home ranges among years that snakes were asymptomatic or symptomatic of SFD and found evidence for altered space use during SFD infection. Snakes increased their maximal home range area (100% minimum convex polygon [MCP]) and doubled their core home range area (50% MCP) when infected. I also found sex-specific effects of SFD on snake behavior and habitat use, with non-gravid females typically most affected by SFD across all examined space use metrics. Symptomatic females rested more and foraged less frequently than expected, while symptomatic males rested less and foraged more frequently than expected. Females were more likely to use dry, southwestern-facing, high elevation sites in early seral stands, conditions favorable to thermoregulation, when symptomatic of SFD. During symptomatic years, snakes selected sites with greater solar exposure, but

only exhibited elevated body temperatures during the fall, likely due to increased surface activity at the end of the active season.

These studies provide insight into external and internal drivers of snake habitat selection. My findings suggest that (1) optimal foraging theory may be applicable to the foraging ecology of low-energy ambush predators and (2) physiological and behavioral adjustments associated with SFD infection can scale up to effect change in habitat use.

## Acknowledgments

I would like to first acknowledge my adviser, Bill Peterman, for his assistance and encouragement in following my research interests. I have not always been confident or assured in my next steps, but Bill has always listened and provided thoughtful advice to help me move forward. I also thank Drs. Pesapane and Matthews for kindly agreeing to be involved in these projects and for their enthusiastic support.

I would like to acknowledge the agencies and people that made these projects possible. First and foremost, I credit my labmate and coauthor Andrew Hoffman for organizing the Vinton Timber Rattlesnake project and for always being eager to share about and revel in exciting developments or even daily minutiae regarding the snakes. I also need to give a special thanks to the field technicians that suffered through chiggers, ticks, scorching heat, and trekking through clear-cuts to assist this project. Thank you to John Buffington, Blaine Hiner, Tyler Lacina, Jennifer Myers, Emma Scott, Sky Stevens, and Zach Truelock. Dr. Randy Junge of the Columbus Zoo conducted all of the snake transmitter implantations. I also thank Bill Borovicka and the U.S. Forest Service: Northern Research Station for providing housing accommodations and logistical support. Funding support was provided by the Ohio Department of Natural Resources—Division of Wildlife and the Ohio Biodiversity Conservation Partnership.

I acknowledge my other wonderful labmates Kate, Meaghan, Phil, Marissa, Ryan, and Andrew W. for your moral support outside of the walls of Kottman Hall and listening to me babble on about snakes. Thanks to Evan for making Columbus a better place to be.

I cannot express the gratitude I have for my undergraduate mentors Dr. Shannon Pittman and Meagan Thomas. We have been through some ups and downs together, and you both have shaped my life in countless ways. Shannon and Meagan, thank you for supporting me and other students in research and in life. Finally, countless thanks go to my wonderfully supportive family. Dad and Caitlin, I know you don't like snakes, but you love me, so I value your encouragement and support in making my own choices and forging a path for myself.

## Vita

B.S. with High Honors in Biology.....2017  
Davidson College, Davidson, North Carolina

## Publications

**Tutterow, A. M.**, Graeter, G. J., & Pittman, S. E. (2017). Bog turtle demographics within the Southern Population. *Copeia*, 105, 293–300.

Zappalorti, R. T., **Tutterow, A. M.**, Lovich, J. E., & Pittman, S. E. (2017). Hatching success and predation of bog turtle (*Glyptemys muhlenbergii*) eggs in New Jersey and Pennsylvania. *Chelonian Conservation and Biology*, 16, 194–202.

## Fields of Study

Major Field: Environment and Natural Resources

## Table of Contents

Abstract .....	ii
Acknowledgments .....	v
Vita .....	vii
List of Tables .....	ix
List of Figures .....	xv
Chapter 1. Prey-Driven Behavioral Habitat Use in a Low-Energy Ambush Predator .....	1
Abstract .....	1
Introduction .....	2
Methods .....	7
Results .....	14
Discussion .....	18
Conclusions .....	26
Literature Cited .....	27
Chapter 2. Multi-scale Effects of Snake Fungal Disease on Individual Behavior and Space Use in Timber Rattlesnakes .....	46
Abstract .....	46
Introduction .....	47
Methods .....	50
Results .....	57
Discussion .....	64
Conclusions .....	71
Literature Cited .....	72
References .....	93
Appendix A. Chapter 1 Supplementary Material .....	105
Appendix B. Chapter 2 Supplementary Material .....	115

## List of Tables

Table 1.1. Fine-scale (5-m) landscape covariates (n = 16) used to describe small mammal spatial distributions in a mixed-use forest in southeastern Ohio. Summary statistics for each continuous variable provide the mean value ( $\pm$ SD) and range of values across 242 camera trap sites.....	34
Table 1.2. Camera trap (n = 242) daily detections of potential prey items for timber rattlesnakes ( <i>Crotalus horridus</i> ) in a mixed-use forest in southeastern Ohio from 2017–2018. Bird detections include common woodland residents, such as wood thrushes ( <i>Hylocichla mustelina</i> ), ovenbirds ( <i>Seiurus aurocapilla</i> ), and Carolina wrens ( <i>Thryothorus ludovicianus</i> ).....	36
Table 1.3. Bayesian zero-inflated (Zi) negative binomial models of mice ( <i>Peromyscus</i> spp.), chipmunk ( <i>Tamias striatus</i> ), and squirrel ( <i>Sciurus</i> spp.) encounter rates across 242 camera sites in a mixed-use forest in southeastern Ohio. We modeled the number of camera days with a species detection, offset by the total number of active camera days, as a function of study year (2017–2018) and remotely-sensed landscape variables (5-m resolution). We report the variables that best described each species’ distribution. Mean coefficient estimates, standard errors ( $\pm$ S.E.) and percentage of the posterior distributions overlapping zero are provided. Refer to Table 1.1 for further descriptions of covariates.	37
Table 2.1. Snake fungal disease (SFD) designations assigned annually (2016–2019) to 41 timber rattlesnakes ( <i>Crotalus horridus</i> ) in southeastern Ohio. Each spring (April–May) and fall (August–September) individual snakes were examined for the presence of skin lesions associated with SFD infection and skin-swabbed and qPCR-tested for the presence of the fungal pathogen <i>Ophidiomyces ophiodiicola</i> . We considered the presence of clinical signs (i.e. lesions) and a positive qPCR test the most conclusive evidence for SFD infection. ....	78
Table 2.2. Bayesian mixed effect models of home range area across 50%, 95%, and 100% minimum convex polygons (MCP) for 15 (n = 9 males and 6 non-gravid females) timber rattlesnakes ( <i>Crotalus horridus</i> ), during years when considered asymptomatic or symptomatic of snake fungal disease (SFD). Mean coefficient estimates, standard errors (S.E.), 95% lower (LCI) and upper (UCI) credible intervals, percentage of the posterior distributions overlapping zero, and percentage of the posterior distributions in the region of practical equivalence (ROPE) are provided for the most parsimonious model at each home range scale. Refer to Table B.1 for further descriptions of candidate models. ....	79

Table 2.3. Multivariate ANOVA (MANOVA) of principal component analysis (PCA) scores of 15 timber rattlesnakes (*Crotalus horridus*) in southeast Ohio during years when asymptomatic or symptomatic of snake fungal disease (SFD). The PCA included eight movement metrics, with principal components (PC) 1 and 2 representing a cumulative 89.8% of the variance. Large, positive scores on PC1 suggest greater home range size (particularly 95% and 100% minimum convex polygons) and greater displacement rates. Large, positive scores on PC2 suggest greater median and mean movement rates. We used an interaction of SFD status and sex to predict PC scores, with a random effect of individual snakes. Mean coefficient estimates, standard errors (S.E.), 95% lower (LCI) and upper (UCI) credible intervals, and percentage of the posterior distributions overlapping zero are provided. .... 80

Table 2.4. Observed frequencies of 15 timber rattlesnakes (*Crotalus horridus*) in southeastern Ohio exhibiting four unique behaviors (resting, foraging, digesting, and ecdysis) when asymptomatic or symptomatic of snake fungal disease (SFD). We compared observed (% of total) and expected frequencies between males (n = 9) and females (n = 6) across each SFD status with a chi-squared test. All snakes were monitored for at least one asymptomatic and symptomatic year each. The contribution (%) of each cell to the chi-square statistic was calculated as  $100 \times \chi^2$ . Bolded cells had a contribution > 10% ..... 81

Table 2.5. Bayesian mixed effects Bernoulli models of site use characteristics of timber rattlesnakes (*Crotalus horridus*) during years unaffected or affected by snake fungal disease (SFD). Each snake was considered asymptomatic or symptomatic of SFD infection for at least one year each. We modeled probability of site use by a symptomatic snake as a function of thirteen geospatial landscape and forest structural variables (5-m resolution), with individual snakes as random effects. We report the variables that best described site use by males and females. Mean coefficient estimates, standard errors ( $\pm$  S.E.) and percentage of the posterior distributions overlapping zero are provided. Refer to Table 1.1 for further descriptions of covariates. .... 82

Table 2.6. Bayesian mixed effect models of external snake body temperatures taken with a digital infrared thermometer at sites (n = 870) used by timber rattlesnakes (*Crotalus horridus*) during years unaffected or affected by snake fungal disease (SFD). Each snake (n = 15) was considered asymptomatic or symptomatic of SFD infection for at least one year each. We modeled snake body temperature as a function of interactive SFD status and season of observation. We defined spring as April–June, summer as July–August, and fall as September–October. We included random effects of individual snakes and month of observation. Mean coefficient estimates, standard errors (S.E.), 95% lower (LCI) and upper (UCI) credible intervals, percentage of the posterior distributions overlapping zero, and percentage of the posterior distributions in the region of practical equivalence (ROPE) are provided for the most parsimonious model. Refer to Table B.6 for further descriptions of candidate models. .... 83

Table 2.7. Bayesian mixed effect model of solar insolation at sites (n = 730) used by timber rattlesnakes (*Crotalus horridus*) during years unaffected or affected by snake fungal disease (SFD). Each snake (n = 15) was considered asymptomatic or symptomatic of SFD infection for at least one year each. We modeled solar insolation (kWH/m<sup>2</sup>), corrected by proportion canopy cover, as a function of additive SFD status and season of observation. We defined spring as April–June, summer as July–August, and fall as September–October. We included random effects of individual snakes and month of observation. Mean coefficient estimates, standard errors (S.E.), 95% lower (LCI) and upper (UCI) credible intervals, percentage of the posterior distributions overlapping zero, and percentage of the posterior distributions in the region of practical equivalence (ROPE) are provided for the most parsimonious model. Refer to Table B.7 for further descriptions of candidate models. .... 84

Table A.1. Landcover types present at the study site, their relative coverage on the landscape, and their representation in our game camera trap dataset for small mammals (242 total camera trap sites). .... 105

Table A.2. Candidate global models describing mice (*Peromyscus* spp.) encounter rates in a mixed-use forest in southeastern Ohio between 2017 and 2018, including variations of zero-inflated (Zi) Poisson and negative binomial models to account for potential temporal variation in small mammal distributions contributing to an excess of zeros. The global set of predictors described forest structure and composition, landscape topography, and year of study (see Table 1.1 for further descriptions of covariates). Median Date refers to the median date of a camera’s active interval and was modeled as a quadratic. We considered diagnostic plots, leave-one-out cross validation (LOO), and Watanabe-Akaike information criterion (WAIC) to determine the most parsimonious model. The best-supported global model (in bold type) was a zero-inflated negative binomial model with year of study explaining the excess of zeros. .... 106

Table A.3. Candidate global models describing chipmunk (*Tamias striatus*) encounter rates in a mixed-use forest in southeastern Ohio between 2017 and 2018, including variations of zero-inflated (Zi) Poisson and negative binomial models to account for potential temporal variation in small mammal distributions contributing to an excess of zeros. The global set of predictors described forest structure and composition, landscape topography, and year of study (see Table 1.1 for further descriptions of covariates). Median Date refers to the median date of a camera’s active interval and was modeled as a quadratic. We considered diagnostic plots, leave-one-out cross validation (LOO), and Watanabe-Akaike information criterion (WAIC) to determine the most parsimonious model. The best-supported global model (in bold type) was a zero-inflated negative binomial model with year of study explaining the excess of zeros. .... 107

Table A.4. Candidate global models describing squirrel (*Sciurus* spp.) encounter rates in a mixed-use forest in southeastern Ohio between 2017 and 2018, including variations of zero-inflated (Zi) Poisson and negative binomial models to account for potential temporal

variation in small mammal distributions contributing to an excess of zeros. The global set of predictors described forest structure and composition, landscape topography, and year of study (see Table 1.1 for further descriptions of covariates). Median Date refers to the median date of a camera's active interval and was modeled as a quadratic. We considered diagnostic plots, leave-one-out cross validation (LOO), and Watanabe-Akaike information criterion (WAIC) to determine the most parsimonious model. The best-supported global model (in bold type) was a zero-inflated negative binomial model with median date of camera deployment and year of study explaining the excess of zeros... 108

Table A.5. Candidate Bayesian zero-inflated (Zi) negative binomial models for mice, chipmunks, and squirrels describing encounter rates from 242 camera traps in a mixed-use forest in southeastern Ohio. The number of camera days with a species' detection (Counts) is offset by the total number of active camera days (Days). Models were reduced from the global (G) set of covariates characterizing forest structure and composition ( $k = 13$ ), landscape topography ( $k = 3$ ), and year of study (2017–2018). Refer to Table 1.1 for descriptions of each covariate. The zero-inflated process was modeled with year and/or median camera deployment date. The most parsimonious model (in bold type) for each species was determined using diagnostic plots, leave-one-out cross validation (LOO), and Watanabe-Akaike information criterion (WAIC). ..... 109

Table A.6. Candidate Bayesian mixed-effects Bernoulli models describing timber rattlesnake (*Crotalus horridus*) foraging as a function of predicted prey encounter rates from a landscape-scale small mammal encounter surface (2017–2018) for a mixed-use forest in southeastern Ohio. Species-level models include predicted daily encounter rates for mice (*Peromyscus* spp.), chipmunks (*Tamias striatus*), and squirrels (*Sciurus* spp.). Cumulative models include the additive daily encounter rate predictions for mice and chipmunks specifically (Cumulative MC) or the contribution of all species (Cumulative Prey). Variation in prey encounter rates and snake identity (Snake), modeled as a random effect, described TRS foraging status (Forage) between 2016–2019. In 2016 and 2019, prey encounter values for each snake location represented the average predicted rate (prey species or species grouping) between 2017 and 2018. We used diagnostic plots and leave-one-out cross validation (LOO) to determine the most parsimonious models, identified as the smallest selection criterion value (in bold type), for combined adult TRS, non-gravid female, and male foraging probabilities among species-level and cumulative models for 2017–2018 and 2016–2019..... 111

Table A.7. Bayesian mixed-effects Bernoulli models of adult timber rattlesnake (*Crotalus horridus*) foraging from 2016–2019, explained by species-level daily rodent encounter rates from landscape-scale prey encounter surfaces of mice (*Peromyscus* spp.), chipmunks (*Tamias striatus*), and squirrels (*Sciurus* spp.) or cumulative prey encounter rates encompassing all prey species. We tested species-level and Cumulative Prey models for non-gravid females ( $n = 16$ ) and males ( $n = 21$ ) separately, and Cumulative Prey models for adults collectively. Mean coefficient estimates, standard errors (S.E.), 95% lower (LCI) and upper (UCI) credible intervals, and percentage of the posterior distributions

overlapping zero are provided. Refer to Table A.6 for further descriptions of candidate models. .... 112

Table B.1. Candidate Bayesian mixed effect models describing home range area across 50%, 95%, and 100% minimum convex polygons (MCP) for 15 (n = 9 males and 6 non-gravid females) timber rattlesnakes (*Crotalus horridus*), during years when considered asymptomatic or symptomatic of snake fungal disease (SFD). We monitored each snake for at least one year in which they were asymptomatic of SFD (SFD = 0) and at least one year in which they exhibited clinical symptoms (SFD = 1). We used additive or interactive combinations of SFD status and sex to predict log-transformed home range area (Area), with individual snakes modeled as random effects. The most parsimonious model (in bold type) for each home range scale was determined using diagnostic plots and leave-one-out cross validation (LOO). .... 115

Table B.2. Principal component analysis (PCA) of eight movement metrics from 15 timber rattlesnakes (*Crotalus horridus*) in southeast Ohio during years when asymptomatic or symptomatic of snake fungal disease. We considered annual summaries of mean and median movement rates, cumulative step lengths, mean and max net squared displacement, and 50%, 95%, and 100% minimum convex polygon (MCP) home range areas. We considered the most informative principal components as those with the greatest eigenvalues and greatest percentage of variability explained within the data. Cumulative variance represents the amount of variance explained by consecutive principal component dimensions. .... 116

Table B.3. Loadings of eight movement metrics from a principal component analysis (PCA) for 15 timber rattlesnakes (*Crotalus horridus*) in southeast Ohio during years when asymptomatic or symptomatic of snake fungal disease. We considered annual summaries of mean and median movement rates (MR), mean and max net squared displacement (NSD), cumulative step lengths (SL) and 50%, 95%, and 100% minimum convex polygon (MCP) home range areas. The first three principal components (PC) explained 94.4% of the variance. We considered variables with loadings close to -1 or 1 to be the most influential variables on a component. .... 117

Table B.4. Coordinates of eight movement metrics from a principal component analysis (PCA) for 15 timber rattlesnakes (*Crotalus horridus*) in southeast Ohio during years when asymptomatic or symptomatic of snake fungal disease. We considered annual summaries of mean and median movement rates (MR), mean and max net squared displacement (NSD), cumulative step lengths (SL) and 50%, 95%, and 100% minimum convex polygon (MCP) home range areas. The first three principal components (PC) explained 94.4% of the variance. .... 118

Table B.5. Candidate Bayesian mixed effect Bernoulli models of site use by timber rattlesnakes (*Crotalus horridus*) during years unaffected or affected by snake fungal disease (SFD). Probability of site use by a snake infected with SFD was modeled as a function of thirteen geospatial landscape and forest structural variables (5-m resolution),

with individual snakes as random effects. Each snake ( $n = 15$ ) was considered asymptomatic or symptomatic of SFD infection for at least one year each. The most parsimonious model (in bold type) for each sex was determined using diagnostic plots and leave-one-out cross validation (LOO)..... 119

Table B.6. Candidate Bayesian mixed effect models of external snake body temperatures taken with a digital infrared thermometer at sites ( $n = 870$ ) used by timber rattlesnakes (*Crotalus horridus*) during years unaffected or affected by snake fungal disease (SFD). Each snake ( $n = 15$ ) was considered asymptomatic or symptomatic of SFD infection for at least one year each. We modeled snake body temperature as a function of additive or interactive combinations of SFD status and season of observation. We defined spring as April–June, summer as July–August, and fall as September–October. We included random effects of individual snakes and month of observation. The most parsimonious model (in bold type) was determined using diagnostic plots and leave-one-out cross validation (LOO)..... 120

Table B.7. Candidate Bayesian mixed effect models of solar insolation at sites ( $n = 730$ ) used by timber rattlesnakes (*Crotalus horridus*) during years unaffected or affected by snake fungal disease (SFD). Each snake ( $n = 15$ ) was considered asymptomatic or symptomatic of SFD infection for at least one year each. We modeled solar insolation ( $\text{kWH/m}^2$ ), corrected by proportion canopy cover (CSI), as a function of additive or interactive combinations of SFD status and season of observation. We defined spring as April–June, summer as July–August, and fall as September–October. We included random effects of individual snakes and month of observation. The most parsimonious model (in bold type) was determined using diagnostic plots and leave-one-out cross validation (LOO)..... 121

## List of Figures

Figure 1.1. Characteristic ambush posture of timber rattlesnakes ( <i>Crotalus horridus</i> ) used to identify foraging locations, including (A) foraging at logs and downed woody debris, (B) vertical-tree foraging, and (C) non-log foraging along the forest floor. Snakes maintain a tight, “S”-shaped coil regardless of foraging orientation. Photo credits to B. Hiner and E. Scott. ....	38
Figure 1.2. Placement of a camera trap with bait for small mammals one meter above and directly overlooking a log in a mature forest site in southeastern Ohio. (B) <i>Tamias striatus</i> and (C) <i>Peromyscus</i> spp. captured on camera at this trap site. ....	39
Figure 1.3. Daily estimated mice ( <i>Peromyscus</i> spp.) encounter rates from 242 camera trap sites distributed in a mixed-use forest in southeastern Ohio. ....	40
Figure 1.4. Daily estimated chipmunk ( <i>Tamias striatus</i> ) encounter rates from 242 camera trap sites distributed in a mixed-use forest in southeastern Ohio. ....	41
Figure 1.5. Daily estimated squirrel ( <i>Sciurus</i> spp.) encounter rates from 242 camera trap sites distributed in a mixed-use forest in southeastern Ohio. ....	42
Figure 1.6. Foraging probability of 37 adult timber rattlesnakes ( <i>Crotalus horridus</i> ) in a mixed-use forest in southeastern Ohio predicted by the cumulative contribution of estimated site-specific, daily encounters with mice ( <i>Peromyscus</i> spp.), chipmunks ( <i>Tamias striatus</i> ), and squirrels ( <i>Sciurus</i> spp.) from 2016–2019. ....	43
Figure 1.7. Adult female (n = 16) timber rattlesnake ( <i>Crotalus horridus</i> ) foraging probabilities in a mixed-use forest in southeastern Ohio predicted by prey encounter rates from 2016-2019. A) Cumulative Prey encounter rate, representing the additive combination of mouse ( <i>Peromyscus</i> spp.), chipmunk ( <i>Tamias striatus</i> ), and squirrel ( <i>Sciurus</i> spp.) site-specific encounter rates; B) mice-specific encounter rate; and C) squirrel-specific encounter rate. ....	44
Figure 1.8. Adult male (n = 21) timber rattlesnake ( <i>Crotalus horridus</i> ) foraging probabilities in a mixed-use forest in southeastern Ohio predicted by prey encounter rates from 2016-2019. Prey-specific foraging models include encounters with A) mice ( <i>Peromyscus</i> spp.), B) chipmunks ( <i>Tamias striatus</i> ), and C) squirrels ( <i>Sciurus</i> spp.). D) Cumulative Prey encounter rate, representing the additive combination of mouse, chipmunk, and squirrel site-specific encounter rates. ....	45

Figure 2.1. Clinical symptoms of snake fungal disease (SFD) in a population of timber rattlesnakes (*Crotalus horridus*) in southeastern Ohio. A–B) Mild clinical signs of SFD. For clarity, we circled observed facial lesions in red. The symptomatic female (top left) and male (top right) were both included in the movement and habitat use analyses. Bottom row: Moderate clinical signs of SFD in other individuals not included in movement and habitat use analyses in this study because of insufficient monitoring of SFD-asymptomatic years. Photo credits to B. Hiner, Z. Truelock, and J. Buffington. .... 85

Figure 2.2. Schematic of a multi-scale, behavior-focused study design to examine multifaceted effects of snake fungal disease (SFD) on the spatial ecology of 15 timber rattlesnakes (*Crotalus horridus*) in southeastern Ohio. .... 86

Figure 2.3. Mean area (ha) of 50%, 95%, and 100% minimum convex polygons (MCP) describing home ranges for 15 timber rattlesnakes (A–C: 6 non-gravid females; D–F: 9 males) during years when asymptomatic or symptomatic of snake fungal disease (SFD). Female home range area increases between years that individuals are asymptomatic of SFD and years in which they exhibit symptoms of SFD infection across all home range scales (A–C). Male home range area increases with SFD infection at the 50% (D) and 100% scales (F), but home range size does not differ at the 95% scale (E). .... 87

Figure 2.4. Principal component analysis biplots, representing gradients in scales of movement for 15 timber rattlesnakes (*Crotalus horridus*) in southeastern OH during years that individuals were Asymptomatic (coded by circles) or Symptomatic (coded by triangles) of snake fungal disease (SFD). Large, positive scores on PC1 suggest greater home range size (particularly 95% and 100% minimum convex polygons) and greater displacement rates. Large, positive scores on PC2 suggest greater median and mean movement rates. A) Male scores on PC1 and PC2. Individuals (n = 9) are coded by color. B) Female scores on PC1 and PC2. Individuals (n = 6) are coded by color. C) Scores of all individuals, coded by sex. Red represents females and gray represents males. .... 88

Figure 2.5. Principal component (PC1) scores, representing gradients in scales of movement for 15 timber rattlesnakes (*Crotalus horridus*) in southeastern OH during years that individuals were asymptomatic or symptomatic of snake fungal disease (SFD). Large, positive scores on PC1 suggest greater home range size (particularly 95% and 100% minimum convex polygons) and greater displacement rates. Large, positive scores on PC2 suggest greater median and mean movement rates. We used an interaction of SFD status and sex (females in red and males in grey) to predict PC scores, with a random effect of individual snake..... 89

Figure 2.6. Probability of site use by six non-gravid female timber rattlesnakes (*Crotalus horridus*) symptomatic of snake fungal disease (SFD) predicted by remotely-sensed (5-m resolution) landscape and forest structural characteristics. A) Distance to nearest stream. B) Forest stand age represents forest management history. C) Moisture gradient (NMDS1) with lower scores representing drier, southwestern-facing slopes. D)

Longitudinal gradient (NMDS3) with higher scores representing higher elevations and western locations..... 90

Figure 2.7. External snake body temperatures taken with a digital infrared thermometer at sites ( $n = 870$ ) used by timber rattlesnakes (*Crotalus horridus*) during years unaffected or affected by snake fungal disease (SFD). We modeled body temperature as an interaction of season of observation and SFD status, with month of observation and individual snakes modeled as random effects. Each snake ( $n = 9$  males and 6 non-gravid females) was considered Asymptomatic or Symptomatic of SFD infection for at least one year each. Asymptomatic years are in blue and Symptomatic years are in orange. We defined Spring as April–June, Summer as July–August, and Fall as September–October. .... 91

Figure 2.8. Estimated solar insolation ( $\text{kWh/m}^2$ ) corrected by observed canopy cover of sites used by 15 timber rattlesnakes (*Crotalus horridus*) in southeastern Ohio. We modeled solar insolation as a function of season of observation and snake fungal disease (SFD) status, with month of observation and individual snakes modeled as random effects. Each snake ( $n = 9$  males and 6 non-gravid females) was considered Asymptomatic or Symptomatic of SFD infection for at least one year each. Asymptomatic years are in blue and Symptomatic years are in orange. We defined Spring as April–June, Summer as July–August, and Fall as September–October. .... 92

Figure A.1. Predicted small mammal prey availability by timber rattlesnake (*Crotalus horridus*) foraging posture orientation. We used a Bayesian multivariate analysis of variance (MANOVA) to examine small mammal prey availability among different foraging orientation types (log-oriented, non-log-oriented, and vertical-tree-oriented) by timber rattlesnakes. We modeled site-specific daily encounter rates of mice (*Peromyscus* spp.), chipmunks (*Tamias striatus*), and squirrels (*Sciurus* spp.) as a function of foraging orientation with the ‘brms’ package in R (Bürkner, 2017; R Core Team 2020). Log-oriented and non-log oriented were the most commonly observed foraging orientations in our population ( $n = 244$  and  $239$ , respectively) and these foraging orientations exhibited the most similar small mammal associations. There was greater uncertainty around the species-level prey availability of vertical-tree foraging sites due to low observations ( $n = 39$ ) of this ambush posture in our population. A) Mice encounters were marginally greater (mean: 1.43 mice/day; 95% CI: 1.31–1.55 mice/day) at sites associated with a vertical-tree foraging orientation than non-log-oriented foraging (mean: 1.41 mice/day; 95% CI: 1.36–1.46 mice/day) or log-oriented foraging (mean: 1.35 mice/day; 95% CI: 1.30–1.40 mice/day), but with overlapping credible intervals among all groups. B) Chipmunk (CM) encounters varied little by foraging orientation type. Log-oriented foraging sites yielded the greatest mean chipmunk encounters (0.60 CM/day; 95% CI: 0.57–0.63 CM/day), followed by non-log-oriented (mean: 0.58 CM/day; 95% CI: 0.55–0.61 CM/day) and vertical-tree-oriented foraging (mean: 0.55 CM/day; 95% CI: 0.48–0.63), but with overlapping credible intervals among all groups. C) Predicted squirrel (SQ) encounters were marginally greater (mean = 0.27 SQ/day; 95% CI: 0.23–0.31 SQ/day) at vertical-tree foraging sites, followed by equal encounters at log-oriented

(mean: 0.24 SQ/day; 95% CI: 0.23–0.26) and non-log-oriented (mean = 0.24 SQ/day; 95% CI: 0.22–0.26) and overlapping credible intervals among all groups. .... 113

Figure B.1. External body temperatures (n = 870) of 15 timber rattlesnakes (*Crotalus horridus*) in southeastern Ohio. We measured body temperature with a digital infrared thermometer. We classified seasons for temperature and solar radiation models based on the partitioning of snake body temperatures between April–June, July–August, and September–October..... 122

Figure B.2. Linear relationship between external snake body temperatures (n = 9 snakes; 46 observations) taken with a digital infrared thermometer and the matching internal snake body temperature recorded hourly with an implanted RFID tag. .... 123

## Chapter 1. Prey-Driven Behavioral Habitat Use in a Low-Energy Ambush Predator

### Abstract

Food acquisition is an important modulator of animal behavior and habitat selection that can affect fitness. Optimal foraging theory predicts that predators should select habitat patches to maximize their foraging success and net energy gain, which predators can achieve by targeting spaces with high prey availability. However, it is debated whether prey availability drives fine-scale habitat selection for predators. We assessed whether an ambush predator, the timber rattlesnake (*Crotalus horridus*), exhibits optimal foraging site selection based on the spatial distribution and availability of prey. We evaluated the spatial concordance of radio-telemetered timber rattlesnake foraging locations and passive infrared game camera trap detections of potential small mammal prey (*Peromyscus* spp., *Tamias striatus*, and *Sciurus* spp.) in a mixed-use forest in southeastern Ohio from 2016–2019. We replicated a characteristic timber rattlesnake ambush position by focusing cameras over logs and modeled small mammal encounters across the landscape in relation to remotely-sensed forest and landscape structural features. To determine whether snakes selectively forage in areas with higher prey availability, we projected the estimated prey spatial relationships across the landscape and modeled their overlap of occurrence with observed timber rattlesnake foraging locations. We broadly predicted that prey availability was greatest in mature deciduous

forests, but *T. striatus* and *Sciurus* spp. exhibited greater spatial heterogeneity compared to *Peromyscus* spp. We also combined predicted species encounter rates to encompass a body size gradient in potential prey. The spatial distribution of cumulative small mammal encounters (i.e. overall prey availability), rather than the distribution of any one species, was highly predictive of snake foraging. Timber rattlesnakes appear to select foraging locations where the probability of encountering prey is greatest. Our study provides evidence for fine-scale optimal foraging in a low-energy, ambush predator and offers new insights into drivers of snake foraging and habitat selection.

## Introduction

Animal activity patterns are governed by the acquisition of spatially and temporally variable resources from the landscape, such as food, mates, shelter, or hospitable environmental conditions. Successfully procuring food is particularly essential for individual survival, growth, reproduction, and ultimately fitness (Tetzlaff et al., 2017). Therefore, it is important to link the distribution and availability of food with an animal's space use to better understand the drivers of movement and habitat selection (Heard et al., 2004; Williams et al., 2013).

Given the fitness trade-offs of investing time and/or energy into one behavior instead of another (Beaupre, 2008; Glaudas & Alexander, 2017), optimal foraging theory predicts that predators should forage where they will have the greatest success (i.e. net energy gain; Charnov, 1976). Optimal foraging theory also provides predictions for foraging habits, such as temporal and spatial patterns of site use, for predators in

resource-patchy environments. For example, optimally foraging predators spend more time foraging (i.e., longer residency time) in high quality patches according to the marginal value theorem (Charnov, 1976; McNair, 1982). Patch residency by predators therefore depends on patch-scale prey availability relative to the surrounding habitat (Charnov, 1976). Additionally, the ideal free distribution (IFD) predicts that predators should disperse to patches proportional to their food abundance (Flaxman & Lou, 2009; Williams et al., 2013). Predators can achieve IFD by either tracking prey densities or environmental gradients in prey foraging habitat (Flaxman & Lou, 2009; Kittle et al., 2017). Under game theory predictions, predators are expected to aggregate in areas where prey are abundant at large spatial scales but less precisely match prey distributions at fine scales (Hammond et al., 2012). Accordingly, wolves (Kittle et al., 2017), sea lions (Womble et al., 2009), and snakes (Madsen & Shine, 1996) have all been documented selecting habitats with higher prey availability at broad (regional or macrohabitat) scales.

A complication to understanding drivers of foraging behavior is that habitat selection can be multi-scale and hierarchical (Johnson, 1980; Mayor et al., 2009). Predators can demonstrate hierarchical foraging behavior as a result of multiple scale-dependent processes, such as predation risk or resource availability (McNeill et al., 2020). Conversely, observed foraging patterns can result from predominantly fine-scale resource selection (Harvey & Weatherhead, 2006). The space use of ectotherms is often driven by microhabitat conditions that affect their ability to thermoregulate, avoid predation, and forage (Harvey & Weatherhead, 2006; Sutton et al., 2017). Therefore, snakes may not distribute themselves proportionally to prey availability (i.e. achieve IFD)

nor forage optimally if prey-rich patches do not coincide with optimal environmental conditions for thermoregulation (Blouin-Demers & Weatherhead, 2001; Carfagno et al., 2006).

Indeed, some studies have found no evidence of snakes selecting prey-rich areas (Carfagno et al., 2006; Sperry & Weatherhead, 2009; Michael et al., 2014). However, other studies have found mixed or scale-dependent support for prey-mediated habitat selection by snakes (Whitaker & Shine, 2003; Glaudas & Rodríguez-Robles, 2011). Multi-scale studies emphasize the importance of habitat structure coinciding with prey availability for snake habitat selection (Heard et al., 2004; Glaudas & Rodríguez-Robles, 2011). Therefore, whether snakes exhibit IFD characteristics or optimally forage remains unresolved. Investigating the spatial overlap of snakes and their prey is essential to understand potential drivers of foraging behavior and habitat selection.

One hypothesis for the spatial overlap of snakes and their small mammal prey is that similar habitat preferences drive spatial interaction (Blouin-Demers & Weatherhead, 2001). Snakes therefore select habitat based on thermoregulation or other habitat requirements and opportunistically forage, which has been observed in generalist predators such as ratsnakes (*Pantherophis* spp.) and Eastern racers (*Coluber constrictor*; Blouin-Demers & Weatherhead, 2001; Carfagno et al., 2006). Snakes that opportunistically forage may have home ranges containing high prey densities, but they may not exhibit fine-scale selection that maximizes potential prey encounters (Sperry & Weatherhead, 2009). An alternative hypothesis is that the spatial distribution of prey abundance drives snake habitat selection (Blouin-Demers & Weatherhead, 2001). Prey-

mediated habitat selection suggests greater alignment of snake space use with prey availability (i.e. demonstrating IFD). This pattern is more likely to be evident in dietary specialists (Madsen & Shine, 1996) or during times of environmental stress such as drought (Whitaker & Shine, 2003).

Although some studies support contrasting hypotheses, not all studies used effective metrics for assessing prey distributions and snake site selection. First, most studies are conducted on a macrohabitat scale, which may not be appropriate when investigating snake habitat selection (Harvey & Weatherhead, 2006). Additionally, researchers typically evaluate prey abundance rather than prey availability. Prey abundance may not equate to prey availability when factors affecting prey detection are not considered (Sperry & Weatherhead, 2009; Reinert et al., 2011). Specifically, prey may be more abundant in some habitat types but more easily detected by the predator in others (i.e. higher catchability; Hopcraft et al., 2005). To our knowledge, no study has estimated prey availability for snakes at a fine scale and assessed prey distributions as a driver of snake foraging site selection.

The paucity of studies examining prey availability at a fine scale may be due to the logistical challenges of determining the exact microhabitats where the predator forages (Glaudas & Rodríguez-Robles, 2011). However, rattlesnake natural history characteristics make them ideal subjects to test hypotheses related to optimal foraging theory. We sought to determine whether foraging site selection of timber rattlesnakes (*Crotalus horridus*; hereafter, TRS) is related to the availability of prey on a fine scale.

Timber rattlesnakes are sit-and-wait ambush predators that may wait at a site for many hours to several days (Clark, 2006). They also have a stereotyped foraging posture, in which they orient their head perpendicular to the long axis of a log or other downed wood while maintaining a tight body coil (Reinert et al., 2011). The species' conspicuous foraging behavior allows for identification of exact foraging sites. In addition, TRS feed almost exclusively on small mammals, primarily shrews (Soricidae), voles (Cricetidae), mice in the genus *Peromyscus*, chipmunks (*Tamias striatus*), and squirrels (primarily *Sciurus carolinensis*; Clark, 2002). This relatively narrow dietary breadth reduces the potential for complex interactive or conflicting relationships between primary prey, alternative prey and TRS foraging preferences (Carfagno et al., 2006).

Our multi-year radio-telemetry study provided a behaviorally and spatially explicit dataset of TRS activity that allowed us to differentiate among behavior-specific site use and account for individual variation in foraging site selection. The primary goals of our study were to define small mammal spatial distributions and their overlap with observed TRS foraging locations at a fine spatial scale to determine whether TRS optimally forage in prey-rich areas. Our approach entailed (1) quantifying small mammal relative availability with widely-distributed camera traps, (2) projecting small mammal encounters across the study area with landscape predictors, and (3) using radio-telemetry-derived TRS behavioral data and the spatially continuous prey encounter surface to assess the predictive strength of prey availability on TRS foraging site selection.

## Methods

### *Study Site*

We conducted our study within a mixed-use forest landscape (approximately 5,000 ha) in southeastern Ohio. Vinton Furnace Experimental Forest (VFEF) consists primarily of second-growth forests punctuated by early-successional stands managed through various silvicultural and management practices (ODNRF, 2020). Forest communities in the region vary along topographic gradients. Ridgetops and southwestern-facing slopes are dominated by mixed oak (*Quercus* spp.) and hickory (*Carya* spp.) assemblages and shrubby (*Vaccinium* spp.) understory. Northeastern-facing slopes and river bottoms harbor mesophytic taxa such as *Acer rubrum*, *Acer saccharum*, and *Ulmus rubra* (Adams & Matthews, 2019).

### *Camera trap design*

Timber rattlesnakes hunt along logs (Reinert et al., 1984) and these microhabitats are also used by small mammals as “runways” (Douglass & Reinert, 1982; Figure 1.1A). To simulate this foraging behavior, we fixed passive infrared game cameras (Moultrie M-888) to metal fence posts approximately one meter above-ground and positioned them directly overlooking the nearest log (> 15 cm diameter) at each site (Figure 1.2). We placed a canister with small holes that contained peanut butter under each camera. Our camera deployment protocol allowed us to obtain fine-scale rodent encounter rates, which we considered more informative of prey availability for TRS than representative macrohabitat-scale estimates of rodent abundance (Reinert et al., 2011).

We deployed game cameras from 2017–2018 at 242 randomly-chosen, unique sites. We stratified these random points across the dominant macrohabitat types (deciduous forest, pine plantations, clear cuts, and burns) to ensure adequate sampling of each land cover type proportional to its prevalence on the landscape. Accordingly, we sampled more sites from deciduous forests (representing approximately 80% of the landscape) than any other forest type (Table A.1). We also set 26 camera traps at previously noted TRS foraging locations. We placed this subset of cameras at observed foraging sites between a day to a few weeks (range 1–86 d; median 15 d) of the snake’s departure from the site.

Game camera active intervals varied by site. We set game cameras at sites for 3–51 days (mean 7.3 d; median 6 d) between 15 June and 13 October 2017 and 4–22 days (mean 8 d; median 6 d) between 24 May and 26 September 2018. We focused our analysis on likely prey items for TRS that were also consistently captured on camera: white-footed/deer mice (*Peromyscus leucopus/maniculatus*), eastern chipmunks (*Tamias striatus*), and eastern gray squirrels/fox squirrels (*Sciurus carolinensis/niger*). We monitored occupancy (presence/absence) of each species during observation windows of roughly 12-hr day (approximately 0700–2000 h) and night (approximately 2100–0600 h) periods. We therefore did not track the number of individuals present during each observation period. Because night intervals spanned two dates, we considered small mammals active in the early morning (e.g., before 0600 h) as present in the night interval of the previous date.

#### ***Landscape variables characterizing small mammal distributions***

Habitat selection for small mammals, particularly as it relates to forest structural features, is typically assessed with microhabitat and vegetation structural characteristics, such as coarse woody debris and leaf litter cover (Nelson et al., 2019). However, it was not feasible to assess microhabitat features for each camera location and across the landscape. Airborne light detection and ranging (LiDAR) can describe horizontal and vertical vegetation structure across large areas, providing a valuable alternative to the use of intensive field-based methods to assess forest structure (Simonson et al., 2014). Schooler and Zald (2019) demonstrated that LiDAR-derived metrics are effective predictors of small mammal diversity in a temperate mixed-forest community. We therefore used LiDAR and other remotely sensed data to quantify forest structure and predict small mammal occupancy across the landscape.

We described landscape composition and structure at each camera location with 16 land-use, floristic, and topographic variables from fine-scale (5-m) stand-level or remotely sensed data for our study area (Table 1.1). Stand-level forest management data, including burn history and stand age, reflect active management at VFEF by the Ohio Division of Forestry and U.S. Forest Service over the past 60 years. We derived topographic variables, such as Beers' aspect (Beers et al., 1966), slope, and elevation from a LiDAR digital terrain model (DTM). To describe forest composition, we considered compositional, multivariate metrics (NMDS1 and NMDS2) that allowed for continuous variation across the landscape. Adams et al., (2019) combined a LiDAR-derived DTM, vegetational plot data, and Landsat 8 OLI imagery to generate floristic gradients for the study area. We sourced the LiDAR-derived DTM from The Ohio

Geographically Referenced Information Program (OGRIP; <https://ogrip.oit.ohio.gov/Home.aspx>) and Landsat 8 Imagery from the United States Geological Survey (USGS; <https://earthexplorer.usgs.gov>), and corrected for known timber harvests occurring after data acquisition (Adams & Matthews, 2018; Adams et al., 2019). We tested for multicollinearity among the predictors with Pearson’s correlation coefficient, and no variables were correlated above 0.7. We scaled and centered all continuous variables to have a mean of zero and standard deviation of one.

### ***Timber rattlesnake radio-telemetry***

As part of an ongoing study, we radio-tracked 37 adult TRS (21 males and 16 non-gravid females) between 2016 and 2019 to obtain behavior-specific spatial data (further described in Hoffman et al., 2020, in review). We relocated snakes 1–3 times per week and classified behavioral state (e.g., ecdysis, resting, foraging) upon relocation, resulting in 522 observed foraging locations. We noted foraging locations when snakes exhibited a characteristic “S”-shaped ambush posture: compactly coiled, with head extending past outer coil, and a greater number of anterior directional changes compared to a resting state (Figure 1.1; Reinert et al., 1984). We also identified the presumed foraging orientation type—log-oriented, non-log-oriented, or vertical-tree-oriented (Reinert et al., 2011; Goetz et al., 2016). We defined a log-oriented posture as when snakes rested on or faced (within 1-m) a log or fallen branch (Figure 1.1A; Reinert et al., 1984). We defined a vertical-tree-oriented posture as when snakes coiled at the base of standing trees, with their heads oriented upwards or facing (within 1-m) a tree (Figure 1.1B; Goetz et al., 2016). We considered snakes coiled in ambush on the forest floor but

not log or vertical-tree-oriented to be in a non-log-oriented posture (Figure 1.1C; Reinert et al., 2011). We found males and non-gravid females in our study equally likely to forage log-oriented ( $n = 244$ ) as non-log-oriented ( $n = 239$ ), and to rarely exhibit a vertical-tree-orientation ( $n = 39$ ). A preliminary analysis showed that foraging orientation type did not affect prey encounter rate for any prey species (Figure A.1). We therefore included all foraging location types in the Snake Foraging Probability models to assess snake foraging spatial concurrence with prey availability.

### ***Small mammal encounter rate models***

We modeled the number of days/nights with a small mammal species' observation using Bayesian zero-inflated generalized linear models (GLM). We considered a zero-inflated framework because of the coarse sampling of small mammals across our site and resulting overdispersion in counts. Ecological datasets often contain a higher frequency of measured zeros than can be accommodated by standard statistical distributions and can therefore violate the assumptions of these distributions (Martin et al., 2005). Zero-inflated models combine two underlying processes, modeling non-zero counts and true zeros with a Poisson or negative binomial process and the potentially false zeros with a binomial process ( $Z_i$ ), generating the probability of measuring a zero in error (Zuur et al., 2009).

We tested the global set of landscape covariates ( $n = 16$ ), year, an offset of the number of active camera days, and  $Z_i$  covariates (i.e. the binomial “false-zero” process) under negative binomial and Poisson distributions, resulting in 10 candidate global models for each species (Tables A.2–A.4). We suspected that interannual variation, likely

representing acorn mast availability (Clotfelter et al., 2007), or the timing of camera placement during each season (i.e. seasonal fluctuations in small mammal activity patterns) could affect our detection success at a particular location. We therefore accounted for temporal variation in species encounter rates for zero-inflated models with the  $Z_i$  term, using no covariates as a null, median date of camera deployment (modeled as a quadratic function), year, and the additive or interactive combinations of median date and year (Tables A.2–A.4). We used diagnostic plots to compare each model’s predictions of the mean and variance and selected the global model of best fit. For each small mammal species, a zero-inflated negative binomial model best represented encounters but the selected  $Z_i$  covariates varied by species (Table A.5).

We examined model coefficients for their magnitude of effect in each selected global model and removed covariates with no or a negligible effect, removed covariates with >15% posterior distribution overlap with zero, and removed covariates with >20% of the posterior within the Region of Practical Equivalence (ROPE; Piironen & Vehtari, 2017). We considered the resulting species model with the lowest leave-one-out statistic (LOO) and Watanabe-Akaike Information Criterion (WAIC) value to be the most parsimonious.

We projected small mammal spatial relationships across the landscape by using the fitted encounter rate model for each species and the corresponding landscape raster surfaces using the ‘raster’ package in R version 3.6.1 (Hijmans 2020; R Core Team 2020). We generated mean encounter probabilities for each species across the study site at a 10-m resolution for 2017 and 2018. In addition to landscapes of species-specific

encounter rates, we considered the dietary breadth of adult TRS, and generated grouped prey landscapes by adding the relevant encounter surfaces together. In one group, we combined mouse and chipmunk encounters (Cumulative MC) because they are most likely to be encountered at logs (Douglass & Reinert, 1982). We also combined mouse, chipmunk and squirrel encounters (Cumulative Prey) to capture the body size gradient in prey selection for adult TRS. We extracted the predicted prey species or prey group encounter rates at every TRS location.

### *Snake foraging models*

We modeled snake foraging using mixed-effects Bernoulli GLMs with foraging behavior as a binomial function of the spatially-explicit small mammal encounter rates. We included a random effect for individual snakes. We tested models with prey type variations for non-gravid adult females (NGF;  $n = 16$ ), adult males ( $n = 21$ ), and the combined adult TRS group ( $n = 37$ ). We excluded gravid females ( $n = 10$ ) because they fast during gestation (Reinert et al., 1984).

We did not monitor small mammal spatial distributions for two years (2016 and 2019) that we tracked snakes. Although we recognize the potential for prey fluctuations in density corresponding with acorn mast cycles (Clotfelter et al., 2007), the predictive landscape metrics we considered did not vary over the course of the study. We therefore generalized our findings from 2017–2018 to all observations from our telemetry study. We estimated small mammal encounter rates, comprising mouse, chipmunk, squirrel, and the cumulative prey surfaces (Cumulative MC and Cumulative Prey) for 2017 and 2018, but used the two-year averaged encounter rates for each species or species group to

represent prey availability in 2016 and 2019. We report results from 2016–2019 but reference the 2017–2018 subset in model selection tables and when applicable in results (see Appendix A for further details). We tested species-level and cumulative prey models for adults collectively, and non-gravid females and males separately. We considered the foraging models with the lowest LOO and WAIC scores as the best-supported model for each group. We used the ‘brms’ package in R to fit all statistical models (Bürkner, 2017).

## Results

### *Prey diversity on camera traps*

Across 242 camera sites and a cumulative 1901 trap days and 1662 trap nights, we successfully captured the dominant prey species of TRS. We detected mice at most sites (61% of sites with  $\geq 1$  detection; Table 1.2) and the most extensively and frequently (range of 0–17 camera days) of any species. We observed chipmunks and squirrels at fewer sites ( $< 50\%$  of sites) and less frequently (maximum of 9 and 6 days, respectively; Table 1.2). In addition to these primary prey items, we also infrequently captured shrews (Soricidae), voles (*Microtus* spp.), and cottontail rabbits (*Sylvilagus floridanus*). We also frequently captured bird species that are potential opportunistic prey sources.

### *Small mammal encounter rate models*

**Mice**—The most explanatory model for daily mice encounters was a zero-inflated ( $Z_i = \text{year}$ ) negative binomial model with year, burn history, and stand age (Table A.5). Mice were most likely to be encountered in non-burns of a younger age (Table 1.3). Mice were encountered approximately twice as frequently in 2018 (2.22 mice/day; 95% CI:

1.94–2.55) than 2017 (0.91 mice/day; 95% CI: 0.70–1.16; Figure 1.3A). Encounters were lowest in burned stands (Table 1.3), at 0.53 mice encounters per day compared to approximately 0.91 encounters/day in other stand types (Figure 1.3B). Stand age was the weakest predictor of mice encounters (Table 1.3), but encounters were generally more frequent in younger stands (Figure 1.3C). Mice could be encountered across the landscape at a range of 0.32–0.81/day in 2017 and 0.84–1.9/day in 2018.

**Chipmunks**—The best-fitting model for daily chipmunk (CM) encounters was a zero-inflated ( $Z_i = \text{year}$ ) negative binomial model with the forest successional gradient (NMDS2), plant species richness (PSR), and slope (Table A.5). Chipmunks were most frequently encountered in stands with taller canopies and greater plant richness, and along steeper slopes (Figure 1.4). The forest successional gradient was the best landscape predictor (Table 1.3) of chipmunk encounter rates (Figure 1.4A). Encountering a chipmunk would take between 1–2.5 days (mean ~1.5 days) in a more mature forest but between 3–16 days (mean 7 days) in a younger stand. Plant species richness had a similar effect size (mean  $0.23 \pm 0.11$ ), increasing from 0.14 CM/day (95% CI: 0.04–0.40) at low plant richness to an estimated 0.74 CM/day (95% CI: 0.37–1.48) in a more speciose stand (Figure 1.4B). Chipmunks were also encountered more frequently along steeper slopes (Figure 1.4C). Chipmunks could be encountered across the landscape at a range of 0.01–1.2/day in 2017 and 0.04–2.8/day in 2018.

**Squirrels**—The most supported model for squirrel (SQ) encounters was a zero-inflated ( $Z_i = \text{median date}^2 + \text{year}$ ) negative binomial model with year, foliage height diversity (FHD), the moisture gradient (NMDS1), NMDS2, overstory density, and

understory density (Table A.5). Squirrels were most frequently encountered in drier areas and stands with taller canopies and greater overstory density, low canopy structural diversity, and low understory density (Table 1.3). Year had the largest effect on squirrel encounters ( $1.05 \pm \text{SE } 0.31$ ), with encounter rate doubling from an estimated 0.16 SQ/day (95% CI: 0.08–0.25) in 2017 to 0.37 SQ/day (95% CI 0.19–0.56) in 2018 (Figure 1.5A).

The forest succession gradient (NMDS2) was the best landscape predictor of squirrel encounter rates, with squirrels ten times more frequently encountered in forest stands with taller canopies (0.38 encounters/day, 95% CI: 0.15–0.93) compared to early seral stands (Figure 1.5B). Squirrels could be encountered within 1–7 days (mean 3 days) in a mature stand versus rarely, if at all, in the youngest stands with low canopy height. Squirrel encounters were negatively associated with NMDS1, suggesting the species' preference for drier, southwestern-facing slopes that harbor nut-bearing trees (Figure 1.5C). Squirrel encounter rate drastically declined with greater understory density, from 0.55 SQ/day (95% CI: 0.17–1.64) in sparse understories to minimal encounters (0.03 SQ/day; 95% CI: 0.01–0.13) in highly vegetated understories (Figure 1.5D). Squirrels were also encountered more frequently at sites with greater overstory density (Figure 1.5E). Additionally, squirrels were negatively associated with foliage height diversity (FHD; Figure 1.5F), suggesting a preference for forests stands of similar height and age (Aber, 1979). Squirrels could be encountered across the landscape at a range of 0.004–1.29/day in 2017 and 0.01–3.2/day in 2018.

### ***Foraging Probability Models***

The Cumulative Prey landscape, representing the overlay of mice, chipmunk, and squirrel daily encounters, was a strong, well-supported predictor ( $1.09 \pm \text{SE } 0.09$ ) of adult TRS foraging probability (Tables A.6–A.7). The probability of snake foraging increased sharply with predicted prey encounter rates (Figure 1.6). Snake foraging probability increased from a minimum of 0.06 (95% CI: 0.04–0.08) associated with an estimated mean prey encounter rate of 0.59 prey/day to 0.69 (95% CI: 0.61–0.76) at an estimated 3.83 prey/day (Figure 1.6).

Cumulative Prey was also the best predictor ( $1.05 \pm \text{SE } 0.15$ ) for non-gravid females in both year groupings (Table A.6). Female foraging probability increased from 0.07 (95% CI: 0.05–0.11) at low estimated prey encounters (0.63 prey/day) to 0.7 (95% CI: 0.55–0.80) at the highest predicted prey encounter rate (3.8 prey/day; Figure 1.7A). In terms of individual prey species, the best-supported species-level model for females included encounter rates for mice ( $1.39 \pm \text{SE } 0.22$ ) and squirrels ( $1.73 \pm \text{SE } 0.72$ ; Table A.7), but with a modest increase in foraging probability associated with mice encounters only (Figure 1.7B) and significant uncertainty around the effects of squirrel encounters only (Figure 1.7C).

For males, the species-level foraging model was marginally more supported in 2016–2019 and the Cumulative Prey model was better-supported in 2017–2018 (Table A.6). There was greater uncertainty around species-level effects on male foraging, particularly for squirrels (Table A.7). The distribution of mice ( $0.75 \pm \text{SE } 0.20$ ) was least predictive of male foraging; foraging probability increased marginally to 0.3 (95% CI: 0.22–0.38) at the greatest predicted encounter rate (1.90 mice/day; Figure 1.8A).

Predicted chipmunk ( $1.09 \pm \text{SE } 0.35$ ) and squirrel ( $2.9 \pm \text{SE } 0.77$ ) encounters had the greatest effects on male foraging (Table A.7). Male foraging probability increased to a maximum of 0.51 (95% CI: 0.29–0.72) at the highest chipmunk encounter rate of 1.81 CH/day (Figure 1.8B). For squirrel encounters, male foraging probability increased sharply to a maximum of 0.62 (95% CI: 0.36–0.83) at high predicted encounters (0.87 SQ/day; Figure 1.8C). Estimated Cumulative Prey encounters also had a strong effect ( $1.14 \pm \text{SE } 0.11$ ) on male foraging probability, similar to trends observed across all adults (Table A.7; Figure 1.8D).

## Discussion

Because ectotherms have reduced demands for regular, frequent foraging and many snakes in particular can be low-energy specialists (Glaudas & Alexander, 2017), prey distribution and availability may be considered unlikely proximate influences on habitat selection (Heard et al., 2004; Carfagno et al., 2006). However, we found that total prey ‘availability’ (measured as cumulative daily prey encounter rates), rather than any one prey type, was overall the best predictor of TRS foraging. Our results suggest that TRS may forage optimally and preferably forage in prey-rich areas according with IFD. Further, our study supports that TRS may attune to fine-scale differences in prey availability despite specializing on common woodland rodents that are generally thought to be widespread.

Previous studies have found support for some overlap in snake and prey distributions across a single, typically macrohabitat scale. The effects of temporal and/or

spatial heterogeneity in prey densities on predator habitat selection is also more straightforward to describe on a broader scale because one can estimate prey abundance/availability and describe snake habitat use within specific habitat types (Glaudas & Rodríguez-Robles, 2011). However, prey may be more abundant in some habitats but more easily detected by the predator in others (i.e. “higher catchability”) due to a lack of cover or camouflage or changes to predator avoidance behavior by prey (Hopcraft et al., 2005). For example, TRS in an agricultural landscape frequently foraged in fields that harbored lower densities of small mammals than surrounding woodlands, likely as a result of increased prey catchability (Wittenberg 2012). Because of the use of both ‘prey availability’ and ‘prey abundance’ interchangeably in the literature, we will hereafter use prey availability to refer to both but will make note of the context in which they are used when possible.

Other studies have shown that snake home ranges generally contain a high proportion of habitat preferred by rodents (i.e. correspondingly high rodent densities), but snakes do not exhibit site selection that would maximize small mammal encounters (Sperry & Weatherhead, 2009; Glaudas & Rodríguez-Robles, 2011; but see Baxley & Qualls, 2009). We expect that we observed a robust, positive association between prey availability and snake foraging on a fine scale partly because we could distinguish foraging site selection from other distinct behaviors shaping site use. Previous snake telemetry studies accounting for prey availability have either aggregated all snake relocations to compare seasonally within home ranges (e.g., Baxley & Qualls, 2009; Sperry & Weatherhead, 2009; Michael et al., 2014) or against random or non-used

locations (Glaudas & Rodríguez-Robles, 2011), rather than accounting for behavior-specific variation in habitat use preferences.

Hoffman et al. (2020) found that site selection associated with foraging, ecdysis, digestion, and gestation in this TRS population could be described by many of the landscape variables used in this study (Table 1.1) at behavior-specific spatial scales (5–105 m). Foraging was negatively associated with temperature and a landscape moisture gradient (indicating drier soils and oak-dominated areas) and these conditions did not describe site use for other behaviors (Hoffman et al., 2020, in review). Importantly, TRS foraging was associated with cooler temperatures than sites associated with other behavioral states, suggesting foraging behavior may be decoupled from snake thermoregulatory needs (Hoffman et al., 2020, in review). Our findings that TRS foraging is associated with greater prey availability but also suboptimal conditions for thermoregulation demonstrate that snakes preferentially seek out prey-rich areas to forage. Habitat structure may therefore incompletely describe foraging behavior, and the prey landscape is an important additional predictor of ambush site selection (Figure 1.6).

Our finding that the Cumulative Prey landscape, instead of any one prey species' distribution, is strongly predictive of TRS foraging can be understood in the context of snake foraging mode and dietary breadth. First, foraging site selection that maximizes encounters across multiple prey species is likely partly due to the sit-and-wait foraging mode of most viperids (Huey & Pianka, 1981; Reinert et al., 1984). Predators using an ambush strategy to hunt are more likely than widely foraging predators to prey on highly mobile species (i.e. species more likely to be encountered), be non-selective in their prey

choices, and therefore consume prey species in proportion to their availability (Huey & Pianka, 1981). Viperid species appear to forage in a two-part process, in which snakes first search the surrounding landscape for a suitable ambush site where prey may be more readily available, and then wait to encounter prey or abandon the site when prey encounters are unlikely (Reinert et al., 1984; Clark, 2006). Clark (2006) monitored foraging TRS with videography and demonstrated that snakes selected ambush sites based on potential contact with multiple prey individuals of the same or a different species, with snakes likely using prey chemical trails for identification of these fine-scale small mammal hotspots. Our results also support that TRS may select ambush sites based on the detection of multiple prey species (Clark, 2004).

Specificity in snake diet also affects the importance of the prey landscape for snake habitat selection. The studies that have most conclusively linked snake space use to the abundance of their prey examined focal snake species which primarily consumed a single prey species (Madsen & Shine, 1996; Heard et al., 2004). With increasing diet generalization, snakes are expected to respond to total prey availability rather than the distribution of any one species (Carfagno et al., 2006). This supports our finding that foraging in TRS, a species that primarily consumes small mammals but does not specialize on any species, positively correlates with the overlapping distributions of multiple potential prey.

The orientation of TRS ambush, such as at log, non-log (i.e. forest floor), or vertical-tree, can suggest but not validate the potential prey species targeted through ambush (Reinert et al., 2011; Goetz et al., 2016). Snakes are more likely to encounter

mice and some squirrel species (including *Tamias striatus* and *S. carolinensis*) across fallen logs (Douglass & Reinert, 1982), shrews and voles on the forest floor through leaf litter and vegetation (Reinert et al., 2011), and *S. carolinensis* at standing trees (Goetz et al., 2016). An alternative explanation to TRS prioritizing multiple prey chemical cues in ambush site selection is that by combining site-specific prey encounter rates for multiple prey species, we negated any prey-specific preferences by snakes. However, we do not believe this to be likely because we did not detect a difference in predicted encounters of any prey species or combined prey grouping for observed snake foraging sites among ambush orientations (e.g., snakes foraging at logs were not more likely to encounter mice than in non-log ambush). Our finding of equally available prey opportunities among ambush orientations further supports that prey identity is potentially less significant than overall prey availability during foraging in this population (Figure A.1).

Although Cumulative Prey emerged as the best-supported model for adults generally, we also found some sex-specific differences in individual prey associations (Table A.7). Mice most reliably predicted female foraging (Figure 1.7B), while chipmunks best predicted male foraging (Figure 1.8B). Timber rattlesnakes exhibit an ontogenetic expansion in diet, with larger snakes (i.e. adult males) able to consume larger prey and a broader diversity of small mammals but still target smaller prey indiscriminately (Clark, 2002; Reinert et al., 2011). We must emphasize however that we did not conduct diet analyses to examine the dietary compositions of snakes in our population, and diet has been shown to vary by population and region (Reinert et al., 2011; Wittenberg, 2012; Goetz et al., 2016). We therefore caution against trying to infer

dietary patterns from the spatial overlap of snakes with individual prey species or from observed ambush orientations (Clark, 2006; Reinert et al., 2011).

Cameras detected mice (*Peromyscus* spp.) much more frequently than chipmunks (*Tamias striatus*) or squirrels (*Sciurus* spp.), and accordingly, encounter rates for mice scaled higher overall (Table 1.2; Figure 1.3). Mice were most frequently captured in non-burned stands (representing 87% of camera sites and 94% of landscape coverage; Table A.1) but of a younger age. White-footed mice in particular are known to generally be robust to disturbance and management for oak-hickory forests (Urban & Swihart, 2011; Nelson et al., 2019), but we expect the negative association with burns is likely due to the age of these stands (minimum age 9). For example, Sasmal et al. (2017) found that *Peromyscus* spp. did not immediately respond negatively to fire in a longleaf pine ecosystem, but abundance gradually decreased with time (three years). Despite the prevalence of mice across our study area, their distribution related very little to that of chipmunks (Pearson's  $r = -0.19$ ) and squirrels (Pearson's  $r = -0.10$ ). Chipmunks and squirrels had the most correlative distributions at the landscape scale (Pearson's  $r = 0.3$ ). These species shared a moderate, positive association with the forest successional gradient (NMDS2). We captured squirrels on camera more intermittently than other rodents, but they exhibited the most complex landscape-scale spatial relationships. Similar to mice and chipmunks, squirrels preferred forest structural characteristics associated with mature forests, including taller canopies and lower understory density, but uniquely with drier, southwestern-facing slopes associated with oaks (Urban & Swihart 2011).

We primarily considered spatial associations of small mammals, but we also observed temporal shifts in availability (Figures 1.3A and 1.5A). Rodent encounter rates greatly increased between the two sampled years (2017–2018), and year was the best predictor in the zero-inflated process models for all species (Table A.5). We believe this pattern likely corresponds to the boom-bust mast cycles of oaks (*Quercus* spp.), beeches (*Fagus* spp.), and hickories (*Carya* spp.) during 2016 and 2017 and the associated stimulus of increased food availability on rodent population dynamics during the following year (Clotfelter et al., 2007). Given our rodent encounter rate patterns, we suspect, but cannot confirm, that 2016 was a poor mast year and from observational data, 2017 represented a better than average mast crop, particularly for black oaks (*Quercus velutina*) at the site (R. Snell, pers. comm.). We emphasize that we did not expect these yearly fluctuations to affect snake spatial associations with small mammals because our remotely-sensed landscape and forest structural characteristics did not change over the course of the study.

Although our study provides a unique, fine-scale link between prey and predator space use, there are some limitations to the inferences we can make. First, an important assumption to behavioral observations during radio-telemetry is continuity in behavior. We monitored snakes during the day and assumed that individuals remained in a behavioral state if we relocated them at the same site and they exhibited the same behavioral state (e.g. ambush posture) across multiple relocations. We therefore cannot account for temporal gaps in spatial data, during which behavioral shifts or additional

ambush site selection/abandonment and any nocturnal foraging patterns may occur (Clark, 2006).

Our field deployment of camera traps was intended to simulate a snake's perspective and represent a conceptual test of estimating prey availability for this species. Improvements to our camera trap protocol would need to occur in any future applications, such as improving prey species' detections and sampling more thoroughly and extensively across habitat types and snake ambush sites specifically. Improved image quality could potentially enhance detection of rarely captured, smaller prey, such as shrews and voles (Table 1.2). Additionally, we used daily species occupancy to account for individual animals moving around or returning to camera sites within a 12-hr interval. Our prey availability metric underestimates true availability. However, we expect this bias to be consistent across all habitats surveyed, which may not be the case in studies using prey abundance as a proxy of availability (Carfagno et al., 2006; Sperry & Weatherhead, 2009).

We also made indirect spatial links between rodents and snakes as our camera locations do not, for the most part, match known TRS foraging locations. We inferred prey availability at snake ambush sites by projecting small mammal spatial relationships across the landscape, which may incompletely capture the spatial heterogeneity of their distributions. However, we found our remotely-sensed landscape-scale covariates (Table 1.1) to have moderately strong effects on rodent encounter rates (Table 1.3). In future studies, we recommend direct quantification of small mammal encounters at observed

ambush sites and other selected behavior-specific sites to more precisely link foraging behavior to prey spatial distributions.

We demonstrated that prey availability can be an important driver of foraging site selection, which corroborates predictions from an optimal foraging framework. However, optimal foraging theory can also be applied to understand temporal patterns of site use by predators (Charnov, 1976). Future work should therefore investigate time spent foraging to assess site residency times (alternatively, “giving-up time”) and potential fitness costs to suboptimal foraging site use. We recommend continued assessment of optimal foraging theory and its corollaries in describing observed foraging behavior, particularly in conventionally underrepresented species in the literature, such as Viperid snakes and other low-energy specialists.

## Conclusions

Multiple factors could affect the relationship between prey availability and snake spatial ecology, including prey behavior and habitat use, the spatial scales of study, snake diet and foraging mode, and environmental fluctuations. We recognize that thermal requirements are the underlying determinant of overall habitat use variation in snakes, but prey availability plays a potentially important and underappreciated role in local habitat selection. We found a strong association between TRS foraging site selection and rodent encounter rates. Our results suggest that TRS can detect fine-scale differences in prey availability and spatially distribute themselves accordingly. We demonstrate that optimal

foraging theory may be applicable to the habitat selection of a low-energy ambush predator.

#### Literature Cited

- Aber, J. D. (1979). Foliage-height profiles and succession in northern hardwood forests. *Ecology*, 60, 18–23.
- Adams, B. T., & Matthews, S. N. (2018). Enhancing forest and shrubland mapping in a managed forest landscape with Landsat–Lidar data fusion. *Natural Areas Journal*, 38, 402–418.
- Adams, B. T., Matthews, S. N., Peters, M. P., Prasad, A. & Iverson, L. R. (2019). Mapping floristic gradients of forest composition using an ordination-regression approach with landsat OLI and terrain data in the Central Hardwoods region. *Forest Ecology and Management*, 434, 87–98.
- Baxley, D. L., & Qualls, C. P. (2009). Black pine snake (*Pituophis melanoleucus lodingi*): spatial ecology and associations between habitat use and prey dynamics. *Journal of Herpetology*, 43, 284–293.
- Beaupre, S. J. (2008). Annual variation in time-energy allocation by timber rattlesnakes (*Crotalus horridus*) in relation to food acquisition. In W. K. Hayes, K.R. Beaman, M.D. Cardwell, & S.P. Bush (Eds.), *Biology of the Rattlesnakes* (pp. 111–122). Loma Linda, California, USA: Loma Linda University Press.
- Beers, T. W., Dress, P. E., & Wensel, L. C. (1966). Notes and observations: Aspect transformation in site productivity research. *Journal of Forestry*, 64, 691–692.

- Blouin-Demers, G., & Weatherhead, P. J. (2001). An experimental test of the link between foraging, habitat selection and thermoregulation in black rat snakes *Elaphe obsoleta obsoleta*. *Journal of Animal Ecology*, 70, 1006–1013.
- Bürkner, P. (2017). brms: An R package for Bayesian multilevel models using Stan. *Journal of Statistical Software*, 80, 1–28.
- Carfagno, G. L. F., Heske, E. J., & Weatherhead, P. J. (2006). Does mammalian prey abundance explain forest-edge use by snakes? *Écoscience*, 13, 293–297.
- Charnov, E. L. (1976). Optimal foraging, the marginal value theorem. *Theoretical Population Biology*, 9, 129–136.
- Clark, R. W. (2002). Diet of the timber rattlesnake, *Crotalus horridus*. *Journal of Herpetology*, 36, 494–499.
- Clark, R. W. (2004). Timber rattlesnakes (*Crotalus horridus*) use chemical cues to select ambush sites. *Journal of Chemical Ecology*, 30, 607–617.
- Clark, R. W. (2006). Fixed videography to study predation behavior of an ambush foraging snake, *Crotalus horridus*. *Copeia*, 2006, 181–187.
- Clotfelter, E. D., Pedersen, A. B., Cranford, J. A., Ram, N., Snajdr, E. A., Nolan, V., Ketterson, E. D. (2007). Acorn mast drives long-term dynamics of rodent and songbird populations. *Oecologia*, 154, 493–503.
- Douglass, N. J., & Reinert, H. K. (1982). The utilization of fallen logs as runways by small mammals. *Proceedings of the Pennsylvania Academy of Science*, 56, 162–164.

- Flaxman, S. M., & Lou, Y. (2009). Tracking prey or tracking the prey's resource? Mechanisms of movement and optimal habitat selection by predators. *Journal of Theoretical Biology*, 256, 187–200.
- Glaudas, X., & Rodríguez-Robles, J. A. (2011). A two-level problem: habitat selection in relation to prey abundance in an ambush predator, the speckled rattlesnake (*Crotalus mitchellii*). *Behaviour*, 148, 1491–1524.
- Glaudas, X., & Alexander, G. J. (2017). Food supplementation affects the foraging ecology of a low-energy, ambush-foraging snake. *Behavioral Ecology and Sociobiology*, 71, 1–11.
- Goetz, S. M., Petersen, C. E., Rose, R. K., Kleopfer, J. D., & Savitzky, A. H. (2016). Diet and foraging behaviors of timber rattlesnakes, *Crotalus horridus*, in eastern Virginia. *Journal of Herpetology*, 50, 520–526.
- Hammond, J. I., Luttbeg, B., Brodin, T., & Sih, A. (2012). Spatial scale influences the outcome of the predator-prey space race between tadpoles and predatory dragonflies: Scale and predator-prey games. *Functional Ecology*, 26, 522–531.
- Harvey, D. S., & Weatherhead, P. J. (2006). A test of the hierarchical model of habitat selection using eastern massasauga rattlesnakes (*Sistrurus catenatus*). *Biological Conservation*, 130, 206–216.
- Heard, G. W., Black, D., & Robertson, P. (2004). Habitat use by the inland carpet python (*Morelia spilota metcalfei*): Seasonal relationships with habitat structure and prey distribution in a rural landscape. *Austral Ecology*, 29, 446–460.

- Hijmans, R. J. (2020). Raster: geographic data analysis and modeling. R Package Version 3.3-13. <<http://CRAN.R-project.org/package=raster>>.
- Hopcraft, J. G. C., Sinclair, A. R. E., & Packer, C. (2005). Planning for success: Serengeti lions seek prey accessibility rather than abundance. *Journal of Animal Ecology*, 74, 559–566.
- Huey, R. B., & Pianka, E. R. (1981). Ecological consequences of foraging mode. *Ecology*, 62, 991–999.
- Johnson, D. H. (1980). The comparison of usage and availability measurements for evaluating resource preference. *Ecology*, 61, 65–71.
- Kittle, A. M., Anderson, M., Avgar, T., Baker, J. A., Brown, G. S., Hagens, J., ... Fryxell, J. M. (2017). Landscape-level wolf space use is correlated with prey abundance, ease of mobility, and the distribution of prey habitat. *Ecosphere*, 8, e01783.
- Madsen, T., & Shine, R. (1996). Seasonal migration of predators and prey—A study of pythons and rats in tropical Australia. *Ecology*, 77, 149–156.
- Martin, T. G., Wintle, B. A., Rhodes, J. R., Kuhnert, P. M., Field, S. A., Low-Choy, S. J., ... Possingham, H. P. (2005). Zero tolerance ecology: improving ecological inference by modelling the source of zero observations. *Ecology Letters*, 8, 1235–1246.
- Mayor, S. J., Schneider, D. C., Schaefer, J. A., & Mahoney, S. P. (2009). Habitat selection at multiple scales. *Ecoscience*, 16, 238–247.

- McNair, J. N. (1982). Optimal giving-up times and the Marginal Value Theorem. *The American Naturalist*, 119, 511–529.
- McNeill, E. P., Thompson, I. D., Wiebe, P. A., Street, G. M., Shuter, J., Rodgers, A. R., & Fryxell, J. M. (2020). Multi-scale foraging decisions made by woodland caribou (*Rangifer tarandus caribou*) in summer. *Canadian Journal of Zoology*, 98, 331–341.
- Michael, D. R., Cunningham, R. B., Macgregor, C., Brown, D., & Lindenmayer, D. B. (2014). The effects of prey, habitat heterogeneity and fire on the spatial ecology of peninsular diamond pythons (*Morelia spilota spilota*). *Austral Ecology*, 39, 181–189.
- Moore, J. A., & Gillingham, J. C. (2006). Spatial ecology and multi-scale habitat selection by a threatened rattlesnake. *Copeia*, 2006, 742–751.
- Nelson, D. L., Kellner, K. F., & Swihart, R. K. (2019). Rodent population density and survival respond to disturbance induced by timber harvest. *Journal of Mammalogy*, 100, 1253–1262.
- Ohio Department of Natural Resources Division of Forestry (ODNRF). (2020). Vinton Furnace State Forest. <<http://forestry.ohiodnr.gov/vintonfurnace>>.
- Piironen, J., & Vehtari, A. (2017). Comparison of Bayesian predictive methods for model selection. *Statistics and Computing*, 27, 711–735.
- R Core Team. (2020). R: A language and environment for statistical computing. Version 3.6.1. R Foundation for Statistical Computing, Vienna, Austria. <<https://www.R-project.org/>>.

- Reinert, H. K., Cundall, D., & Bushar, L. M. (1984). Foraging behavior of the timber rattlesnake, *Crotalus horridus*. *Copeia*, 1984, 976–981.
- Reinert, H. K., MacGregor, G. A., Esch, M., Bushar, L. M., & Zappalorti, R. T. (2011). Foraging ecology of timber rattlesnakes, *Crotalus horridus*. *Copeia*, 2011, 430–442.
- Schooler, S. L., & Zald, H. S. J. (2019). Lidar prediction of small mammal diversity in Wisconsin, USA. *Remote Sensing*, 11(19), 2222.
- Simonson, W. D., Allen, H. D., & Coomes, D. A. (2014). Applications of airborne lidar for the assessment of animal species diversity. *Methods in Ecology and Evolution*, 5, 719–729.
- Sperry, J. H., and P. J. Weatherhead. (2009). Does prey availability determine seasonal patterns of habitat selection in Texas ratsnakes. *Journal of Herpetology*, 43, 55–64.
- Sutton, W. B., Wang, Y., Schweitzer, C. J., & McClure, C. J. W. (2017). Spatial ecology and multi-scale habitat selection of the Copperhead (*Agkistrodon contortrix*) in a managed forest landscape. *Forest Ecology and Management*, 391, 469–481.
- Tetzlaff, S. J., Carter, E. T., DeGregorio, B. A., Ravesi, M. J., & Kingsbury, B. A. (2017). To forage, mate, or thermoregulate: Influence of resource manipulation on male rattlesnake behavior. *Ecology and Evolution*, 7, 6606–6613.
- Urban, N. A., & Swihart, R. K. (2011). Small mammal responses to forest management for oak regeneration in southern Indiana. *Forest Ecology and Management*, 261, 353–361.

- Whitaker, P. B., & Shine, R. (2003). A radiotelemetric study of movements and shelter-site selection by free-ranging brownsnakes (*Pseudonaja textilis*). *Herpetological Monographs*, 17, 130–144.
- Williams, A. C., Flaherty, S. E., & Flaxman, S. M. (2013). Quantitative tests of multitrophic ideal free distribution theory. *Animal Behaviour*, 86, 577–586.
- Wittenberg, R. D. (2012). Foraging ecology of the timber rattlesnake (*Crotalus horridus*) in a fragmented agricultural landscape. *Herpetological Conservation and Biology*, 7, 449–461.
- Womble, J. N., Sigler, M. F., & Willson, M. F. (2009). Linking seasonal distribution patterns with prey availability in a central-place forager, the Steller sea lion. *Journal of Biogeography*, 36, 439–451.
- Zuur, A. F., Ieno, E. N., Walker, N. J., Saveliev, A. A., & Smith, G. M. (2009). Mixed effects models and extensions in ecology with R. Springer, New York, New York, USA.

Table 1.1. Fine-scale (5-m) landscape covariates (n = 16) used to describe small mammal spatial distributions in a mixed-use forest in southeastern Ohio. Summary statistics for each continuous variable provide the mean value ( $\pm$  SD) and range of values across 242 camera trap sites.

Type	Variable	Description/Interpretation	Summary Statistics (Mean $\pm$ SD, range)
<b>Forest Management</b>	<b>Presence of burns</b> (Burn)	Presence/absence of burned stands (No. camera sites).	Burns = 31 Non-burns = 211
	<b>Stand age</b> (Age)	Approximate stand age (years), reflecting forest management activity.	72 $\pm$ 47, 4–151
<b>Topography</b>	<b>Beers' transformed aspect index</b> (Beers)	Transforms circular aspect to a range of xeric southwest to mesic northeast aspects.	0.95 $\pm$ 0.69, 0–2
	<b>Elevation</b> (DEM)	LiDAR-derived Digital Terrain Model (m).	258.4 $\pm$ 18.5, 203–292
	<b>Slope</b>	Slope (degrees).	15.3 $\pm$ 7.6, 0–36.9
	<b>Stream distance</b> (Stream)	Distance to the nearest stream (m).	154 $\pm$ 91, 1–381
<b>Multipurpose — Ordination Axes</b>	<b>NMDS axis 1 of floristic variation</b> (NMDS1)	Ordination axis representing a moisture and topographic gradient. Large, negative values represent drier southwestern facing slopes and positive values represent floodplains.	-0.006 $\pm$ 0.236, -0.516–0.981

Continued

Table 1.1 Continued

Type	Variable	Description/Interpretation	Summary Statistics (Mean $\pm$ SD, range)
<b>Multipurpose — Ordination Axes</b>	<b>NMDS axis 2 of floristic variation (NMDS2)</b>	Ordination axis representing a forest structural and successional gradient. Large, positive values are associated with taller canopies and mature forests.	-0.048 $\pm$ 0.199, -0.760–0.420
<b>Vegetation Structure &amp; Composition</b>	<b>Canopy surface height (CHM)</b>	Canopy height model representing the maximum canopy height (m).	16.3 $\pm$ 10.7, 0–40
	<b>MacArthur's Foliage Height Diversity (FHD)</b>	Shannon's diversity of vegetation hits throughout the vertical profile (3 vertical layers, 0–5, 5–25, and >25 m) of each point location.	0.70 $\pm$ 0.26, 0–1.04
	<b>Enhanced vegetation index (EVI)</b>	Vegetation “greenness” or productivity.	0.703 $\pm$ 0.109, 0.095–0.878
	<b>Plant species richness (PSR)</b>	Number of woody plant taxa.	14.6 $\pm$ 1.5, 7.8–18.7
	<b>Overstory density (OVE)</b>	Amount of overstory (i.e., $\geq$ 8-cm DBH) foliage (stems/ha).	18.5 $\pm$ 24.2, 0–132.2
	<b>Understory density (UND)</b>	Amount of understory (<8-cm DBH) foliage (stems/ha).	164.2 $\pm$ 37.9, 41.9–316.6
	<b>Tree density (TDE)</b>	Combined density of overstory and understory size classes of woody plants (stems/ha)	444.7 $\pm$ 130.5, 56.3–954.6
	<b>Skewness of LiDAR returns (SKE)</b>	Skewness of LiDAR returns is expected to be greater (i.e., longer tail) for mature stands compared to younger stands.	0.93 $\pm$ 1.18, -0.06–8.45

Table 1.2. Camera trap (n = 242) daily detections of potential prey items for timber rattlesnakes (*Crotalus horridus*) in a mixed-use forest in southeastern Ohio from 2017–2018. Bird detections include common woodland residents, such as wood thrushes (*Hylocichla mustelina*), ovenbirds (*Seiurus aurocapilla*), and Carolina wrens (*Thryothorus ludovicianus*).

	<b>Sites with ≥ 1 Detection</b>	<b>Sites with &gt; 1 Detection</b>	<b>Maximum Detections (Days)</b>
<b>Mice</b> ( <i>Peromyscus</i> spp.)	148 (61%)	86 (36%)	17
<b>Eastern chipmunks</b> ( <i>Tamias striatus</i> )	89 (37%)	48 (20%)	9
<b>Squirrels</b> ( <i>Sciurus</i> spp.)	70 (29%)	15 (6%)	6
<b>Shrews</b> (Soricidae)	14 (6%)	2 (0.8%)	2
<b>Voles</b> ( <i>Microtus</i> spp.)	1 (0.4%)	0	1
<b>Eastern cottontails</b> ( <i>Sylvilagus floridanus</i> )	25 (10%)	8 (3%)	3
<b>Birds</b>	124 (51%)	65 (27%)	11

Table 1.3. Bayesian zero-inflated (Zi) negative binomial models of mice (*Peromyscus* spp.), chipmunk (*Tamias striatus*), and squirrel (*Sciurus* spp.) encounter rates across 242 camera sites in a mixed-use forest in southeastern Ohio. We modeled the number of camera days with a species detection, offset by the total number of active camera days, as a function of study year (2017–2018) and remotely-sensed landscape variables (5-m resolution). We report the variables that best described each species’ distribution. Mean coefficient estimates, standard errors ( $\pm$  S.E.) and percentage of the posterior distributions overlapping zero are provided. Refer to Table 1.1 for further descriptions of covariates.

	Mice	Chipmunks	Squirrels
<b>Year</b>	0.56 ( $\pm$ 0.17) <1%		1.05 ( $\pm$ 0.31) <1%
<b>Burn</b>	-0.52 ( $\pm$ 0.19) <1%		
<b>Age</b>	-0.09 ( $\pm$ 0.06) 7%		
<b>Slope</b>		0.19 ( $\pm$ 0.09) 3%	
<b>NMDS1</b>			-0.24 ( $\pm$ 0.14) 4%
<b>NMDS 2</b>		0.27 ( $\pm$ 0.10) <1%	0.38 ( $\pm$ 0.17) 1%
<b>PSR</b>		0.23 ( $\pm$ 0.11) 2%	
<b>FHD</b>			-0.41( $\pm$ 0.22) 3%
<b>OVE</b>			0.3 ( $\pm$ 0.14) 2%
<b>UND</b>			-0.4 ( $\pm$ 0.17) 1%
<b>Zi: (Median camera deployment date)<sup>2</sup></b>			-1.52 ( $\pm$ 1.16) 5%
<b>Zi: Year</b>	-3.56 ( $\pm$ 2.09) 1%	-4.02 ( $\pm$ 2.04) 0	1.21 ( $\pm$ 2.8) 30%



Figure 1.1. Characteristic ambush posture of timber rattlesnakes (*Crotalus horridus*) used to identify foraging locations, including (A) foraging at logs and downed woody debris, (B) vertical-tree foraging, and (C) non-log foraging along the forest floor. Snakes maintain a tight, “S”-shaped coil regardless of foraging orientation. Photo credits to B. Hiner and E. Scott.



Figure 1.2. Placement of a camera trap with bait for small mammals one meter above and directly overlooking a log in a mature forest site in southeastern Ohio. (B) *Tamias striatus* and (C) *Peromyscus* spp. captured on camera at this trap site.

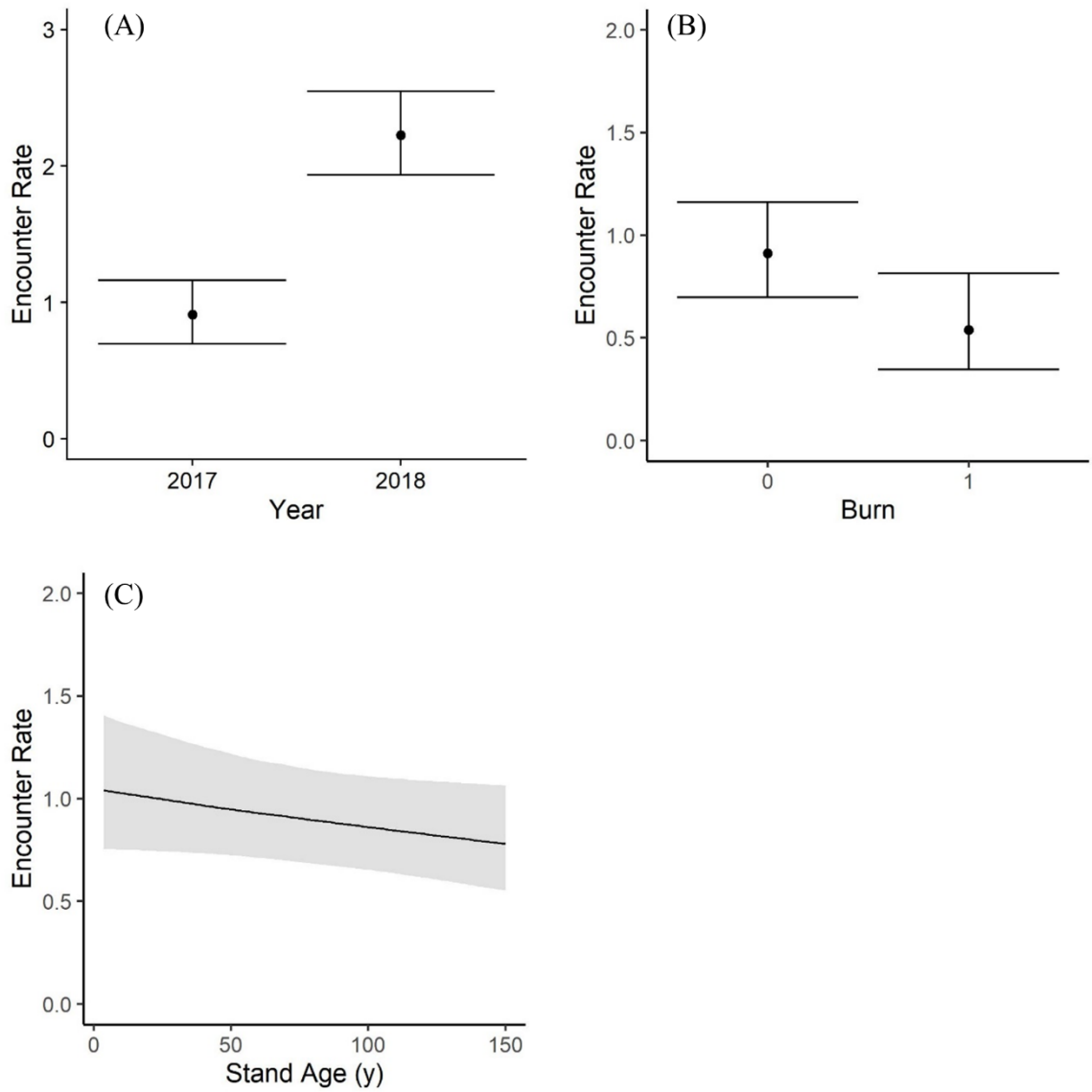


Figure 1.3. Daily estimated mice (*Peromyscus* spp.) encounter rates from 242 camera trap sites distributed in a mixed-use forest in southeastern Ohio.

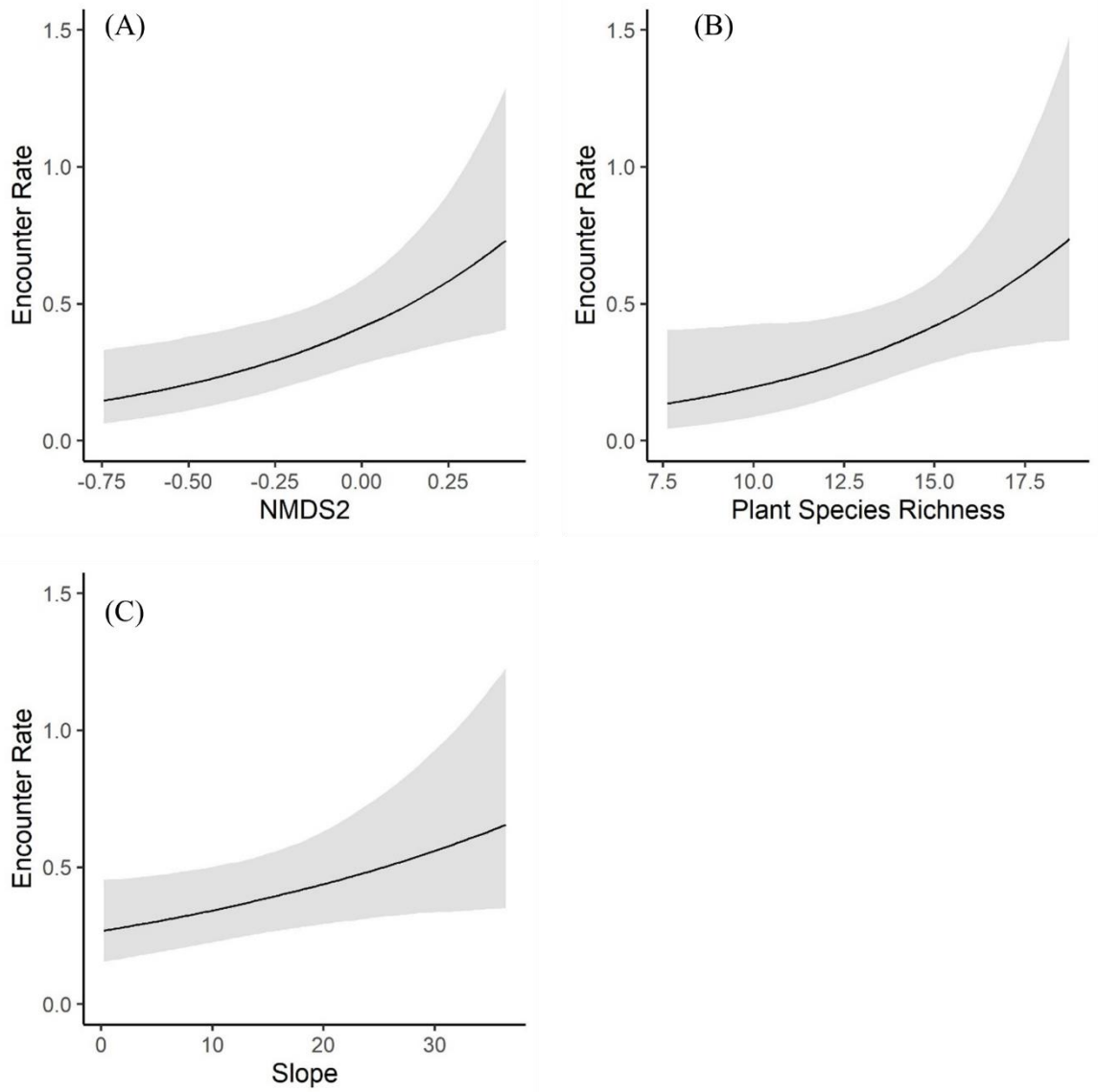


Figure 1.4. Daily estimated chipmunk (*Tamias striatus*) encounter rates from 242 camera trap sites distributed in a mixed-use forest in southeastern Ohio.

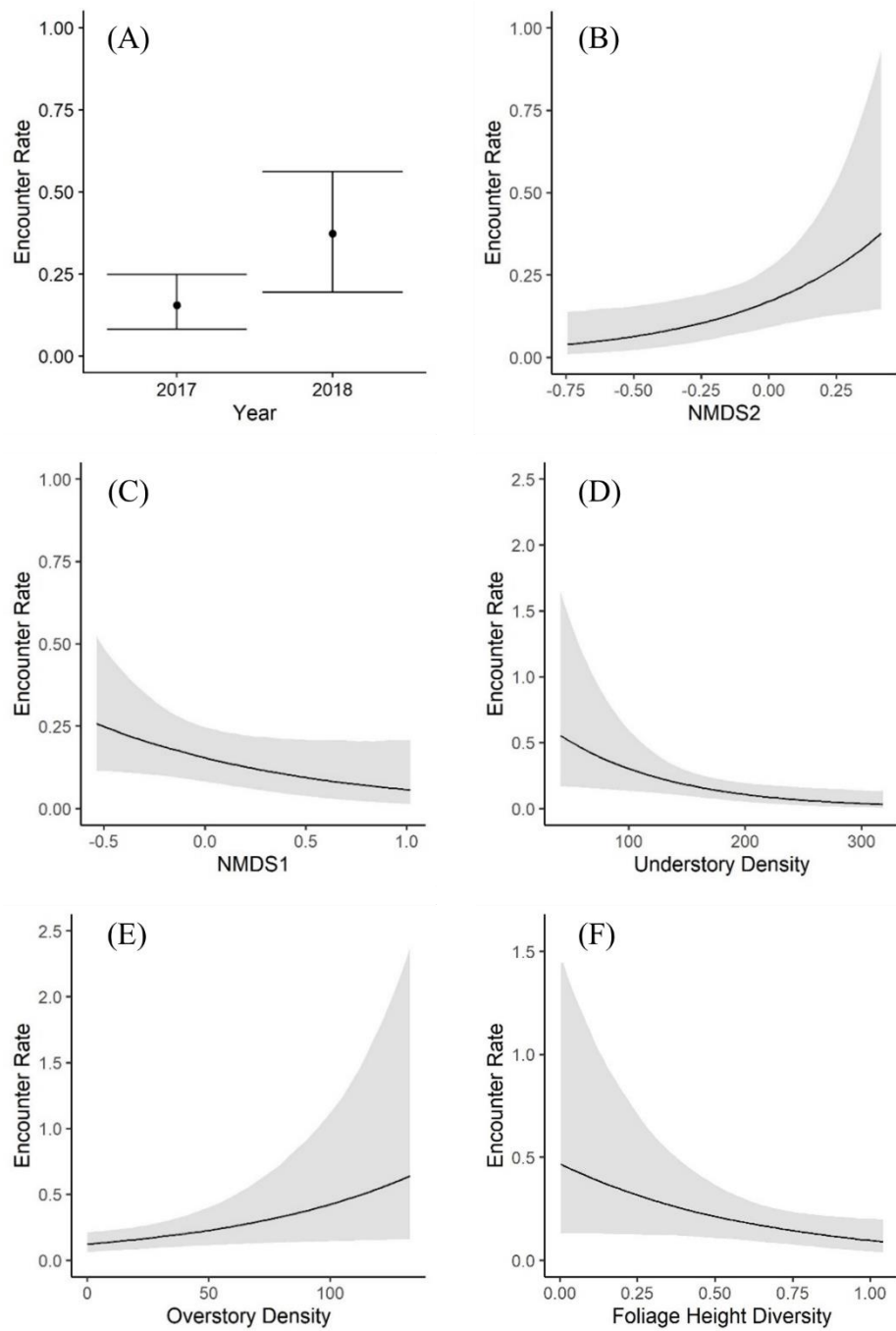


Figure 1.5. Daily estimated squirrel (*Sciurus* spp.) encounter rates from 242 camera trap sites distributed in a mixed-use forest in southeastern Ohio.

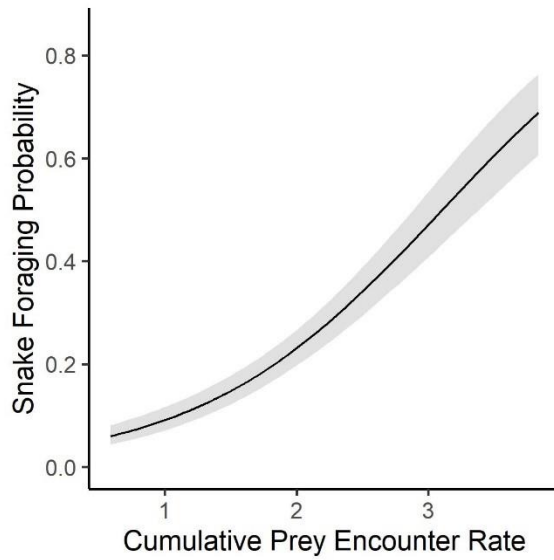


Figure 1.6. Foraging probability of 37 adult timber rattlesnakes (*Crotalus horridus*) in a mixed-use forest in southeastern Ohio predicted by the cumulative contribution of estimated site-specific, daily encounters with mice (*Peromyscus* spp.), chipmunks (*Tamias striatus*), and squirrels (*Sciurus* spp.) from 2016–2019.

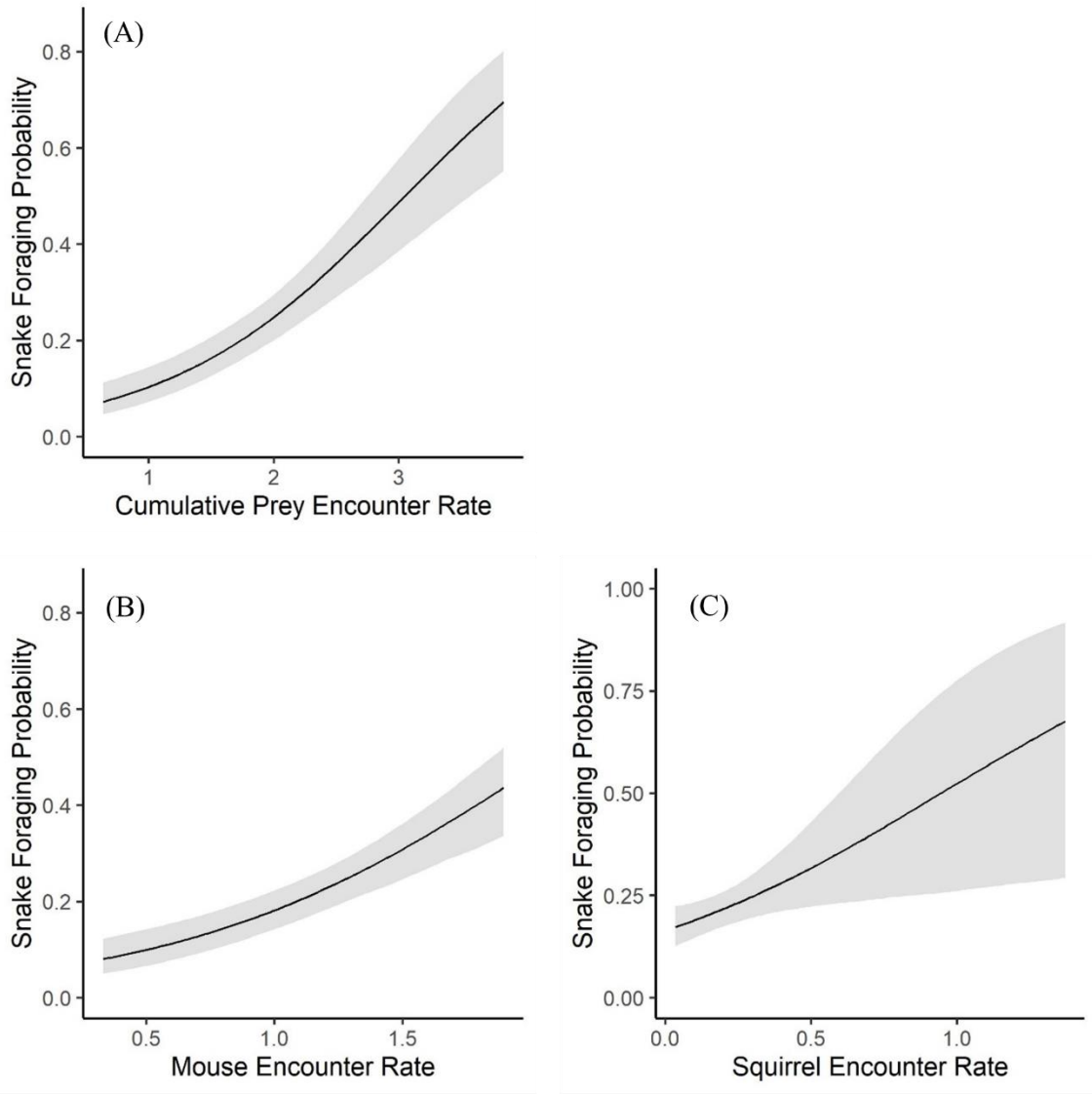


Figure 1.7. Adult female ( $n = 16$ ) timber rattlesnake (*Crotalus horridus*) foraging probabilities in a mixed-use forest in southeastern Ohio predicted by prey encounter rates from 2016-2019. A) Cumulative Prey encounter rate, representing the additive combination of mouse (*Peromyscus* spp.), chipmunk (*Tamias striatus*), and squirrel (*Sciurus* spp.) site-specific encounter rates; B) mice-specific encounter rate; and C) squirrel-specific encounter rate.

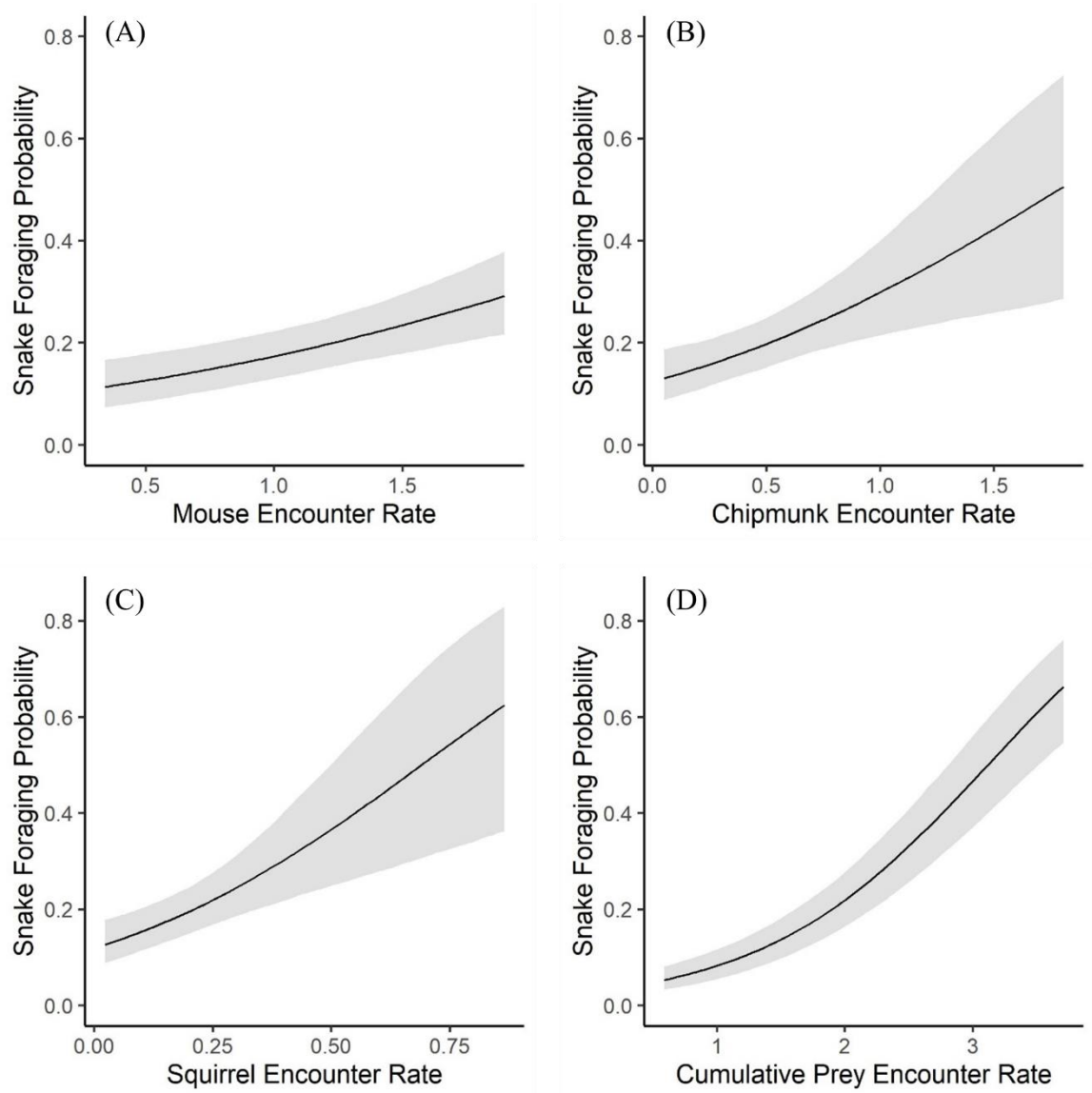


Figure 1.8. Adult male ( $n = 21$ ) timber rattlesnake (*Crotalus horridus*) foraging probabilities in a mixed-use forest in southeastern Ohio predicted by prey encounter rates from 2016-2019. Prey-specific foraging models include encounters with A) mice (*Peromyscus* spp.), B) chipmunks (*Tamias striatus*), and C) squirrels (*Sciurus* spp.). D) Cumulative Prey encounter rate, representing the additive combination of mouse, chipmunk, and squirrel site-specific encounter rates.

## Chapter 2. Multi-scale Effects of Snake Fungal Disease on Individual Behavior and Space Use in Timber Rattlesnakes

### Abstract

Emerging mycoses pose a significant threat to wildlife populations. However, sub-lethal effects of fungal pathogens on hosts, such as inducing atypical behavior and space use, are not commonly addressed. Snake fungal disease (SFD) is caused by *Ophidiomyces ophiodiicola* and is associated with a suite of symptoms that can range in severity, but typically results in mild skin lesions that can be resolved with ecdysis. Infection with SFD may drive snakes to select warmer areas of the landscape for thermoregulation, but also push snakes towards ‘risky’ behaviors, such as basking in open-canopy habitat (increased predation risk) and increased surface activity during colder months (increased exposure risk). We radio-telemetered and assessed the SFD infection status of 41 timber rattlesnakes (*Crotalus horridus*) in southeastern Ohio between 2016 and 2019. We examined individual-level effects of SFD infection on 15 snakes that each exhibited at least one ‘healthy’ year and at least one SFD-symptomatic year. We monitored outcomes of SFD infection on snake body temperature, behavior, movement, site use, and home ranges. Snakes increased their maximal home range area (100% minimum convex polygon [MCP]) and doubled their core home range area (50% MCP) when infected. However, we did not observe a concurrent increase in the rate of movement during infected years. Snakes were more likely to select sites closer to streams

during infection, most likely to access high humidity conditions and mitigate evaporative water loss. During symptomatic years, snakes selected sites with greater solar exposure, but only exhibited elevated body temperatures during the fall, likely due to increased surface activity at the end of the active season. We additionally found sex-specific effects of SFD on snake behavior and habitat use. Symptomatic females rested more and foraged less frequently than expected, while symptomatic males rested less and foraged more frequently than expected. Females were more likely to use dry, southwestern-facing, high elevation sites in early seral stands, conditions favorable to thermoregulation, during symptomatic years. Understanding shifts in the habitat use of individuals across different physiological or behavioral states is particularly important for informing habitat requirements of this and other imperiled species.

## Introduction

Emerging infectious diseases are increasingly recognized as a global threat to wildlife populations and biodiversity (Fisher et al., 2012). Fungal pathogens specifically have become more prevalent and have received greater scrutiny in recent decades, perhaps because of changes in temperature and precipitation patterns associated with climate change (Lorch et al., 2016). An upsurge in the occurrence of fungal pathogens has been linked to dramatic population declines in bats with white-nose syndrome (Blehart et al., 2009), amphibians with chytridiomycosis (Skerratt et al., 2007), and snakes with snake fungal disease (hereafter, SFD; Clark et al., 2011).

Pathogens can also impose fitness consequences to wildlife populations without contributing directly to mortality (Agugliaro et al., 2019). Considering that individuals have limited energy and time to devote to physiological or behavioral functions, energy-allocation trade-offs (EATOs) represent sublethal effects by which pathogens can affect hosts (Lind et al., 2019). The impact of EATOs can scale from individual physiology to behavior, space use, and fitness-related metrics. For example, resolving an active infection can be energetically costly and suppress reproductive behavior (Lind et al., 2019) or reduce locomotion capacity (Tetzlaff et al., 2017). However, individual outcomes and the resiliency of infected free-ranging animals are relatively understudied in wildlife disease (Scheele et al., 2014), particularly for infections that rarely result in direct mortality and are likely to be resolved (Lind et al., 2018).

Snake fungal disease, caused by the fungus *Ophidiomyces ophiodiicola* (hereafter, *Oo*), often results in mild cases of dermatitis that can be cleared by ecdysis (i.e. shedding; Allender et al., 2015b; Lorch et al., 2016). Minor skin lesions, such as scale abnormalities and scabs, are typical of the disease (Figure 2.1), but symptoms can range in severity depending on the location of the lesions (Baker et al., 2019). Lesions on the eyes, loreal pit (in pit vipers), or cloaca can cause disfigurement and interfere with essential physiological functions (Baker et al., 2019). Severe cases of SFD may also require successive bouts of ecdysis to effectively eliminate the fungus, which could be energetically costly (Dupoué et al., 2015). For some snake populations, SFD infection patterns appear to be cyclical and chronic (Lorch et al., 2016; McCoy et al., 2017), with infection severity peaking in cooler months, ebbing in warmer months, and individual

infection status and severity fluctuating annually (Lind et al., 2018). Transmission of SFD can occur through contact with *Oo* in the environment or other infected individuals, making species that use communal hibernacula particularly vulnerable to infection (Long et al., 2019). For these populations overwintering in refugia, individuals are likely to exhibit new symptoms post-egress, typically recover during summer months, but potentially experience a resurgence of symptoms during the cooler months of fall if the infection has not resolved (Lorch et al., 2016).

Pathogens often impair physiological performance of hosts and can significantly affect individual space use and the overall spatial organization of wildlife populations (Binning et al., 2017; Brandell et al., 2020). In response to an infection, ectotherms can raise their core temperature above its normal range by moving to warmer habitat areas, referred to as behavioral fever (Richards-Zawacki, 2010; Rakus et al., 2017). Behavioral fever provides a mechanistic link between disease, physiology, behavior, and space use in ectotherms. Infection by *Oo* initiates a physiological cascade of events in snakes, including a mobilized immune response, an increased frequency of ecdysis, and elevated baseline metabolic rate (Lorch et al., 2015; Agugliaro et al., 2019), which are most efficiently performed at warmer temperatures. These physiological processes are energetically costly (Dupoué et al., 2015; Agugliaro et al., 2019), likely necessitating time-energy allocation away from other essential functions such as foraging and reduced movement (Tetzlaff et al., 2017). Infected snakes tend to select open-canopy, exposed sites to efficiently raise their body temperature, sometimes during inopportune periods that healthy snakes would not be active (Lorch et al., 2015). Thus, these conditions may

also predispose infected snakes to additional forms of mortality, such as predation or exposure (Lorch et al., 2016).

Assessing habitat use across different physiological or behavioral states is particularly important for understanding the comprehensive habitat requirements of imperiled species. To our knowledge, no study has monitored SFD infection outcomes, and consistency of behavior, habitat, and space use of individual snakes across years. We examined multi-scale effects of SFD infection on timber rattlesnakes (*Crotalus horridus*; hereafter, TRS) through a behavioral and spatial lens (Figure 2.2). Multi-year monitoring of snakes enabled us to track physiological/behavioral status, SFD presence, and space use in individuals over time, and make individual-level comparisons in spatial parameters. We predicted that snakes with SFD would maintain elevated body temperatures across the active season, spend more time in ecdysis or rest compared to foraging or digestion, move less frequently, select sites conducive for optimal thermoregulation, and exhibit smaller home range areas relative to years that they were healthy.

## Methods

### *Radiotelemetry*

We radio-tracked 41 telemetered snakes 2–3 times per week between 2016 and 2019 as part of an on-going study. At every snake location, we classified behavior into five behavioral categories: gestation, ecdysis, digestion, foraging, and resting. We verified that females were gravid by sonogram in early spring. We noted locations

preceding ecdysis when snakes developed blue or cloudy eyes and a dull, dusky skin color. We noted digestion locations when we observed a snake with a food bolus. However, we infrequently detected snakes digesting meals and these observations are likely biased towards snakes digesting larger meals. We identified foraging behavior following previous descriptions of stereotyped ambush posture (Reinert et al., 2011). When snakes did not clearly exhibit the four other distinct behaviors, and were not actively moving, we designated snake behavior as “resting.” We also recorded microhabitat variables for snake locations (described below in Thermal regime).

#### *SFD classification*

We evaluated each snake for SFD symptoms each spring (April–June) and fall (August–September). We recorded clinical signs of SFD infection, such as the presence of scale abnormalities, scabs, and necrotic scales (Baker et al., 2019; Figure 2.1). We then used cotton-tipped applicators to swab TRS skin thoroughly across the body on dorsal, lateral, and ventral surfaces, and around the eyes and loreal pits, paying particular attention to any observable lesions on each individual. Individual applicators were analyzed for the presence of *Oo* DNA with quantitative polymerase chain reaction (qPCR), reported per  $\mu\text{g}$  of total DNA (Allender et al., 2015a). A negative *Oo* test could result from true absence of the pathogen, poor DNA quantity of the sample from inadequate swabbing or low prevalence of *Oo* DNA on the epidermis, or poor quality of the sample due to DNA degradation.

Annual presence of the fungal pathogen from skin swabs did not strongly correlate with clinical signs of SFD infection (Pearson’s  $r = 0.44$ ) in our population.

Hileman et al. (2018) also found a high false negative probability (0.73) associated with *Oo* qPCR of one skin-swab applicator for snakes that exhibited clinical signs of SFD infection. We therefore classified yearly infection status based on both qPCR test results and observed lesions, resulting in four potential yearly infection designations (Table 2.1). Snakes ‘presumed healthy’ were asymptomatic and tested negative for *Oo*; snakes considered ‘possibly infected’ were asymptomatic but tested positive for *Oo* at least once during a particular year; snakes ‘presumed infected’ were symptomatic (i.e. lesions present) but tested negative for *Oo* or were not tested in a particular year; snakes considered ‘infected’ exhibited clinical symptoms of SFD infection and tested positive for the presence of *Oo* (Table 2.1).

#### *Individual-level Analyses*

Previous studies have found moderate rates (15–38%, on average) of terrestrial snakes with no discernible clinical symptoms testing positive for the presence of *Oo* DNA (Hileman et al., 2018; McKenzie et al., 2019). These individuals may only be carriers of the pathogen or may be in early infection stages (McKenzie et al., 2019). Therefore, we collapsed the four yearly infection designations (Table 2.1) into a binomial SFD infection status of ‘asymptomatic’ (Categories 0–1) or ‘symptomatic’ (Categories 2–3). We selected 15 snakes ( $n = 9$  males and 6 non-gravid females) that we monitored for at least one asymptomatic year and one symptomatic year to analyze the effects of SFD infection on behavior, movement, habitat use, and home ranges.

#### *Spatial Ecology*

**Home range**—We calculated 50%, 95% and 100% minimum convex polygons (MCP) in the ‘adehabitatHR’ package in R (Calenge, 2020). We considered the MCP to be the best descriptor of home range size in this population due to the relatively coarse resolution of radio-telemetry relocations (one–three relocations per week) in this study. Preliminary home range analyses for this population have shown that fixed and autocorrelated kernel density methods may overestimate home range area (unpublished data). We assessed generalized linear mixed effects models at each home range MCP scale. We modeled home range area as a function of SFD infection status and sex, with individual snakes modeled as random effects. We tested for both additive and interactive effects of infection status with sex, and log-transformed home range area prior to analyses to reduce skewness.

**Movement patterns**—We analyzed movement characteristics of snakes between asymptomatic and symptomatic years with step length and net squared displacement in the ‘amt’ package in R (Signer et al., 2019). We calculated movement rate as step length divided by lag time between relocation days. We summarized mean, median, and max movement rate, mean and max net squared displacement, and cumulative step lengths for each snake per year. We used principal component analysis (PCA) to reduce annual movement parameters to fewer, representative linear combinations of the variables. We examined mean movement rate, median movement rate, cumulative step lengths, max net squared displacement, mean net squared displacement, 50% MCP, 95% MCP, and 100% MCP. All variables were positively correlated above 0.4. We assessed each variable for outliers and univariate normality and performed log or square-root transformations of

variables when necessary. We assessed multivariate normality, skewness, and kurtosis with the Mardia-Test in the ‘mvn’ package in R (Korkmaz et al., 2014). We used the size of eigenvalues and the proportion of variability in data explained by each principal component to determine the number of relevant principal component axes for interpretation. We assessed principal component scores of individuals with multivariate ANOVA (MANOVA), including an interaction of sex and infection status, and a random effect of individual snakes.

**Behavior**—We examined potential shifts in the frequency of observed behaviors (ecdysis, digestion, foraging, and resting) for males and females during SFD infection with a chi-squared test. To determine the parameters most different from expected frequencies, we calculated the contribution of any given cell to the chi-square statistic with  $\frac{r^2}{\chi^2}$ .

**Site use**—We used thirteen geospatial (5-m resolution) forest structural, landscape, and topographic metrics to examine site selection differences during SFD symptomatic years. Previous work from this population has shown that landscape conditions selected for foraging contrast with landscape characteristics of sites selected for other behaviors, such as ecdysis and digestion (Hoffman et al., 2020, in review). We therefore excluded foraging locations to permit direct assessment of behavioral site selection driven by thermoregulatory needs. We modeled the probability of site use by SFD symptomatic snakes as a Bernoulli variable against sites selected when snakes were asymptomatic of SFD. We considered mixed effects models in a Bayesian framework to

assess potentially distinctive landscape and forest structural characteristics associated with SFD for each sex, with individual snakes included as random effects.

### *Thermal regime*

**Body Temperature**—Between 2017 and 2019, we used a digital laser infrared thermometer to record snake external body temperatures and temperatures of the substrate adjacent to a snake in both sunspots and shaded areas. We also implanted intraperitoneal RFID WeePits (Alpha Mach WeeTag) to a subset of snakes ( $n = 9$ ) in 2017 to record hourly internal body temperatures. To account for missing external snake temperatures for 2017 ( $n = 125$  observations), we regressed external snake body temperatures against the corresponding hourly internal body temperature for each available snake ( $n = 46$  observations). We rounded down to the nearest hourly internal temperature for snake observations between minutes 00–15, we took the average of two hourly temperatures for snake observations between minutes 16–29, and we rounded internal temperatures up to the value at the nearest hour for snake observations between minutes 30–59. We scaled and centered new data ( $n = 125$  observations) based on the mean and standard deviation of the training dataset and predicted external body temperatures from the recorded internal body temperature.

We modeled external snake body temperatures as a function of additive or interactive combinations of SFD status and season. We assigned seasons of observations by examining similarities in snake body temperature profiles among months (Figure B.1). We classified spring as April–June, summer as July–August, and fall as September–October.

**Canopy cover and solar insolation**—We recorded canopy cover above a snake's location with a densiometer in 2016. We used fisheye lens attachments for smart phones in 2017–2019 to assess canopy cover with hemispherical photos at a subset of snake locations. We took each canopy photo one-meter above-ground, with the phone positioned level, faced towards due north, and pointed towards the forest canopy above the snake's location. We analyzed field-derived hemispherical photos of the forest canopy to estimate proportion cover and generate corrected solar insolation estimates for each snake location. Prior to analyses, we eliminated any canopy photos that were out of focus or contained pixels that were over or under-exposed. We also eliminated photos that contained obstructions to the canopy or sun flares. We used functions from the image analysis packages 'EBImage' and 'ImageJ' to binarize the images in R (Pau et al., 2010). From the binarized images, we calculated the proportion of canopy pixels to all pixels (vegetation and sky) for each canopy photo. We used a 3-m digital elevation model (<https://www.usgs.gov/core-science-systems/national-geospatial-program/national-map>) to estimate the monthly average of solar insolation (kWH/m<sup>2</sup>) from half-hour samples for each location during the location's associated month and year of observation. We calculated the insolation value (INS) corrected by observed canopy cover proportion (PCAN) for each location as:  $CSI = INS * (1 - PCAN)$ .

To determine whether SFD symptomatic snakes select sites with greater solar exposure, we modeled CSI as a function of additive or interactive combinations of SFD symptomatic status and season, and random effects of month of observation and individual snake. We square-root transformed CSI prior to analyses to improve

normality. We modeled seasonal and monthly effects of accumulated solar insolation to account for greater solar exposure in the spring (April–June) than fall (September–October) of each year. We analyzed corrected solar insolation (CSI) for 730 TRS locations between 2016–2019.

### *Statistical Analyses*

We used the ‘brms’ package in R to fit all statistical models (Bürkner 2017). We examined model coefficients for their magnitude of effect in each selected global model and removed covariates with no or a negligible effect, removed covariates with >15% posterior distribution overlap with zero, and removed covariates with >20% of the posterior within the Region of Practical Equivalence (ROPE; Piironen & Vehtari, 2017). We considered the resulting model with the lowest leave-one-out statistic (LOO) to be the most parsimonious.

## Results

### *SFD classifications*

We monitored seven of fifteen snakes for three years. Of these individuals, we monitored five snakes for one asymptomatic year and two symptomatic years, and two snakes for two asymptomatic years and one symptomatic year. We tracked the remaining eight snakes for two years, each representing an asymptomatic year and a symptomatic year.

### *Spatial Ecology*

**Home range**—Mixed effects models of home range area generated sex-specific and home range scale-specific results (Table 2.2). Sex had the greatest effect on home range area across all scales, with male home ranges scaling larger than female home ranges (Table 2.2). Mean home range area increased for both sexes between asymptomatic and symptomatic years at the 50% and 100% MCP scales, but this pattern was only apparent for female home ranges at the 95% scale (Figure 2.3). We found the greatest effect of SFD infection status on home range size for both sexes at the 50% MCP scale (Table 2.2). The best-supported model at the 50% MCP scale was an additive combination of SFD status and sex (Table B.1). Infection status strongly predicted home range area ( $0.59 \pm \text{SE } 0.29$ ; Table 2.2). The mean home range area for males and females increased approximately 1.8 times during SFD symptomatic years (Figure 2.3A, 2.3D). Male home range size increased from 6.4 ha (95% CI: 3.2–13.3 ha) when asymptomatic of SFD to 11.6 ha (95% CI: 5.9–23.2 ha) during SFD symptomatic years (Figure 2.3D). Female home range size increased from 2.5 ha (95% CI: 1.1–5.9 ha) when asymptomatic of SFD to 4.5 ha (95% CI: 1.9–10.5 ha) during SFD symptomatic years (Figure 2.3A).

We observed the weakest effects of SFD infection on home range area at the 95% MCP scale (Table 2.2). The best-supported model for 95% MCPs was an interaction of sex and SFD status (Table B.1). The effect size of the SFD by sex interaction was  $0.49 \pm \text{SE } 0.38$  (Table 2.2). Male home range size was unaffected by SFD status, but female home range area increased 1.8 times with SFD infection (Figure 2.3B, 2.3E). Female home range area increased from 6.6 ha (95% CI: 3.1–14.8 ha) when snakes were unaffected by SFD to 11.9 ha (95% CI: 5.5–25.2 ha) during SFD symptomatic years,

although credible intervals were large (Figure 2.3B). At the 100% MCP scale, the best-supported model was an additive combination of SFD status and sex (Table B.1).

Infection status had an effect size of  $0.38 \pm \text{SE } 0.19$  (Table 2.2). Mean home range area for males increased 47% with SFD, from 36.3 ha (95% CI: 20.3–66.1 ha) during asymptomatic years to 53.4 ha (95% CI: 30.4–94.2 ha) during SFD symptomatic years (Figure 2.3F). Mean home range area for females increased 47% with SFD, from 8.7 ha (95% CI: 4.2–18.1 ha) during asymptomatic years to 12.8 ha (95% CI: 6.2–25.9 ha) during symptomatic years (Figure 2.3C).

**Movement patterns**—We did not detect a systematic change in any individual movement metric with SFD infection status. The movement PCA separated the eight movement metrics into two representative principal components (PC), which accounted for a cumulative 89.8% of the variance (Table B.2). The first PC alone accounted for 81.1% of the variance (Table B.2). Every metric contributed approximately equally to PC1, with median movement rate represented the least (axis loading of 0.29) and 95% and 100% MCPs contributing the most (axis loadings of 0.38) and scaling highest on PC1 (Table B.3; Table B.4). Further, PC1 correlated strongly with the 95% and 100% MCPs (Pearson's  $r = 0.97$ ). Principal Component 2 accounted for 8.7% of the variance in movement. Median movement rate primarily contributed to PC2 (axis loading of 0.77), followed by mean net squared displacement (axis loading of -0.41), and mean movement rate (axis loading of 0.33; Table B.3). No variable other than median movement rate (Pearson's  $r = 0.64$ ) was correlated with PC2 at  $r > |0.3|$ .

We observed sex-specific patterns within the movement gradients. Individual males did not exhibit a consistent trend in PC scoring with SFD infection (Figure 2.4A). However, individual females tended to score more positively on PC1 with infection and reduce their scores on PC2 with infection (Figure 2.4B). Overall, females scaled negatively on PC1 and males tended to scale positively because of their larger home ranges (Figure 2.4C). Accordingly, sex accounted for the most variation in PC1 scores ( $-4.16 \pm \text{SE } 1.20$ ), followed by the interaction of SFD status and sex ( $1.45 \pm \text{SE } 0.91$ ; Table 2.3). The interaction of SFD status and sex had the greatest effect ( $-0.68 \pm \text{SE } 0.52$ ) on PC2 (Table 2.3). Between infection states, PC1 scores increased (Figure 2.5A) but PC2 scores decreased for females, suggesting that females increased their home range size and displacement but reduced their overall movement rates when symptomatic (Figure 2.5B). The mean PC1 score for females increased from  $-2.9$  (95% CI:  $-4.8$ – $1.0$ ) when asymptomatic to  $-1.58$  (95% CI:  $-3.4$ – $0.2$ ) when symptomatic. The mean PC2 score for females declined from  $0.3$  (95% CI:  $-0.4$ – $1.1$ ) when asymptomatic to  $-0.24$  (95% CI:  $-0.96$ – $0.5$ ) when symptomatic, but with wide and partially overlapping credible intervals (Figure 2.5B). Males did not exhibit shifts in either principal component metric when they were symptomatic (Figure 2.5).

**Behavior**—We observed nonrandom behavioral frequencies by snakes ( $\chi^2 = 39.1$ ,  $\text{df} = 9$ ,  $p < 0.05$ ), with sex-specific shifts in time spent performing particular behaviors during infection (Table 2.4). Females spent more time resting when symptomatic (69% frequency) than asymptomatic (54%), less time foraging when symptomatic (16% vs. 27% frequency), and less time digesting meals when symptomatic

(3% frequency) than asymptomatic (7% frequency; Table 2.4). Conversely, males spent less time resting when symptomatic (53%) than asymptomatic (64%), more time foraging when symptomatic (25% vs. 16% frequency), but digested meals at approximately the same frequency (5-6%; Table 2.4). Both sexes underwent ecdysis at approximately the same frequency between asymptomatic and symptomatic years (Table 2.4). However, we observed males in ecdysis marginally more frequently (16%) than expected (14.4%; Table 2.4)

**Site use**—Site use patterns for symptomatic snakes differed strongly by sex. Female symptomatic site use could be predicted by many landscape metrics, but male site use was weakly predicted by only two of these (Table 2.5). Only distance to nearest stream predicted symptomatic site use for both sexes, with infected snakes more likely to occupy sites closer to streams (Table 2.5). Stream distance also had a greater magnitude of effect on female site use than males (Table 2.5). From the most parsimonious model of site use by symptomatic females (Table B.5), stream distance ( $-0.58 \pm 0.16$ ), stand age ( $-0.56 \pm 0.19$ ), NMDS1 ( $-0.47 \pm 0.15$ ), and NMDS3 ( $0.42 \pm 0.16$ ) had the greatest effects on site use (Table 2.5). Symptomatic females were most likely to be observed closer to streams and in younger stands on drier, southwestern-facing slopes (Figure 2.6). The probability of site use for an infected female peaked at 0.85 (95% CI: 0.57–0.96) for sites closest to streams compared to a probability of 0.35 (95% CI: 0.11–0.69) for sites farthest from streams (351.5 m; Figure 2.6A). Infected females were also more likely to occupy early seral forest stands (0.83; 95% CI: 0.53–0.96) compared to mature stands (0.49; 95% CI: 0.19–0.78; Figure 2.6B). The probability of site use for an SFD-symptomatic female

steeply declined from 0.86 (95% CI: 0.57–0.97) at negative scores on the NMDS1 gradient (indicating drier conditions such as ridgetops and southwestern-facing slopes) to a minimum of 0.21 (95% CI: 0.04–0.59) at positive NMDS1 scores indicative of floodplains and bottomlands (Figure 2.6C). The positive association of infected female site use with NMDS3 corroborated their preference for western-facing locations and higher elevations (Figure 2.6D).

The most parsimonious model of symptomatic male site use included stream distance and Beers' transformed aspect (Table B.5). However, these metrics weakly predicted site use by an infected snake (Table 2.5). Symptomatic males were marginally more likely to occupy sites closer to streams and on northeast-facing slopes (Table 2.5). Symptomatic male site use peaked at 0.66 (95% CI: 0.48–0.80) at sites closest to streams and declined to 0.44 (95% CI: 0.27–0.63) at sites most distant from streams. Infected males were also slightly more likely (0.66; 95% CI: 0.49–0.80) to occupy northeast-facing sites than southwest-facing sites (0.47; 95% CI: 0.30–0.63) on Beers' transformed aspect index.

#### *Thermal regime*

**Body Temperature**—Internal snake body temperatures corresponded strongly with external snake body temperatures, allowing for precise estimates of missing external snake body temperatures (Figure B.2). The most-supported model of variation in external snake body temperatures included an interaction of SFD status and season of observation (Table B.6). Without considering seasonal effects, overall snake body temperature declined with SFD infection, but by less than a degree of difference ( $-0.75 \pm \text{SE } 0.48$ ;

Table 2.6). Overall, the range of snake body temperatures was similar between spring and summer, but the range was significantly lower for snakes in both infection statuses during the fall ( $-3.56 \pm \text{SE } 1.57$ ; Table 2.6). We also observed the greatest difference in snake body temperature between asymptomatic and symptomatic years in the fall ( $2.91 \pm \text{SE } 0.85$ ; Table 2.6). Mean snake body temperature during the fall increased from  $21.8^{\circ}\text{C}$  (95% CI:  $19.4\text{--}24.2^{\circ}\text{C}$ ) during asymptomatic years to  $24.0^{\circ}\text{C}$  (95% CI:  $21.7\text{--}26.3^{\circ}\text{C}$ ) in symptomatic years (Figure 2.7).

**Canopy cover**—The most parsimonious model of CSI included additive SFD infection status and season of observation, with month of observation and individual snake as random effects (Table B.7). Symptomatic snakes tended to occupy sites with slightly greater solar exposure than asymptomatic snakes ( $0.57 \pm \text{SE } 0.34\text{--}0.80$ ; Table 2.7). Across both infection statuses, corrected solar insolation was approximately equivalent between spring and summer, but significantly lower in the fall ( $-2.07 \pm \text{SE } 0.65$ ; Table 2.7). During spring months, CSI increased marginally from  $52.3 \text{ kWh/m}^2$  (95% CI:  $39.8\text{--}66.6 \text{ kWh/m}^2$ ) during asymptomatic years to  $60.9 \text{ kWh/m}^2$  (95% CI:  $47.3\text{--}76.0 \text{ kWh/m}^2$ ) during symptomatic years (Figure 2.8). During fall months, CSI increased marginally from  $26.6 \text{ kWh/m}^2$  (95% CI:  $16.5\text{--}39.5 \text{ kWh/m}^2$ ) during asymptomatic years to  $32.8 \text{ kWh/m}^2$  (95% CI:  $21.6\text{--}46.8 \text{ kWh/m}^2$ ) during symptomatic years (Figure 2.8).

## Discussion

Alternative disease outcomes, such as EATOs, are less commonly examined but tend to focus on physiological metrics (e.g., glucocorticoids or body condition) that serve as fitness surrogates (Lind et al., 2018). However, it is imperative to link physiological processes to other domains and disciplines such as behavior, space use, and survival or reproduction effort to effectively scale physiological phenomena to population responses (Ames et al., 2020). We compared behavior, movement patterns, habitat use, and home ranges among years that snakes were asymptomatic or symptomatic of SFD and found evidence for altered space use during SFD infection. Females tended to be most affected by SFD across all examined metrics, but particularly in home range size, movement patterns, and site use.

Infected snakes generally increased their home range size, displacement, and cumulative step lengths, but moved at slower rates (Figure 2.4C). Tetzlaff et al. (2017) also found SFD infected eastern massasauga rattlesnakes (*Sistrurus catenatus*) to move less frequently across the active season than uninfected snakes. Therefore, minimizing the regularity of movement and the energetic costs of locomotion are likely EATO compromises when infected (Binning et al., 2017). Infrequent, long-distance movements could account for the comparable or larger home range areas that we observed at the 95% or 100% MCP scale and concurrent reduction in overall movement rate. However, we observed the largest effect of SFD infection for both sexes at the 50% MCP scale, where rare, long-distance movements would not be detected. It is important to note that home range metrics such as MCPs do not account for temporal variation in movement, but

instead measure the most concentrated centers of movement activity. This difference in movement pattern assessment explains the separation of movement distance measures (PC1), such as MCPs, cumulative step lengths and displacement, from movement rate measures (PC2) in the PCA.

Females increased their home range size at all MCP scales (50%, 95%, and 100% MCP) with infection (Figure 2.3A–C), but males only increased their home range area at the 50% and 100% MCP levels (Figure 2.3D, 2.3F). We believe the disparity in home range patterns with SFD is due to natural variation in the scale of movement between males and females. During asymptomatic years, male home ranges were on average 5.8 times larger than female home ranges at the 95% scale. Females therefore had greater movement potential than males, whereas males may approach their maximum movement capacity during healthy years. Breeding season movements (July–August) typically account for large-scale movements by healthy males (Waldron et al., 2006). When severely symptomatic, we did not observe males breeding (A. Hoffman, pers. comm.), but breeding is also a rarely observed behavior. Importantly, symptomatic male home ranges at the 95% MCP scale were equivalent in size to asymptomatic home range area (Figure 2.3E). Thus, males maintained large home ranges when symptomatic despite potentially not breeding during those years. The fitness implications of infected snakes expending comparable or additional energy towards movement and habitat selection, particularly when in a compromised condition are unknown (Mccoy et al., 2017; Agugliaro et al., 2019).

We observed distinct and contrasting behavioral shifts for both sexes associated with SFD infection (Table 2.4). Females spent more time resting than foraging or digesting when symptomatic while males spent more time foraging than resting when symptomatic. Reduced overall activity (i.e. greater rest time) for symptomatic females coincides with their lower movement rates and infrequent, but long-distance movements. Given that symptomatic females foraged less frequently than expected, their site choice is also more likely to be guided by thermoregulatory needs rather than the distribution of prey. In contrast, we found males in ambush posture more frequently than expected during symptomatic years. We also observed an equivalent frequency of digestion observations between asymptomatic and symptomatic years in males, suggesting that symptomatic males potentially needed to exert more time/effort foraging to successfully obtain meals. Lind et al. (2017) did not examine foraging effort (time spent foraging) but found a negative trend between SFD infection severity and foraging success (proportion of captures with a food bolus) in pigmy rattlesnakes (*Sistrurus miliarius*). The potentially lower foraging efficiency of symptomatic males could in turn be the result of males foraging in sub-optimal areas for prey availability or during seasons or years with lower prey abundance (Chapter 1). We observed males in ecdysis marginally more frequently than expected (Table 2.4), but we did not find strong evidence for increased time spent in ecdysis with SFD infection for both sexes. This apparent contradictory finding for the prevalence of ecdysis could be due to the longer duration of ecdysis (1–2 weeks) relative to short-term behaviors such as foraging or resting, making it easier to incompletely

characterize the duration of the behavior (e.g., record a snake as resting as opposed to ecdysis).

Snakes make behavioral adjustments to access optimal thermoregulatory conditions for physiological performance (Dupoué et al., 2015). Infected snakes may seek out sites with ideal thermoregulatory conditions and return periodically to these areas, accounting for larger home ranges at the 50% MCP scale during infection. Symptomatic females selected specific landscape characteristics potentially to facilitate basking and ecdysis, but males did not exhibit as much selectivity in site use during infection. Females selected for landscape conditions that would increase solar exposure, such as southwestern-facing slopes (Figure 2.6C) and younger-aged stands (Figure 2.6B). However, drier, southwestern-facing slopes would also likely increase evaporative water loss (EWL; Lillywhite and Sheehy 2016), necessitating use of humid microclimates, such as sites closer to streams, to complete ecdysis (Dupoué et al., 2015). For example, Agugliaro et al. (2019) found pigmy rattlesnakes to exhibit 30–40% elevated EWL during SFD infection, primarily lost cutaneously. Due to the highly impermeable structure of the epidermis in snakes, ecdysis or skin irregularities, such as lesions associated with SFD, can dramatically increase EWL (Lillywhite and Maderson 1982; Dupoué et al., 2015; Agugliaro et al., 2019). Therefore, the use of sites in hot, dry conditions might exacerbate already elevated EWL levels in infected snakes. We found that both sexes preferred sites closer to streams and consistently selected sites with greater solar exposure (Figure 2.8), which suggests there could be an effort to balance EWL with behavioral fever during infection.

Hoffman et al. (2020, in review) assessed multi-scale landscape associations of behavioral site selection within this TRS population. They found that snakes selected landscape characteristics across different spatial scales for each behavior (foraging, digestion, ecdysis, and gestation), but ultimately, thermoregulatory-driven behaviors such as digestion, ecdysis, and gestation exhibited more spatial overlap than foraging. Sites selected for foraging accounted for a quarter of our SFD symptomatic male behavioral observations (Table 2.4), possibly explaining the lack of selectivity in site use models for males that excluded these foraging locations. Compared to other snakes in this population, symptomatic snakes from this study selected sites most analogously to ecdysis locations. Six of the nine covariates (Table 2.5) in the most parsimonious symptomatic site use models for females and males combined exhibited the same directional effects as those in the general ecdysis model by Hoffman et al. (2020, in review), including younger stand age, lower canopy height, drier conditions (NMDS1), higher elevations (NMDS3), flatter slopes, and sites closer to streams.

Interestingly, symptomatic snakes appeared to select sites with slightly cooler estimated temperatures from our temperature model, possibly indicating that symptomatic individuals are taking advantage of fine-scale variation in landscape temperature (e.g., canopy gaps or forest edges) instead of exclusively selecting hotter areas of the landscape. This apparent conflict in the predicted selected temperature by symptomatic snakes could result from a discontinuity in the spatial scale of the temperature model (5-m) and the scale at which snakes can behaviorally adjust their body temperature. For example, the landscape-scale temperature model did not correlate with

field-measured substrate temperatures associated with snake locations (Pearson's  $r = 0.06$ ).

In contrast to our predictions, we did not consistently observe elevated body temperatures for snakes during symptomatic years. We found symptomatic snakes to exhibit marginally cooler body temperatures in spring, suggesting earlier egress (emergence from hibernacula) dates during symptomatic years. Winter surface activity has been documented in other temperate TRS populations affected by SFD (Clark et al., 2015; McBride et al., 2015). Our earliest recorded date of surface activity occurred in February in an SFD symptomatic individual, when all other snakes remained in hibernacula. For the subset of individuals with different SFD infection statuses across years and known egress times ( $n = 5$ ), the date of egress decreased with SFD infection for four of five snakes, with snakes emerging from hibernacula 9–19 days earlier during symptomatic years. In contrast to spring temperature ranges, snakes exhibited warmer body temperatures and selected sites with greater solar insolation in the fall during SFD-symptomatic years. On average, snakes were 2°C hotter during the fall in symptomatic than asymptomatic years (Figure 2.7). Tetzlaff et al. (2017) also found that body temperatures did not differ between SFD infected and uninfected eastern massasauga rattlesnakes for the majority of the active season, but infected snakes exhibited higher body temperatures at the end of the active season. This finding of comparatively warmer snake body temperatures during the fall can be attributed to infected snakes increasing their surface activity in the fall and completing ingress later than healthy snakes. The

estimated date of ingress of our snakes increased with SFD infection for most (8/13) individuals by 2–41 days during symptomatic years.

Although this study provides novel findings for habitat associations of SFD-infected snakes, there are several limitations that should be considered. Due to our lab testing regimen in the spring and fall of each year, we were not able to consider state transitions in infection during the course of a year. Therefore, we were unable to accurately assess when an individual had fully recovered if testing SFD positive in the spring and negative in the fall or predict the onset of infection for individuals that newly tested SFD positive in the fall. We expected that most snakes with an active infection in the spring would recover by the fall, but this did not always occur (i.e. some snakes tested positive in both the spring and fall). We also did not rank infection severity to examine behavior and habitat use within infected individuals, which has been shown to be an important source of variation in previous physiology-focused studies on SFD (McCoy et al., 2017; Lind et al., 2018). Including individuals experiencing a range of symptom severity likely moderated the magnitude of effects we observed. Therefore, our results can be considered conservative estimates of the effects of SFD on snake spatial ecology.

Importantly, we also demonstrated behavioral responses to SFD that potentially constrain individual energy budgets, such as increased foraging effort but reduced success (in males), reduced foraging effort and success (in females), and increased long-distance movement frequency (both sexes). Additionally, the evident shift in space use patterns that we observed in six females warrants further consideration of sex-specific infection outcomes. This is the only study to our knowledge that demonstrates sex-

specific responses to *Oo* infection. No study has found evidence for sex-specific differences in SFD symptom severity, or physiological and short-term behavioral responses to infection (Mccoy et al., 2017; Tetzlaff et al., 2017; Agugliaro et al., 2019; Long et al., 2019). Our findings ultimately have implications for resource allocation strategies and population stability. As capital breeders, TRS and other Viperid snakes rely on stored energy to fuel reproduction and therefore, reproduce infrequently (e.g., 2–4 year intervals in TRS; Brown, 1991; Martin, 1993; Bonnet et al., 1998; Brown, 2016). Infection with SFD and associated compensatory behaviors (e.g., reduced foraging frequency) could prevent females from reaching a threshold of energy acquisition for reproduction, delaying reproduction cycles, or affecting litter characteristics (Lind et al., 2018; Lind et al., 2019). Our results therefore require further investigation of the implications of infection-altered behavior and space use as it relates to population dynamics and disease transmission.

## Conclusions

Understanding habitat use for individuals in various physiological and behavioral states is essential for developing comprehensive management strategies for imperiled wildlife. Our study examined consistency in long-term behavior, site selection, and space use in a TRS population affected by SFD. We identified potential coping strategies to SFD, such as site use that balances thermoregulatory needs with risk of dehydration. Although comprising a relatively small sample of individuals, this study demonstrates the

need for long-term behavioral monitoring of afflicted populations for a comprehensive understanding of SFD impacts to snake populations.

#### Literature Cited

- Agugliaro, J., Lind, C. M., Lorch, J. M., & Farrell, T. M. (2019). An emerging fungal pathogen is associated with increased resting metabolic rate and total evaporative water loss rate in a winter-active snake. *Functional Ecology*, 34, 486–496.
- Allender, M. C., Bunick, D., Dzhaman, E., Burrus, L., & Maddox, C. (2015a). Development and use of a real-time polymerase chain reaction assay for the detection of *Ophidiomyces ophiodiicola* in snakes. *Journal of Veterinary Diagnostic Investigation*, 27, 217–220.
- Allender, M. C., Raudabaugh, D. B., Gleason, F. H., & Miller, A. N. (2015b). The natural history, ecology, and epidemiology of *Ophidiomyces ophiodiicola* and its potential impact on free-ranging snake populations. *Fungal Ecology*, 17, 187–196.
- Ames, E. M., Gade, M. R., Nieman, C. L., Wright, J. R., Tonra, C. M., Marroquin, C. M., Tutterow, A. M., & Gray, S. M. (2020). Striving for population-level conservation: integrating physiology across the biological hierarchy. *Conservation Physiology*, 8, coaa019.
- Baker, S. J., Haynes, E., Gramhofer, M., Stanford, K., Bailey, S., Christman, M., Conley, K., Frasca, S. Jr., Ossiboff, R. J., LoBato, D., & Allender, M. C. (2019). Case definition and diagnostic testing for snake fungal disease. *Herpetological Review*, 50, 279–285.

- Binning, S. A., Shaw, A. K., & Roche, D. G. (2017). Parasites and host performance: incorporating infection into our understanding of animal movement. *Integrative and Comparative Biology*, 57, 267–280.
- Bonnet, X., Bradshaw, D., & Shine, R. (1998). Capital versus income breeding: an ectothermic perspective. *Oikos*, 83, 333–342.
- Brandell, E. E., Fountain-Jones, N. M., Gilbertson, M. L. J., Cross, P. C., Hudson, P. J., Smith, D. W., Stahler, D. R., Packer, C., & Craft, M. E. (2020). Group density, disease, and season shape territory size and overlap of social carnivores. *Journal of Animal Ecology*, 00, 1–15.
- Brown, W. S. (1991). Female reproductive ecology in a northern population of the timber rattlesnake, *Crotalus horridus*. *Herpetologica*, 47, 101–115.
- Brown, W. S. (2016). Lifetime reproduction in a northern metapopulation of timber rattlesnakes (*Crotalus horridus*). *Herpetologica*, 72, 331–342.
- Clark, R. W., Marchand, M. N., Clifford, B. J., Stechert, R., & Stephens, S. (2011). Decline of an isolated timber rattlesnake (*Crotalus horridus*) population: Interactions between climate change, disease, and loss of genetic diversity. *Biological Conservation*, 144, 886–891.
- Dupoué, A., Stahlschmidt, Z. R., Michaud, B., & Lourdais, O. (2015). Physiological state influences evaporative water loss and microclimate preference in the snake *Vipera aspis*. *Physiology & Behavior*, 144, 82–89.

- Fisher, M. C., Henk, D. A., Briggs, C. J., Brownstein, J. S., Madoff, L. C., McCraw, S. L., & Gurr, S. J. (2012). Emerging fungal threats to animal, plant and ecosystem health. *Nature*, 484, 186–194.
- Hileman, E. T., Allender, M. C., Bradke, D. R., Faust, L. J., Moore, J. A., Ravesi, M. J., & Tetzlaff, S. J. (2018). Estimation of *Ophidiomyces* prevalence to evaluate snake fungal disease risk. *The Journal of Wildlife Management*, 82, 173–181.
- Korkmaz, S., Goksuluk, D., & Zararsiz, G. (2014). MVN: An R package for assessing multivariate normality. *The R Journal*, 6, 151–162.
- Lillywhite, H. B., & Maderson, P. F. A. (1982). Skin structure and permeability. In C. Gans, and F. H. Pough (Eds.), *Biology of the Reptilia. Volume 12: Physiological Ecology* (pp. 397–442). New York, New York, USA: Academic Press.
- Lillywhite, H. B., & Sheehy, III, C. M. (2016). Synchrony of ecdysis in snakes. *Herpetological Conservation and Biology*, 11, 286–292.
- Lind, C., Moore, I. T., Akçay, Ç., Vernasco, B. J., Lorch, J. M., & Farrell, T. M. (2018). Patterns of circulating corticosterone in a population of rattlesnakes afflicted with snake fungal disease: stress hormones as a potential mediator of seasonal cycles in disease severity and outcomes. *Physiological and Biochemical Zoology*, 91, 765–775.
- Lind, C. M., Lorch, J. M., Moore, I. T., Vernasco, B. J., & Farrell, T. M. (2019). Seasonal sex steroids indicate reproductive costs associated with snake fungal disease. *Journal of Zoology*, 307, 104–110.

- Long, R. B., Love, D., Seeley, K. E., Patel, S., Allender, M. C., Garner, M. M., & Ramer, J. (2019). Host factors and testing modality agreement associated with *Ophidiomyces* infection in a free-ranging snake population in southeast Ohio, USA. *Journal of Zoo and Wildlife Medicine*, 50, 405–413.
- Lorch, J. M., Knowles, S., Lankton, J. S., Michell, K., Edwards, J. L., Kapfer, J. M., ... D. S. Blehert. (2016). Snake fungal disease: an emerging threat to wild snakes. *Philosophical Transactions of the Royal Society B: Biological Sciences*, 371, 20150457.
- Martin, W. H. (1993). Reproduction of the timber rattlesnake (*Crotalus horridus*) in the Appalachian Mountains. *Journal of Herpetology*, 27, 133–143.
- McBride, M. P., Wojick, K. B., Georoff, T. A., Kimbro, J., Garner, M. M., Wang, X., Childress, A. L., & Wellehan, J. F. X. (2015). *Ophidiomyces ophiodiicola* dermatitis in eight free-ranging timber rattlesnakes (*Crotalus horridus*) from Massachusetts. *Journal of Zoo and Wildlife Medicine*, 46, 86–94.
- McCoy, C. M., Lind, C. M., & Farrell, T. M. (2017). Environmental and physiological correlates of the severity of clinical signs of snake fungal disease in a population of pigmy rattlesnakes, *Sistrurus miliarius*. *Conservation Physiology*, 5, cow077.
- McKenzie, J. M., Price, S. J., Fleckenstein, J. L., Drayer, A. N., Connette, G. M., Bohuski, E., & Lorch, J. M. (2019). Field diagnostics and seasonality of *Ophidiomyces ophiodiicola* in wild snake populations. *EcoHealth*, 16, 141–150.

- Pau, G., Fuchs, F., Sklyar, O., Boutros, M., & Huber, W. (2010). EBImage—an R package for image processing with applications to cellular phenotypes. *Bioinformatics*, 26, 979–981.
- Rakus, K., Ronsmans, M., & Vanderplasschen, A. (2017). Behavioral fever in ectothermic vertebrates. *Developmental & Comparative Immunology*, 66, 84–91.
- Richards-Zawacki, C. L. (2010). Thermoregulatory behaviour affects prevalence of chytrid fungal infection in a wild population of Panamanian golden frogs. *Proceedings of the Royal Society B: Biological Sciences*, 277, 519–528.
- Scheele, B. C., Guarino, F., Osborne, W., Hunter, D. A., Skerratt, L. F. & Driscoll, D. A. (2014). Decline and re-expansion of an amphibian with high prevalence of chytrid fungus. *Biological Conservation*, 170, 86–91.
- Signer, J., Fieberg, J. & Avgar, T. (2019). Animal movement tools (amt): R package for managing tracking data and conducting habitat selection analyses. *Ecology and Evolution*, 9, 880–890.
- Skerratt, L. F., Berger, L., Speare, R., Cashins, S., McDonald, K. R., Phillott, A. D., Hines, H. B., & Kenyon, N. (2007). Spread of chytridiomycosis has caused the rapid global decline and extinction of frogs. *EcoHealth*, 4, 125–134.
- Tetzlaff, S. J., Ravesi, M. J., Allender, M. C., Carter, E. T., DeGregorio, B. A., Josimovich, J. M., & Kingsbury, B. A. (2017). Snake fungal disease affects behavior of free-ranging massasauga rattlesnakes (*Sistrurus catenatus*). *Herpetological Conservation and Biology*, 12, 624–634.

Waldron, J. L., Lanham, J. D., & Bennett, S. H. (2006). Using behaviorally-based seasons to investigate canebrake rattlesnake (*Crotalus horridus*) movement patterns and habitat selection. *Herpetologica*, 62, 389–398.

Table 2.1. Snake fungal disease (SFD) designations assigned annually (2016–2019) to 41 timber rattlesnakes (*Crotalus horridus*) in southeastern Ohio. Each spring (April–May) and fall (August–September) individual snakes were examined for the presence of skin lesions associated with SFD infection and skin-swabbed and qPCR-tested for the presence of the fungal pathogen *Ophidiomyces ophiodiicola*. We considered the presence of clinical signs (i.e. lesions) and a positive qPCR test the most conclusive evidence for SFD infection.

Status	Category	Lesions	Positive Test	Males	Females	Total
asymptomatic	<b>(0) Presumed healthy</b>	No	No	24	13	<b>37</b>
	<b>(1) Possibly infected</b>	No	Yes	8	8	<b>16</b>
Symptomatic	<b>(2) Presumed infected</b>	Yes	No	3	4	<b>7</b>
	<b>(3) Infected</b>	Yes	Yes	16	12	<b>28</b>
<b>Total</b>				51	37	<b>88</b>

Table 2.2. Bayesian mixed effect models of home range area across 50%, 95%, and 100% minimum convex polygons (MCP) for 15 (n = 9 males and 6 non-gravid females) timber rattlesnakes (*Crotalus horridus*), during years when considered asymptomatic or symptomatic of snake fungal disease (SFD). Mean coefficient estimates, standard errors (S.E.), 95% lower (LCI) and upper (UCI) credible intervals, percentage of the posterior distributions overlapping zero, and percentage of the posterior distributions in the region of practical equivalence (ROPE) are provided for the most parsimonious model at each home range scale. Refer to Table B.1 for further descriptions of candidate models.

	Covariate	Estimate	S.E.	95% LCI	95% UCI	Overlap Zero (%)	ROPE (%)
<b>50% MCP</b>	SFD	0.59	0.29	0.03	1.16	1.9	0
	Sex	-0.95	0.53	-2.02	0.11	3.8	0.6
	SFD: Sex	0.49	0.38	-0.25	1.23	9.4	9.7
<b>95% MCP</b>	SFD	0.10	0.22	-0.34	0.55	32.4	36.7
	Sex	-1.49	0.51	-2.49	0.52	0.2	0
<b>100% MCP</b>	SFD	0.38	0.19	-0.01	0.76	2.6	1.7
	Sex	-1.43	0.45	-2.32	-0.53	0.3	0

Table 2.3. Multivariate ANOVA (MANOVA) of principal component analysis (PCA) scores of 15 timber rattlesnakes (*Crotalus horridus*) in southeast Ohio during years when asymptomatic or symptomatic of snake fungal disease (SFD). The PCA included eight movement metrics, with principal components (PC) 1 and 2 representing a cumulative 89.8% of the variance. Large, positive scores on PC1 suggest greater home range size (particularly 95% and 100% minimum convex polygons) and greater displacement rates. Large, positive scores on PC2 suggest greater median and mean movement rates. We used an interaction of SFD status and sex to predict PC scores, with a random effect of individual snakes. Mean coefficient estimates, standard errors (S.E.), 95% lower (LCI) and upper (UCI) credible intervals, and percentage of the posterior distributions overlapping zero are provided.

<b>Covariate</b>	<b>Estimate</b>	<b>S.E.</b>	<b>95% LCI</b>	<b>95% UCI</b>	<b>Overlap Zero (%)</b>
<b>PC1-Intercept</b>	1.26	0.73	-0.17	2.71	4.2
<b>PC2-Intercept</b>	-0.06	0.31	-0.67	0.54	42.1
<b>PC1-SFD</b>	-0.14	0.54	-1.22	0.94	38.8
<b>PC1-Sex</b>	-4.16	1.20	-6.51	-1.76	0.08
<b>PC1-SFD: Sex</b>	1.45	0.91	-0.35	3.28	5.6
<b>PC2-SFD</b>	0.10	0.31	-0.51	0.70	37.5
<b>PC2-Sex</b>	0.40	0.50	-0.59	1.39	20.4
<b>PC2-SFD: Sex</b>	-0.68	0.52	-1.69	0.39	9.0

Table 2.4. Observed frequencies of 15 timber rattlesnakes (*Crotalus horridus*) in southeastern Ohio exhibiting four unique behaviors (resting, foraging, digesting, and ecdysis) when asymptomatic or symptomatic of snake fungal disease (SFD). We compared observed (% of total) and expected frequencies between males (n = 9) and females (n = 6) across each SFD status with a chi-squared test. All snakes were monitored for at least one asymptomatic and symptomatic year each. The contribution (%) of each cell to the chi-square statistic was calculated as  $100 * \frac{r^2}{\chi^2}$ . Bolded cells had a contribution > 10%.

		Female— Asymptomatic	Female— Symptomatic	Male— Asymptomatic	Male— Symptomatic
<b>Rest</b>	<i>Observed</i>	109 (54%)	<b>214 (69%)</b>	247 (64%)	<b>302 (53%)</b>
	<i>Expected</i>	118.1	183.9	226.2	343.8
	<i>Contribution</i>	1.8%	12.6%	4.9%	12.9%
<b>Forage</b>	<i>Observed</i>	55 (27%)	51 (16%)	<b>61 (16%)</b>	<b>147 (25%)</b>
	<i>Expected</i>	42.5	66.2	81.5	123.8
	<i>Contribution</i>	9.3%	8.9%	13.1%	11.1%
<b>Digest</b>	<i>Observed</i>	14 (7%)	<b>9 (3%)</b>	22 (5%)	39 (6%)
	<i>Expected</i>	11.4	17.7	21.8	33.1
	<i>Contribution</i>	1.5%	11.0%	0%	2.7%
<b>Ecdysis</b>	<i>Observed</i>	23 (11%)	39 (12%)	55 (14%)	97 (16%)
	<i>Expected</i>	29.0	45.1	55.5	84.4
	<i>Contribution</i>	3.2%	2.1%	0%	4.8%

Table 2.5. Bayesian mixed effects Bernoulli models of site use characteristics of timber rattlesnakes (*Crotalus horridus*) during years unaffected or affected by snake fungal disease (SFD). Each snake was considered asymptomatic or symptomatic of SFD infection for at least one year each. We modeled probability of site use by a symptomatic snake as a function of thirteen geospatial landscape and forest structural variables (5-m resolution), with individual snakes as random effects. We report the variables that best described site use by males and females. Mean coefficient estimates, standard errors ( $\pm$  S.E.) and percentage of the posterior distributions overlapping zero are provided. Refer to Table 1.1 for further descriptions of covariates.

	<b>Non-gravid Females (n = 6)</b>	<b>Males (n = 9)</b>
<b>CHM</b>	-0.27 ( $\pm$ 0.16) 1.7%	
<b>mTemp</b>	-0.29 ( $\pm$ 0.15) 2.1%	
<b>NMDS1</b>	-0.47 ( $\pm$ 0.15) 0%	
<b>NMDS3</b>	0.42 ( $\pm$ 0.16) 0.2%	
<b>Slope</b>	-0.24 ( $\pm$ 0.14) 2.2%	
<b>Stream</b>	-0.58 ( $\pm$ 0.16) 0%	-0.22 ( $\pm$ 0.08) 0.5%
<b>Age</b>	-0.56 ( $\pm$ 0.19) 0.1%	
<b>UND</b>	-0.29 ( $\pm$ 0.17) 6.5%	
<b>Beers</b>		0.27 ( $\pm$ 0.08) 0%

Table 2.6. Bayesian mixed effect models of external snake body temperatures taken with a digital infrared thermometer at sites (n = 870) used by timber rattlesnakes (*Crotalus horridus*) during years unaffected or affected by snake fungal disease (SFD). Each snake (n = 15) was considered asymptomatic or symptomatic of SFD infection for at least one year each. We modeled snake body temperature as a function of interactive SFD status and season of observation. We defined spring as April–June, summer as July–August, and fall as September–October. We included random effects of individual snakes and month of observation. Mean coefficient estimates, standard errors (S.E.), 95% lower (LCI) and upper (UCI) credible intervals, percentage of the posterior distributions overlapping zero, and percentage of the posterior distributions in the region of practical equivalence (ROPE) are provided for the most parsimonious model. Refer to Table B.6 for further descriptions of candidate models.

<b>Covariate</b>	<b>Estimate</b>	<b>S.E.</b>	<b>95% LCI</b>	<b>95% UCI</b>	<b>Overlap Zero (%)</b>	<b>ROPE (%)</b>
<b>Intercept</b>	25.37	0.98	23.52	27.42	0	0
<b>SFD</b>	-0.75	0.48	-1.69	0.19	5.7	24.4
<b>Summer</b>	0.52	1.50	-2.66	3.46	32.0	28.6
<b>Fall</b>	-3.56	1.57	-6.86	-0.55	1.5	0
<b>SFD: Summer</b>	1.74	0.68	0.40	3.10	0.41	0
<b>SFD: Fall</b>	2.91	0.85	1.23	4.57	0.01	0

Table 2.7. Bayesian mixed effect model of solar insolation at sites ( $n = 730$ ) used by timber rattlesnakes (*Crotalus horridus*) during years unaffected or affected by snake fungal disease (SFD). Each snake ( $n = 15$ ) was considered asymptomatic or symptomatic of SFD infection for at least one year each. We modeled solar insolation ( $\text{kWh/m}^2$ ), corrected by proportion canopy cover, as a function of additive SFD status and season of observation. We defined spring as April–June, summer as July–August, and fall as September–October. We included random effects of individual snakes and month of observation. Mean coefficient estimates, standard errors (S.E.), 95% lower (LCI) and upper (UCI) credible intervals, percentage of the posterior distributions overlapping zero, and percentage of the posterior distributions in the region of practical equivalence (ROPE) are provided for the most parsimonious model. Refer to Table B.7 for further descriptions of candidate models.

<b>Covariate</b>	<b>Estimate</b>	<b>S.E.</b>	<b>95% LCI</b>	<b>95% UCI</b>	<b>Overlap Zero (%)</b>	<b>ROPE (%)</b>
<b>Intercept</b>	7.24	0.47	6.31	8.16	0	0
<b>SFD</b>	0.57	0.12	0.34	0.80	0	0
<b>Summer</b>	-0.43	0.64	-1.7	0.88	19.5	20
<b>Fall</b>	-2.07	0.65	-3.36	-0.74	0.4	0



Figure 2.1. Clinical symptoms of snake fungal disease (SFD) in a population of timber rattlesnakes (*Crotalus horridus*) in southeastern Ohio. A–B) Mild clinical signs of SFD. For clarity, we circled observed facial lesions in red. The symptomatic female (top left) and male (top right) were both included in the movement and habitat use analyses. Bottom row: Moderate clinical signs of SFD in other individuals not included in movement and habitat use analyses in this study because of insufficient monitoring of SFD-asymptomatic years. Photo credits to B. Hiner, Z. Truelock, and J. Buffington.

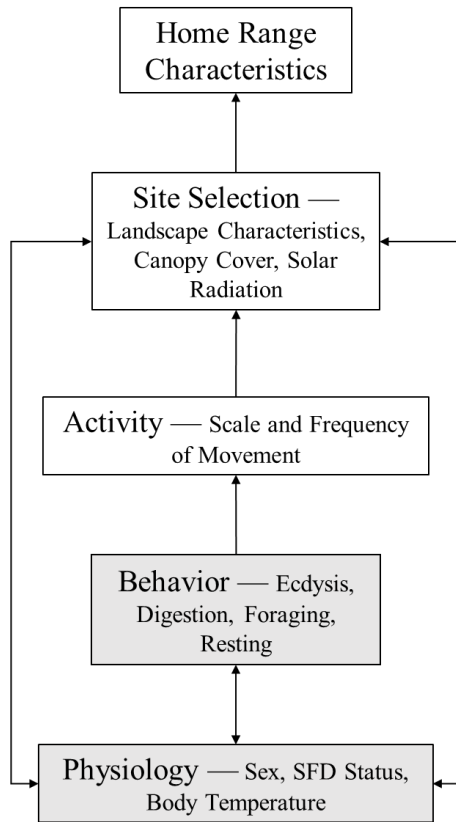


Figure 2.2. Schematic of a multi-scale, behavior-focused study design to examine multifaceted effects of snake fungal disease (SFD) on the spatial ecology of 15 timber rattlesnakes (*Crotalus horridus*) in southeastern Ohio.

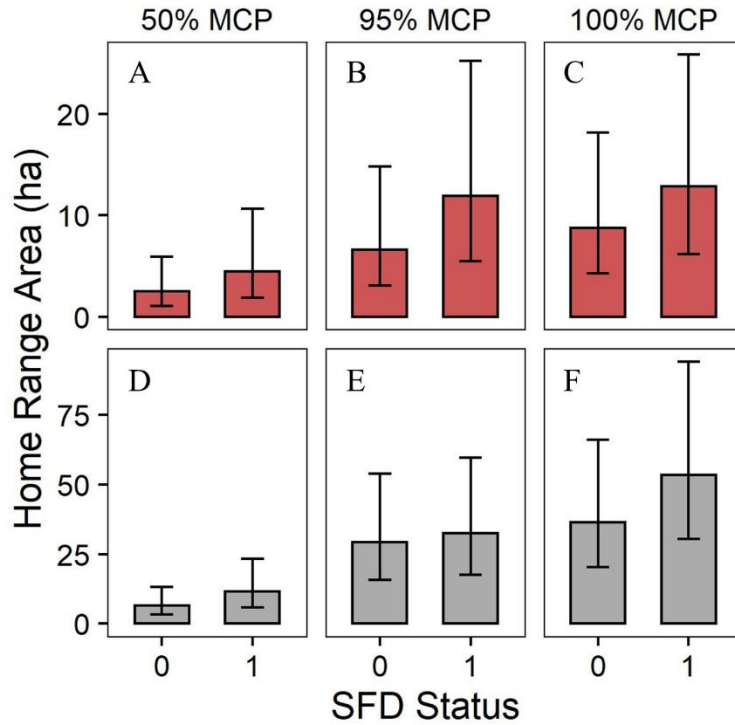


Figure 2.3. Mean area (ha) of 50%, 95%, and 100% minimum convex polygons (MCP) describing home ranges for 15 timber rattlesnakes (A–C: 6 non-gravid females; D–F: 9 males) during years when asymptomatic or symptomatic of snake fungal disease (SFD). Female home range area increases between years that individuals are asymptomatic of SFD and years in which they exhibit symptoms of SFD infection across all home range scales (A–C). Male home range area increases with SFD infection at the 50% (D) and 100% scales (F), but home range size does not differ at the 95% scale (E).

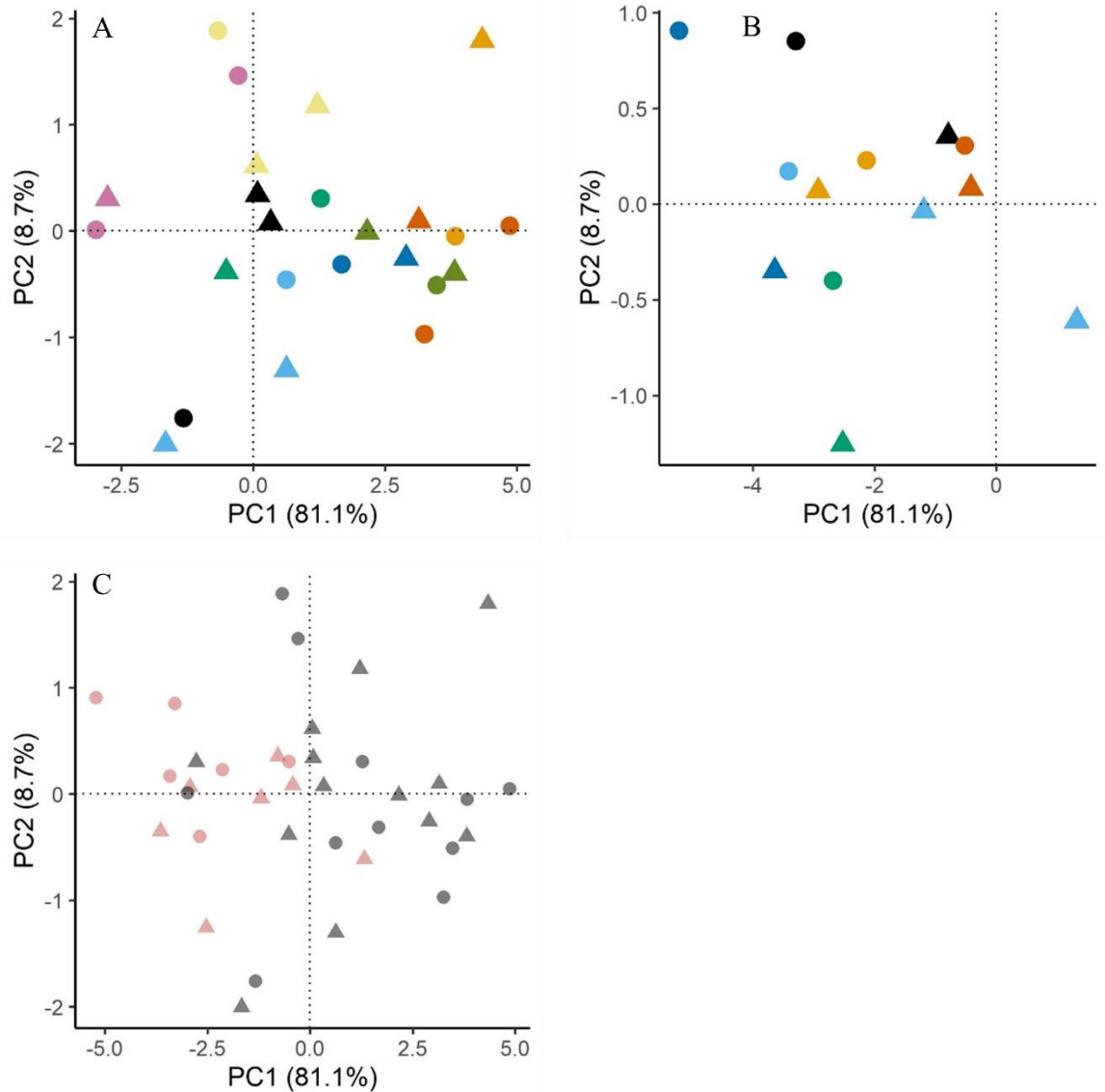


Figure 2.4. Principal component analysis biplots, representing gradients in scales of movement for 15 timber rattlesnakes (*Crotalus horridus*) in southeastern OH during years that individuals were Asymptomatic (coded by circles) or Symptomatic (coded by triangles) of snake fungal disease (SFD). Large, positive scores on PC1 suggest greater home range size (particularly 95% and 100% minimum convex polygons) and greater displacement rates. Large, positive scores on PC2 suggest greater median and mean movement rates. A) Male scores on PC1 and PC2. Individuals (n = 9) are coded by color. B) Female scores on PC1 and PC2. Individuals (n = 6) are coded by color. C) Scores of all individuals, coded by sex. Red represents females and gray represents males.

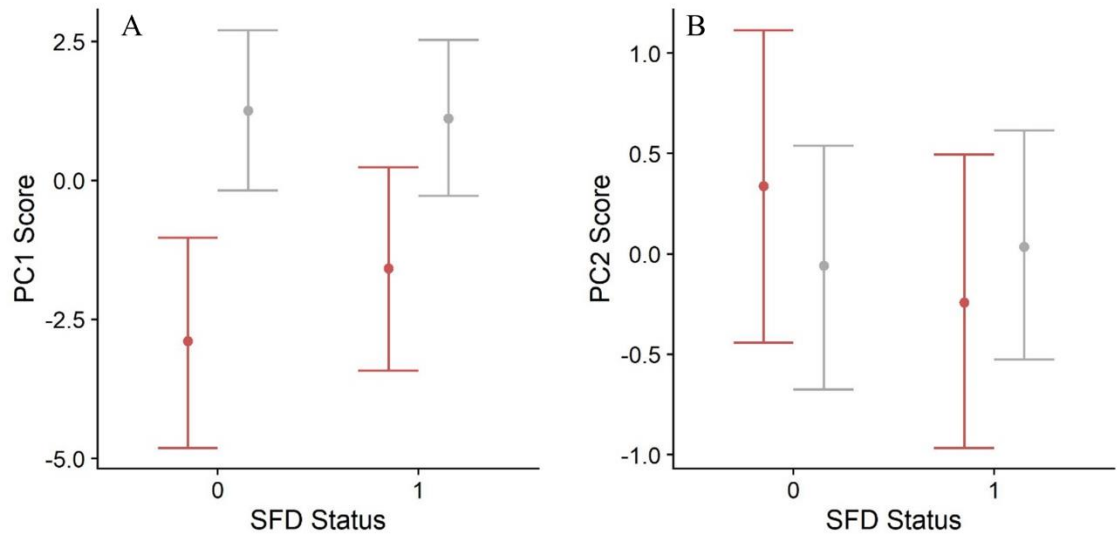


Figure 2.5. Principal component (PC1) scores, representing gradients in scales of movement for 15 timber rattlesnakes (*Crotalus horridus*) in southeastern OH during years that individuals were asymptomatic or symptomatic of snake fungal disease (SFD). Large, positive scores on PC1 suggest greater home range size (particularly 95% and 100% minimum convex polygons) and greater displacement rates. Large, positive scores on PC2 suggest greater median and mean movement rates. We used an interaction of SFD status and sex (females in red and males in grey) to predict PC scores, with a random effect of individual snake.

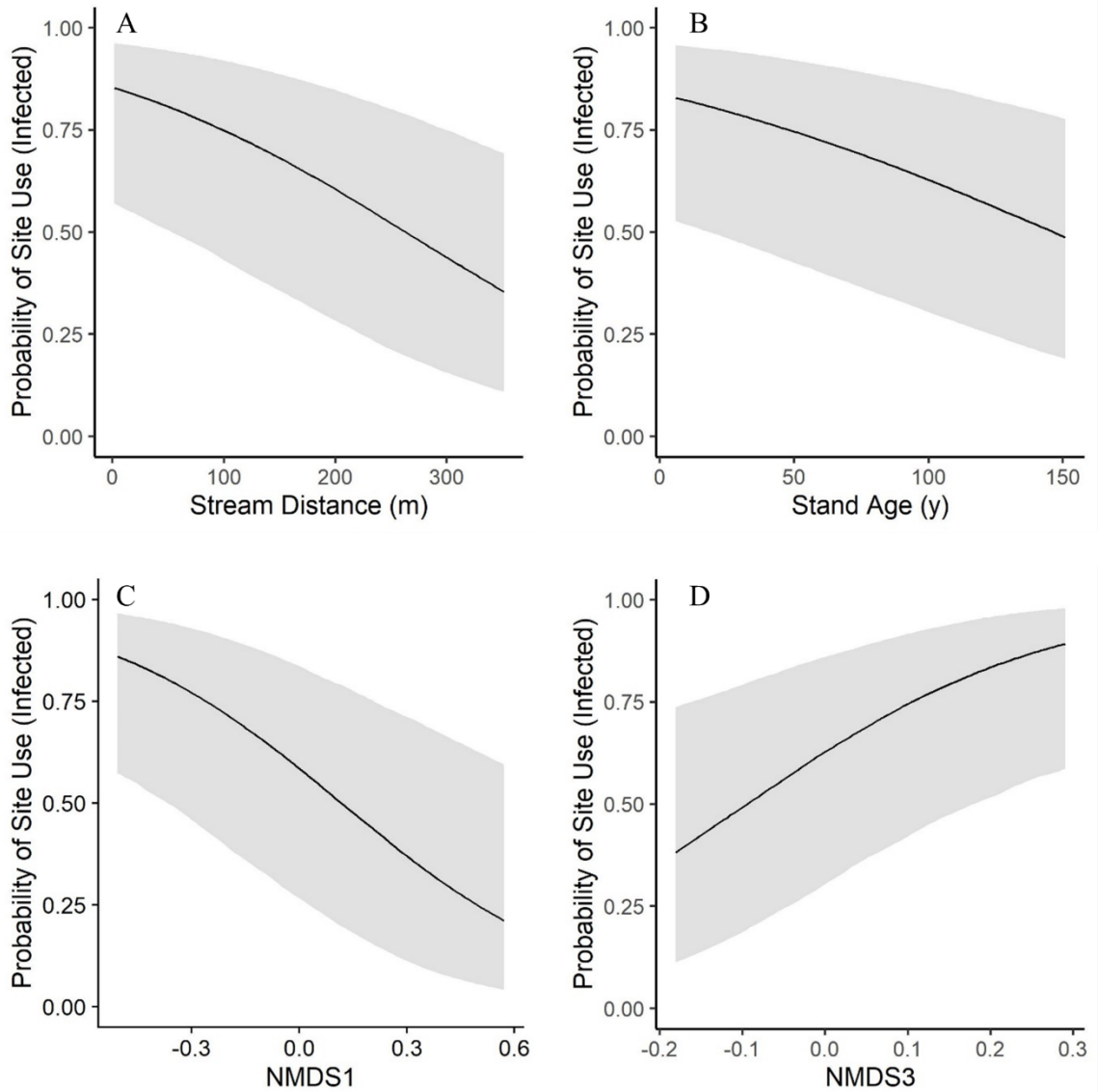


Figure 2.6. Probability of site use by six non-gravid female timber rattlesnakes (*Crotalus horridus*) symptomatic of snake fungal disease (SFD) predicted by remotely-sensed (5-m resolution) landscape and forest structural characteristics. A) Distance to nearest stream. B) Forest stand age represents forest management history. C) Moisture gradient (NMDS1) with lower scores representing drier, southwestern-facing slopes. D) Longitudinal gradient (NMDS3) with higher scores representing higher elevations and western locations.

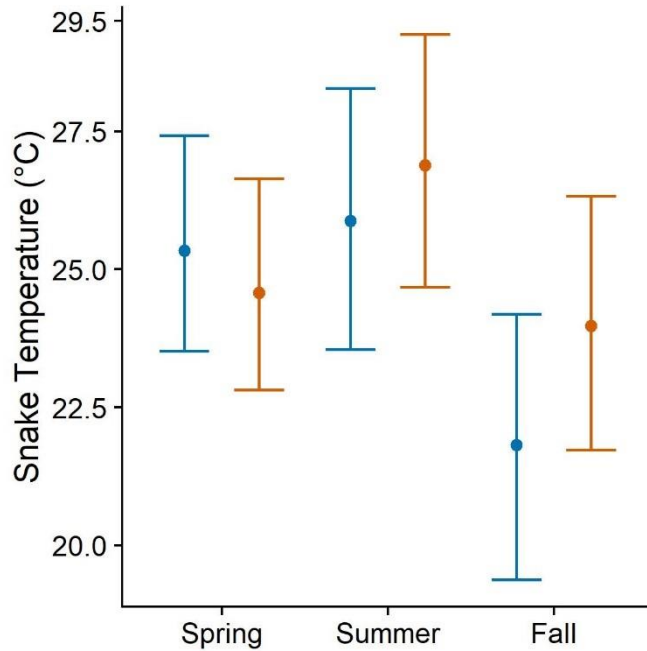


Figure 2.7. External snake body temperatures taken with a digital infrared thermometer at sites ( $n = 870$ ) used by timber rattlesnakes (*Crotalus horridus*) during years unaffected or affected by snake fungal disease (SFD). We modeled body temperature as an interaction of season of observation and SFD status, with month of observation and individual snakes modeled as random effects. Each snake ( $n = 9$  males and 6 non-gravid females) was considered Asymptomatic or Symptomatic of SFD infection for at least one year each. Asymptomatic years are in blue and Symptomatic years are in orange. We defined Spring as April–June, Summer as July–August, and Fall as September–October.

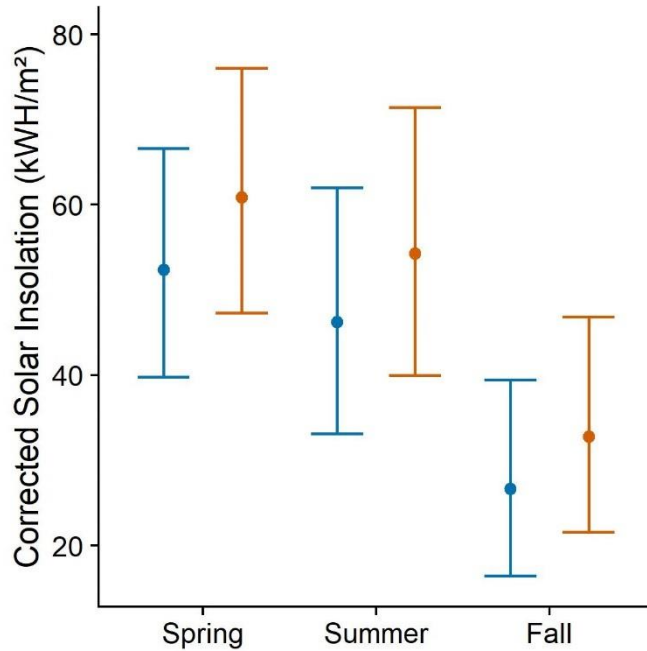


Figure 2.8. Estimated solar insolation ( $\text{kWH/m}^2$ ) corrected by observed canopy cover of sites used by 15 timber rattlesnakes (*Crotalus horridus*) in southeastern Ohio. We modeled solar insolation as a function of season of observation and snake fungal disease (SFD) status, with month of observation and individual snakes modeled as random effects. Each snake ( $n = 9$  males and 6 non-gravid females) was considered Asymptomatic or Symptomatic of SFD infection for at least one year each. Asymptomatic years are in blue and Symptomatic years are in orange. We defined Spring as April–June, Summer as July–August, and Fall as September–October.

## References

- Aber, J. D. (1979). Foliage-height profiles and succession in northern hardwood forests. *Ecology*, 60, 18–23.
- Adams, B. T., & Matthews, S. N. (2018). Enhancing forest and shrubland mapping in a managed forest landscape with Landsat–Lidar data fusion. *Natural Areas Journal*, 38, 402–418.
- Adams, B. T., Matthews, S. N., Peters, M. P., Prasad, A. & Iverson, L. R. (2019). Mapping floristic gradients of forest composition using an ordination-regression approach with landsat OLI and terrain data in the Central Hardwoods region. *Forest Ecology and Management*, 434, 87–98.
- Agugliaro, J., Lind, C. M., Lorch, J. M., & Farrell, T. M. (2019). An emerging fungal pathogen is associated with increased resting metabolic rate and total evaporative water loss rate in a winter-active snake. *Functional Ecology*, 34, 486–496.
- Allender, M. C., Bunick, D., Dzhaman, E., Burrus, L., & Maddox, C. (2015a). Development and use of a real-time polymerase chain reaction assay for the detection of *Ophidiomyces ophiodiicola* in snakes. *Journal of Veterinary Diagnostic Investigation*, 27, 217–220.

- Allender, M. C., Raudabaugh, D. B., Gleason, F. H., & Miller, A. N. (2015b). The natural history, ecology, and epidemiology of *Ophidiomyces ophiodiicola* and its potential impact on free-ranging snake populations. *Fungal Ecology*, 17, 187–196.
- Ames, E. M., Gade, M. R., Nieman, C. L., Wright, J. R., Tonra, C. M., Marroquin, C. M., Tutterow, A. M., & Gray, S. M. (2020). Striving for population-level conservation: integrating physiology across the biological hierarchy. *Conservation Physiology*, 8, coaa019.
- Baker, S. J., Haynes, E., Gramhofer, M., Stanford, K., Bailey, S., Christman, M., Conley, K., Frasca, S. Jr., Ossiboff, R. J., LoBato, D., & Allender, M. C. (2019). Case definition and diagnostic testing for snake fungal disease. *Herpetological Review*, 50, 279–285.
- Baxley, D. L., & Qualls, C. P. (2009). Black pine snake (*Pituophis melanoleucus lodingi*): spatial ecology and associations between habitat use and prey dynamics. *Journal of Herpetology*, 43, 284–293.
- Beaupre, S. J. (2008). Annual variation in time-energy allocation by timber rattlesnakes (*Crotalus horridus*) in relation to food acquisition. In W. K. Hayes, K.R. Beaman, M.D. Cardwell, & S.P. Bush (Eds.), *Biology of the Rattlesnakes* (pp. 111–122). Loma Linda, California, USA: Loma Linda University Press.
- Beers, T. W., Dress, P. E., & Wensel, L. C. (1966). Notes and observations: Aspect transformation in site productivity research. *Journal of Forestry*, 64, 691–692.

- Binning, S. A., Shaw, A. K., & Roche, D. G. (2017). Parasites and host performance: incorporating infection into our understanding of animal movement. *Integrative and Comparative Biology*, 57, 267–280.
- Blouin-Demers, G., & Weatherhead, P. J. (2001). An experimental test of the link between foraging, habitat selection and thermoregulation in black rat snakes *Elaphe obsoleta obsoleta*. *Journal of Animal Ecology*, 70, 1006–1013.
- Bonnet, X., Bradshaw, D., & Shine, R. (1998). Capital versus income breeding: an ectothermic perspective. *Oikos*, 83, 333–342.
- Brandell, E. E., Fountain-Jones, N. M., Gilbertson, M. L. J., Cross, P. C., Hudson, P. J., Smith, D. W., Stahler, D. R., Packer, C., & Craft, M. E. (2020). Group density, disease, and season shape territory size and overlap of social carnivores. *Journal of Animal Ecology*, 00, 1–15.
- Brown, W. S. (1991). Female reproductive ecology in a northern population of the timber rattlesnake, *Crotalus horridus*. *Herpetologica*, 47, 101–115.
- Brown, W. S. (2016). Lifetime reproduction in a northern metapopulation of timber rattlesnakes (*Crotalus horridus*). *Herpetologica*, 72, 331–342.
- Bürkner, P. (2017). brms: An R package for Bayesian multilevel models using Stan. *Journal of Statistical Software*, 80, 1–28.
- Carfagno, G. L. F., Heske, E. J., & Weatherhead, P. J. (2006). Does mammalian prey abundance explain forest-edge use by snakes? *Écoscience*, 13, 293–297.
- Charnov, E. L. (1976). Optimal foraging, the marginal value theorem. *Theoretical Population Biology*, 9, 129–136.

- Clark, R. W. (2002). Diet of the timber rattlesnake, *Crotalus horridus*. *Journal of Herpetology*, 36, 494–499.
- Clark, R. W. (2004). Timber rattlesnakes (*Crotalus horridus*) use chemical cues to select ambush sites. *Journal of Chemical Ecology*, 30, 607–617.
- Clark, R. W. (2006). Fixed videography to study predation behavior of an ambush foraging snake, *Crotalus horridus*. *Copeia*, 2006, 181–187.
- Clark, R. W., Marchand, M. N., Clifford, B. J., Stechert, R., & Stephens, S. (2011). Decline of an isolated timber rattlesnake (*Crotalus horridus*) population: Interactions between climate change, disease, and loss of genetic diversity. *Biological Conservation*, 144, 886–891.
- Clotfelter, E. D., Pedersen, A. B., Cranford, J. A., Ram, N., Snajdr, E. A., Nolan, V., Ketterson, E. D. (2007). Acorn mast drives long-term dynamics of rodent and songbird populations. *Oecologia*, 154, 493–503.
- Douglass, N. J., & Reinert, H. K. (1982). The utilization of fallen logs as runways by small mammals. *Proceedings of the Pennsylvania Academy of Science*, 56, 162–164.
- Dupoué, A., Stahlschmidt, Z. R., Michaud, B., & Lourdais, O. (2015). Physiological state influences evaporative water loss and microclimate preference in the snake *Vipera aspis*. *Physiology & Behavior*, 144, 82–89.
- Fisher, M. C., Henk, D. A., Briggs, C. J., Brownstein, J. S., Madoff, L. C., McCraw, S. L., & Gurr, S. J. (2012). Emerging fungal threats to animal, plant and ecosystem health. *Nature*, 484, 186–194.

- Flaxman, S. M., & Lou, Y. (2009). Tracking prey or tracking the prey's resource? Mechanisms of movement and optimal habitat selection by predators. *Journal of Theoretical Biology*, 256, 187–200.
- Glaudas, X., & Rodríguez-Robles, J. A. (2011). A two-level problem: habitat selection in relation to prey abundance in an ambush predator, the speckled rattlesnake (*Crotalus mitchellii*). *Behaviour*, 148, 1491–1524.
- Glaudas, X., & Alexander, G. J. (2017). Food supplementation affects the foraging ecology of a low-energy, ambush-foraging snake. *Behavioral Ecology and Sociobiology*, 71, 1–11.
- Goetz, S. M., Petersen, C. E., Rose, R. K., Kleopfer, J. D., & Savitzky, A. H. (2016). Diet and foraging behaviors of timber rattlesnakes, *Crotalus horridus*, in eastern Virginia. *Journal of Herpetology*, 50, 520–526.
- Hammond, J. I., Luttbeg, B., Brodin, T., & Sih, A. (2012). Spatial scale influences the outcome of the predator-prey space race between tadpoles and predatory dragonflies: Scale and predator-prey games. *Functional Ecology*, 26, 522–531.
- Harvey, D. S., & Weatherhead, P. J. (2006). A test of the hierarchical model of habitat selection using eastern massasauga rattlesnakes (*Sistrurus catenatus*). *Biological Conservation*, 130, 206–216.
- Heard, G. W., Black, D., & Robertson, P. (2004). Habitat use by the inland carpet python (*Morelia spilota metcalfei*): Seasonal relationships with habitat structure and prey distribution in a rural landscape. *Austral Ecology*, 29, 446–460.

- Hijmans, R. J. (2020). Raster: geographic data analysis and modeling. R Package Version 3.3-13. <<http://CRAN.R-project.org/package=raster>>.
- Hileman, E. T., Allender, M. C., Bradke, D. R., Faust, L. J., Moore, J. A., Ravesi, M. J., & Tetzlaff, S. J. (2018). Estimation of *Ophidiomyces* prevalence to evaluate snake fungal disease risk. *The Journal of Wildlife Management*, 82, 173–181.
- Hopcraft, J. G. C., Sinclair, A. R. E., & Packer, C. (2005). Planning for success: Serengeti lions seek prey accessibility rather than abundance. *Journal of Animal Ecology*, 74, 559–566.
- Huey, R. B., & Pianka, E. R. (1981). Ecological consequences of foraging mode. *Ecology*, 62, 991–999.
- Johnson, D. H. (1980). The comparison of usage and availability measurements for evaluating resource preference. *Ecology*, 61, 65–71.
- Kittle, A. M., Anderson, M., Avgar, T., Baker, J. A., Brown, G. S., Hagens, J., ... Fryxell, J. M. (2017). Landscape-level wolf space use is correlated with prey abundance, ease of mobility, and the distribution of prey habitat. *Ecosphere*, 8, e01783.
- Korkmaz, S., Goksuluk, D., & Zararsiz, G. (2014). MVN: An R Package for Assessing Multivariate Normality. *The R Journal*, 6, 151–162.
- Lillywhite, H. B., & Maderson, P. F. A. (1982). Skin structure and permeability. In C. Gans, and F. H. Pough (Eds.), *Biology of the Reptilia. Volume 12: Physiological Ecology* (pp. 397–442). New York, New York, USA: Academic Press.

- Lillywhite, H. B., & Sheehy, III, C. M. (2016). Synchrony of ecdysis in snakes. *Herpetological Conservation and Biology*, 11, 286–292.
- Lind, C., Moore, I. T., Akçay, Ç., Vernasco, B. J., Lorch, J. M., & Farrell, T. M. (2018). Patterns of circulating corticosterone in a population of rattlesnakes afflicted with snake fungal disease: stress hormones as a potential mediator of seasonal cycles in disease severity and outcomes. *Physiological and Biochemical Zoology*, 91, 765–775.
- Lind, C. M., Lorch, J. M., Moore, I. T., Vernasco, B. J., & Farrell, T. M. (2019). Seasonal sex steroids indicate reproductive costs associated with snake fungal disease. *Journal of Zoology*, 307, 104–110.
- Long, R. B., Love, D., Seeley, K. E., Patel, S., Allender, M. C., Garner, M. M., & Ramer, J. (2019). Host factors and testing modality agreement associated with *Ophidiomyces* infection in a free-ranging snake population in southeast Ohio, USA. *Journal of Zoo and Wildlife Medicine*, 50, 405–413.
- Lorch, J. M., Knowles, S., Lankton, J. S., Michell, K., Edwards, J. L., Kapfer, J. M., ... D. S. Blehert. (2016). Snake fungal disease: an emerging threat to wild snakes. *Philosophical Transactions of the Royal Society B: Biological Sciences*, 371, 20150457.
- Madsen, T., & Shine, R. (1996). Seasonal migration of predators and prey—A study of pythons and rats in tropical Australia. *Ecology*, 77, 149–156.
- Martin, T. G., Wintle, B. A., Rhodes, J. R., Kuhnert, P. M., Field, S. A., Low-Choy, S. J., ... Possingham, H. P. (2005). Zero tolerance ecology: improving ecological

- inference by modelling the source of zero observations. *Ecology Letters*, 8, 1235–1246.
- Martin, W. H. (1993). Reproduction of the timber rattlesnake (*Crotalus horridus*) in the Appalachian Mountains. *Journal of Herpetology*, 27, 133–143.
- Mayor, S. J., Schneider, D. C., Schaefer, J. A., & Mahoney, S. P. (2009). Habitat selection at multiple scales. *Ecoscience*, 16, 238–247.
- McBride, M. P., Wojick, K. B., Georoff, T. A., Kimbro, J., Garner, M. M., Wang, X., Childress, A. L., & Wellehan, J. F. X. (2015). *Ophidiomyces ophiodiicola* dermatitis in eight free-ranging timber rattlesnakes (*Crotalus horridus*) from Massachusetts. *Journal of Zoo and Wildlife Medicine*, 46, 86–94.
- McCoy, C. M., Lind, C. M., & Farrell, T. M. (2017). Environmental and physiological correlates of the severity of clinical signs of snake fungal disease in a population of pigmy rattlesnakes, *Sistrurus miliarius*. *Conservation Physiology*, 5, cow077.
- McKenzie, J. M., Price, S. J., Fleckenstein, J. L., Drayer, A. N., Connette, G. M., Bohuski, E., & Lorch, J. M. (2019). Field diagnostics and seasonality of *Ophidiomyces ophiodiicola* in wild snake populations. *EcoHealth*, 16, 141–150.
- McNeill, E. P., Thompson, I. D., Wiebe, P. A., Street, G. M., Shuter, J., Rodgers, A. R., & Fryxell, J. M. (2020). Multi-scale foraging decisions made by woodland caribou (*Rangifer tarandus caribou*) in summer. *Canadian Journal of Zoology*, 98, 331–341.
- McNair, J. N. (1982). Optimal giving-up times and the Marginal Value Theorem. *The American Naturalist*, 119, 511–529.

- Michael, D. R., Cunningham, R. B., Macgregor, C., Brown, D., & Lindenmayer, D. B. (2014). The effects of prey, habitat heterogeneity and fire on the spatial ecology of peninsular diamond pythons (*Morelia spilota spilota*). *Austral Ecology*, 39, 181–189.
- Moore, J. A., & Gillingham, J. C. (2006). Spatial ecology and multi-scale habitat selection by a threatened rattlesnake. *Copeia*, 2006, 742–751.
- Nelson, D. L., Kellner, K. F., & Swihart, R. K. (2019). Rodent population density and survival respond to disturbance induced by timber harvest. *Journal of Mammalogy*, 100, 1253–1262.
- Ohio Department of Natural Resources Division of Forestry (ODNRF). (2020). Vinton Furnace State Forest. <<http://forestry.ohiodnr.gov/vintonfurnace>>.
- Pau, G., Fuchs, F., Sklyar, O., Boutros, M., & Huber, W. (2010). EBImage—an R package for image processing with applications to cellular phenotypes. *Bioinformatics*, 26, 979–981.
- Piironen, J., & Vehtari, A. (2017). Comparison of Bayesian predictive methods for model selection. *Statistics and Computing*, 27, 711–735.
- R Core Team. (2020). R: A language and environment for statistical computing. Version 3.6.1. R Foundation for Statistical Computing, Vienna, Austria. <<https://www.R-project.org/>>.
- Rakus, K., Ronsmans, M., & Vanderplasschen, A. (2017). Behavioral fever in ectothermic vertebrates. *Developmental & Comparative Immunology*, 66, 84–91.

- Reinert, H. K., Cundall, D., & Bushar, L. M. (1984). Foraging behavior of the timber rattlesnake, *Crotalus horridus*. *Copeia*, 1984, 976–981.
- Reinert, H. K., MacGregor, G. A., Esch, M., Bushar, L. M., & Zappalorti, R. T. (2011). Foraging ecology of timber rattlesnakes, *Crotalus horridus*. *Copeia*, 2011, 430–442.
- Richards-Zawacki, C. L. (2010). Thermoregulatory behaviour affects prevalence of chytrid fungal infection in a wild population of Panamanian golden frogs. *Proceedings of the Royal Society B: Biological Sciences*, 277, 519–528.
- Scheele, B. C., Guarino, F., Osborne, W., Hunter, D. A., Skerratt, L. F. & Driscoll, D. A. (2014). Decline and re-expansion of an amphibian with high prevalence of chytrid fungus. *Biological Conservation*, 170, 86–91.
- Schooler, S. L., & Zald, H. S. J. (2019). Lidar prediction of small mammal diversity in Wisconsin, USA. *Remote Sensing*, 11(19), 2222.
- Signer, J., Fieberg, J. & Avgar, T. (2019). Animal movement tools (amt): R package for managing tracking data and conducting habitat selection analyses. *Ecology and Evolution*, 9, 880–890.
- Simonson, W. D., Allen, H. D., & Coomes, D. A. (2014). Applications of airborne lidar for the assessment of animal species diversity. *Methods in Ecology and Evolution*, 5, 719–729.
- Skerratt, L. F., Berger, L., Speare, R., Cashins, S., McDonald, K. R., Phillott, A. D., Hines, H. B., & Kenyon, N. (2007). Spread of chytridiomycosis has caused the rapid global decline and extinction of frogs. *EcoHealth*, 4, 125–134.

- Sperry, J. H., and P. J. Weatherhead. (2009). Does prey availability determine seasonal patterns of habitat selection in Texas ratsnakes. *Journal of Herpetology*, 43, 55–64.
- Sutton, W. B., Wang, Y., Schweitzer, C. J., & McClure, C. J. W. (2017). Spatial ecology and multi-scale habitat selection of the Copperhead (*Agkistrodon contortrix*) in a managed forest landscape. *Forest Ecology and Management*, 391, 469–481.
- Tetzlaff, S. J., Carter, E. T., DeGregorio, B. A., Ravesi, M. J., & Kingsbury, B. A. (2017). To forage, mate, or thermoregulate: Influence of resource manipulation on male rattlesnake behavior. *Ecology and Evolution*, 7, 6606–6613.
- Tetzlaff, S. J., Ravesi, M. J., Allender, M. C., Carter, E. T., DeGregorio, B. A., Josimovich, J. M., & Kingsbury, B. A. (2017). Snake fungal disease affects behavior of free-ranging massasauga rattlesnakes (*Sistrurus catenatus*). *Herpetological Conservation and Biology*, 12, 624–634.
- Urban, N. A., & Swihart, R. K. (2011). Small mammal responses to forest management for oak regeneration in southern Indiana. *Forest Ecology and Management*, 261, 353–361.
- Waldron, J. L., Lanham, J. D., & Bennett, S. H. (2006). Using behaviorally-based seasons to investigate canebrake rattlesnake (*Crotalus horridus*) movement patterns and habitat selection. *Herpetologica*, 62, 389–398.
- Whitaker, P. B., & Shine, R. (2003). A radiotelemetric study of movements and shelter-site selection by free-ranging brownsnakes (*Pseudonaja textilis*). *Herpetological Monographs*, 17, 130–144.

- Williams, A. C., Flaherty, S. E., & Flaxman, S. M. (2013). Quantitative tests of multitrophic ideal free distribution theory. *Animal Behaviour*, 86, 577–586.
- Wittenberg, R. D. (2012). Foraging ecology of the timber rattlesnake (*Crotalus horridus*) in a fragmented agricultural landscape. *Herpetological Conservation and Biology*, 7, 449–461.
- Womble, J. N., Sigler, M. F., & Willson, M. F. (2009). Linking seasonal distribution patterns with prey availability in a central-place forager, the Steller sea lion. *Journal of Biogeography*, 36, 439–451.
- Zuur, A. F., Ieno, E. N., Walker, N. J., Saveliev, A. A., & Smith, G. M. (2009). Mixed effects models and extensions in ecology with R. Springer, New York, New York, USA.

## Appendix A. Chapter 1 Supplementary Material

Table A.1. Landcover types present at the study site, their relative coverage on the landscape, and their representation in our game camera trap dataset for small mammals (242 total camera trap sites).

Landcover Class	Landscape Coverage	Camera Coverage
Mature Deciduous	80%	183 (75%)
Burns (& partial harvest with burn)	6%	31 (13%)
Clearcuts	11%	23 (10%)
Pines	3%	5 (2%)
<b>Total Sites</b>		242

Table A.2. Candidate global models describing mice (*Peromyscus* spp.) encounter rates in a mixed-use forest in southeastern Ohio between 2017 and 2018, including variations of zero-inflated (Zi) Poisson and negative binomial models to account for potential temporal variation in small mammal distributions contributing to an excess of zeros. The global set of predictors described forest structure and composition, landscape topography, and year of study (see Table 1.1 for further descriptions of covariates). Median Date refers to the median date of a camera's active interval and was modeled as a quadratic. We considered diagnostic plots, leave-one-out cross validation (LOO), and Watanabe-Akaike information criterion (WAIC) to determine the most parsimonious model. The best-supported global model (in bold type) was a zero-inflated negative binomial model with year of study explaining the excess of zeros.

Distribution	Zi Formula	LOO	WAIC
Poisson	None	-6.3	-6.1
	Median Date + Median Date <sup>2</sup>	-6.5	-6.3
	Median Date + Median Date <sup>2</sup> + Year	-2.4	-2.2
	(Median Date + Median Date <sup>2</sup> ) * Year	-3.2	-3
	Year	-1.5	-1.4
Negative Binomial	None	-2	-2.1
	Median Date + Median Date <sup>2</sup>	-2.2	-2.2
	Median Date + Median Date <sup>2</sup> + Year	-0.8	-0.8
	(Median Date + Median Date <sup>2</sup> ) * Year	-1.3	-1.2
	<b>Year</b>	<b>0</b>	<b>0</b>

Table A.3. Candidate global models describing chipmunk (*Tamias striatus*) encounter rates in a mixed-use forest in southeastern Ohio between 2017 and 2018, including variations of zero-inflated (Zi) Poisson and negative binomial models to account for potential temporal variation in small mammal distributions contributing to an excess of zeros. The global set of predictors described forest structure and composition, landscape topography, and year of study (see Table 1.1 for further descriptions of covariates). Median Date refers to the median date of a camera's active interval and was modeled as a quadratic. We considered diagnostic plots, leave-one-out cross validation (LOO), and Watanabe-Akaike information criterion (WAIC) to determine the most parsimonious model. The best-supported global model (in bold type) was a zero-inflated negative binomial model with year of study explaining the excess of zeros.

Distribution		Zi Formula	LOO	WAIC
Poisson		None	-9.7	-9.3
		Median Date + Median Date <sup>2</sup>	-10.1	-9.7
		Median Date + Median Date <sup>2</sup> + Year	-5.4	-4.8
		(Median Date + Median Date <sup>2</sup> ) * Year	-7.3	-6.9
		Year	-5.3	-4.7
Negative Binomial		None	-3.4	-3.4
		Median Date + Median Date <sup>2</sup>	-3.5	-3.6
		Median Date + Median Date <sup>2</sup> + Year	0	0
		(Median Date + Median Date <sup>2</sup> ) * Year	-0.8	-0.7
		<b>Year</b>	-0.1	-0.2

Table A.4. Candidate global models describing squirrel (*Sciurus* spp.) encounter rates in a mixed-use forest in southeastern Ohio between 2017 and 2018, including variations of zero-inflated (Zi) Poisson and negative binomial models to account for potential temporal variation in small mammal distributions contributing to an excess of zeros. The global set of predictors described forest structure and composition, landscape topography, and year of study (see Table 1.1 for further descriptions of covariates). Median Date refers to the median date of a camera's active interval and was modeled as a quadratic. We considered diagnostic plots, leave-one-out cross validation (LOO), and Watanabe-Akaike information criterion (WAIC) to determine the most parsimonious model. The best-supported global model (in bold type) was a zero-inflated negative binomial model with median date of camera deployment and year of study explaining the excess of zeros.

Distribution	Zi Formula	LOO	WAIC
Poisson	None	-1.6	-1.9
	Median Date + Median Date <sup>2</sup>	-0.3	-0.3
	Median Date + Median Date <sup>2</sup> + Year	0	0
	(Median Date + Median Date <sup>2</sup> ) * Year	-0.2	-0.2
	Year	-2.1	-2.4
Negative Binomial	None	-1.4	-1.4
	Median Date + Median Date <sup>2</sup>	-0.4	-0.2
	<b>Median Date + Median Date<sup>2</sup> + Year</b>	-0.1	0
	(Median Date + Median Date <sup>2</sup> ) * Year	-0.5	-0.5
	Year	-1.5	-1.6

Table A.5. Candidate Bayesian zero-inflated (Zi) negative binomial models for mice, chipmunks, and squirrels describing encounter rates from 242 camera traps in a mixed-use forest in southeastern Ohio. The number of camera days with a species' detection (Counts) is offset by the total number of active camera days (Days). Models were reduced from the global (G) set of covariates characterizing forest structure and composition ( $k = 13$ ), landscape topography ( $k = 3$ ), and year of study (2017–2018). Refer to Table 1.1 for descriptions of each covariate. The zero-inflated process was modeled with year and/or median camera deployment date. The most parsimonious model (in bold type) for each species was determined using diagnostic plots, leave-one-out cross validation (LOO), and Watanabe-Akaike information criterion (WAIC).

<b>Species &amp; Candidate Models</b>	<b>LOO</b>	<b>WAIC</b>
<b>Mice (<i>Peromyscus</i> spp.)</b>		
[G] Counts ~ Year + Burn + Age + Beers + DEM + Slope + Stream + NMDS1 + NMDS2 + CHM + FHD + EVI + PSR + OVE + UND + TDE + SKE + offset(log(Days)), Zi ~ Year	-9.6	-8.8
[M1] Counts ~ Year + Burn + CHM + OVE + Age + offset(log(Days)), Zi ~ Year	-0.9	-1
[M2] Counts ~ Year + Burn + CHM + Age + offset(log(Days)), Zi ~ Year	-0.1	0
<b>[M3] Counts ~ Year + Burn + Age + offset(log(Days)), Zi ~ Year</b>	0	-0.1
<b>Chipmunks (<i>Tamias striatus</i>)</b>		
[G] Counts ~ Year + Burn + Age + Beers + DEM + Slope + Stream + NMDS1 + NMDS2 + CHM + FHD + EVI + PSR + OVE + UND + TDE + SKE + offset(log(Days)), Zi ~ Year	-13.6	-12.9
[C1] Counts ~ Slope + NMDS2 + PSR + OVE + UND + offset(log(Days)), Zi ~ Year	-1.9	-1.8
<b>[C2] Counts ~ Slope + NMDS2 + PSR + offset(log(Days)), Zi ~ Year</b>	0	0
<b>Squirrels (<i>Sciurus</i> spp.)</b>		
[G] Counts ~ Year + Burn + Age + Beers + DEM + Slope + Stream + NMDS1 + NMDS2 + CHM + FHD + EVI + PSR + OVE + UND + TDE + SKE + offset(log(Days)), Zi ~ Median Date + Median Date <sup>2</sup> + Year	-8.2	-7.5
[S1] Counts ~ Year + Burn + Beers + NMDS1 + NMDS2 + FHD + PSR + OVE + UND + offset(log(Days)), Zi ~ Median Date + Median Date <sup>2</sup> + Year	-0.8	-0.7

Continued

Table A.5 Continued

<b>Species &amp; Candidate Models</b>	<b>LOO</b>	<b>WAIC</b>
[S2] Counts ~ Year + Burn + NMDS1 + NMDS2 + FHD + PSR + OVE + UND + offset(log(Days)), Zi ~ Median Date + Median Date <sup>2</sup> + Year	-0.5	-0.5
[S3] Counts ~ Year + NMDS1 + NMDS2 + FHD + OVE + UND + offset(log(Days)), Zi ~ Median Date + Median Date <sup>2</sup> + Year	0	0

Table A.6. Candidate Bayesian mixed-effects Bernoulli models describing timber rattlesnake (*Crotalus horridus*) foraging as a function of predicted prey encounter rates from a landscape-scale small mammal encounter surface (2017–2018) for a mixed-use forest in southeastern Ohio. Species-level models include predicted daily encounter rates for mice (*Peromyscus* spp.), chipmunks (*Tamias striatus*), and squirrels (*Sciurus* spp.). Cumulative models include the additive daily encounter rate predictions for mice and chipmunks specifically (Cumulative MC) or the contribution of all species (Cumulative Prey). Variation in prey encounter rates and snake identity (Snake), modeled as a random effect, described TRS foraging status (Forage) between 2016–2019. In 2016 and 2019, prey encounter values for each snake location represented the average predicted rate (prey species or species grouping) between 2017 and 2018. We used diagnostic plots and leave-one-out cross validation (LOO) to determine the most parsimonious models, identified as the smallest selection criterion value (in bold type), for combined adult TRS, non-gravid female, and male foraging probabilities among species-level and cumulative models for 2017–2018 and 2016–2019.

<b>Candidate Models</b>	<b>2017–2018</b>	<b>2016–2019</b>
<b>Non-Gravid Females</b>	n = 16	n = 16
<i>Species-level</i>		
[1a] Forage ~ Mice + Chipmunks + Squirrels + (1  Snake)	-1.9	-0.8
[1b] Forage ~ Mice + Squirrels + (1  Snake)	-1.5	-0.2
<i>Cumulative</i>		
[2] Forage ~ Cumulative MC + (1  Snake)	-1.6	-1.1
<b>[3a] Forage ~ Cumulative Prey + (1  Snake)</b>	<b>0</b>	<b>0</b>
<b>Males</b>	n = 15	n = 21
<i>Species-level</i>		
<b>[1a] Forage ~ Mice + Chipmunks + Squirrels + (1  Snake)</b>	-0.5	0
<i>Cumulative</i>		
[2] Forage ~ Cumulative MC + (1  Snake)	-4.0	-6.7
<b>[3a] Forage ~ Cumulative Prey + (1  Snake)</b>	<b>0</b>	-1.3
<b>Adults</b>	n = 31	n = 37
<i>Cumulative</i>		
[2] Forage ~ Cumulative MC + (1  Snake)	-8	-6.6
<b>[3a] Forage ~ Cumulative Prey + (1  Snake)</b>	<b>-2.3</b>	<b>0</b>
<b>[3b] Forage ~ Cumulative Prey * Sex + (1 Snake)</b>	<b>0</b>	-0.4

Table A.7. Bayesian mixed-effects Bernoulli models of adult timber rattlesnake (*Crotalus horridus*) foraging from 2016–2019, explained by species-level daily rodent encounter rates from landscape-scale prey encounter surfaces of mice (*Peromyscus* spp.), chipmunks (*Tamias striatus*), and squirrels (*Sciurus* spp.) or cumulative prey encounter rates encompassing all prey species. We tested species-level and Cumulative Prey models for non-gravid females (n = 16) and males (n = 21) separately, and Cumulative Prey models for adults collectively. Mean coefficient estimates, standard errors (S.E.), 95% lower (LCI) and upper (UCI) credible intervals, and percentage of the posterior distributions overlapping zero are provided. Refer to Table A.6 for further descriptions of candidate models.

	Covariate	Estimate	S.E.	95% LCI	95% UCI	Overlap Zero (%)
<b>Females</b>	Mice	1.39	0.22	0.94	1.83	0
	Squirrels	1.73	0.72	0.34	3.12	0.75
	Cumulative Prey	1.05	0.15	0.76	1.34	0
<b>Males</b>	Mice	0.75	0.20	0.38	1.15	0.03
	Chipmunks	1.09	0.35	0.4	1.78	0.13
	Squirrels	2.9	0.77	1.41	4.42	0.03
	Cumulative Prey	1.14	0.11	0.92	1.37	0
<b>All Adults</b>	Cumulative Prey	1.09	0.09	0.91	1.27	0

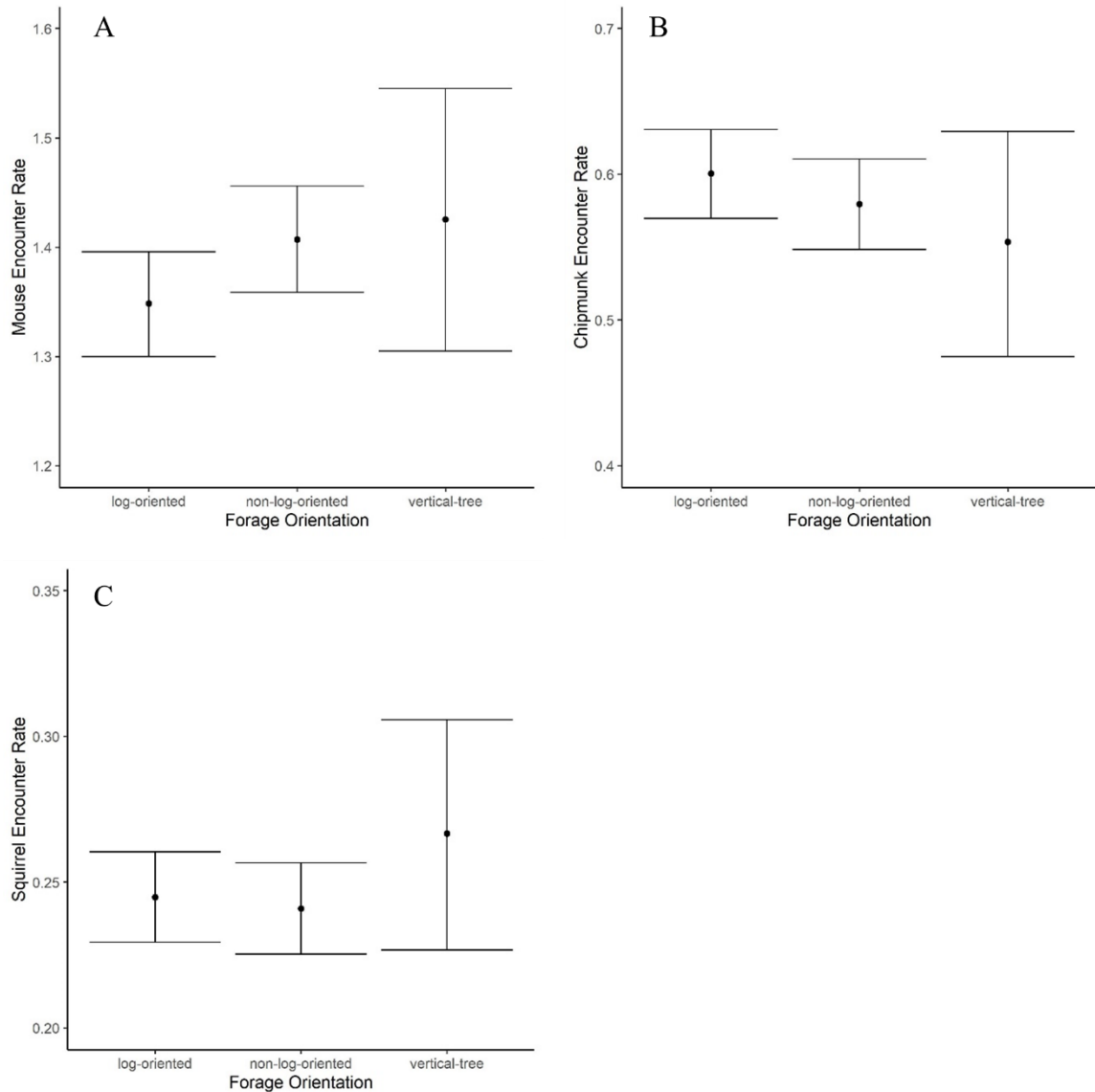


Figure A.1. Predicted small mammal prey availability by timber rattlesnake (*Crotalus horridus*) foraging posture orientation. We used a Bayesian multivariate analysis of variance (MANOVA) to examine small mammal prey availability among different foraging orientation types (log-oriented, non-log-oriented, and vertical-tree-oriented) by timber rattlesnakes. We modeled site-specific daily encounter rates of mice (*Peromyscus* spp.), chipmunks (*Tamias striatus*), and squirrels (*Sciurus* spp.) as a function of foraging orientation with the ‘brms’ package in R (Bürkner, 2017; R Core Team 2020). Log-oriented and non-log oriented were the most commonly observed foraging orientations in our population (n = 244 and 239, respectively) and these foraging orientations exhibited the most similar small mammal associations. There was greater uncertainty around the species-level prey availability of vertical-tree foraging sites due to low observations (n = 39) of this ambush posture in our population. A) Mice encounters were marginally greater (mean: 1.43 mice/day; 95% CI: 1.31–1.55 mice/day) at sites associated with a

vertical-tree foraging orientation than non-log-oriented foraging (mean: 1.41 mice/day; 95% CI: 1.36–1.46 mice/day) or log-oriented foraging (mean: 1.35 mice/day; 95% CI: 1.30–1.40 mice/day), but with overlapping credible intervals among all groups. B) Chipmunk (CM) encounters varied little by foraging orientation type. Log-oriented foraging sites yielded the greatest mean chipmunk encounters (0.60 CM/day; 95% CI: 0.57–0.63 CM/day), followed by non-log-oriented (mean: 0.58 CM/day; 95% CI: 0.55–0.61 CM/day) and vertical-tree-oriented foraging (mean: 0.55 CM/day; 95% CI: 0.48–0.63), but with overlapping credible intervals among all groups. C) Predicted squirrel (SQ) encounters were marginally greater (mean = 0.27 SQ/day; 95% CI: 0.23–0.31 SQ/day) at vertical-tree foraging sites, followed by equal encounters at log-oriented (mean: 0.24 SQ/day; 95% CI: 0.23–0.26) and non-log-oriented (mean = 0.24 SQ/day; 95% CI: 0.22–0.26) and overlapping credible intervals among all groups.

## Appendix B. Chapter 2 Supplementary Material

Table B.1. Candidate Bayesian mixed effect models describing home range area across 50%, 95%, and 100% minimum convex polygons (MCP) for 15 (n = 9 males and 6 non-gravid females) timber rattlesnakes (*Crotalus horridus*), during years when considered asymptomatic or symptomatic of snake fungal disease (SFD). We monitored each snake for at least one year in which they were asymptomatic of SFD (SFD = 0) and at least one year in which they exhibited clinical symptoms (SFD = 1). We used additive or interactive combinations of SFD status and sex to predict log-transformed home range area (Area), with individual snakes modeled as random effects. The most parsimonious model (in bold type) for each home range scale was determined using diagnostic plots and leave-one-out cross validation (LOO).

<b>MCP-scale &amp; Candidate Models</b>	<b>LOO</b>
<hr/> MCP–50%	
[G] Log (Area) ~ SFD * Sex + (1 Snake)	-1.2
<b>[1] Log (Area) ~ SFD + Sex + (1 Snake)</b>	0
[2] Log (Area) ~ SFD + (1 Snake)	-0.8
[3] Log (Area) ~ Sex + (1 Snake)	-1.6
<hr/> MCP–95%	
<b>[G] Log (Area) ~ SFD * Sex + (1 Snake)</b>	0
[1] Log (Area) ~ SFD + Sex + (1 Snake)	-0.8
[2] Log (Area) ~ SFD + (1 Snake)	-1.0
[3] Log (Area) ~ Sex + (1 Snake)	-0.5
<hr/> MCP–100%	
[G] Log (Area) ~ SFD * Sex + (1 Snake)	0
<b>[1] Log (Area) ~ SFD + Sex + (1 Snake)</b>	-0.7
[2] Log (Area) ~ SFD + (1 Snake)	-1.3
[3] Log (Area) ~ Sex + (1 Snake)	-1.5

Table B.2. Principal component analysis (PCA) of eight movement metrics from 15 timber rattlesnakes (*Crotalus horridus*) in southeast Ohio during years when asymptomatic or symptomatic of snake fungal disease. We considered annual summaries of mean and median movement rates, cumulative step lengths, mean and max net squared displacement, and 50%, 95%, and 100% minimum convex polygon (MCP) home range areas. We considered the most informative principal components as those with the greatest eigenvalues and greatest percentage of variability explained within the data. Cumulative variance represents the amount of variance explained by consecutive principal component dimensions.

<b>Components</b>	<b>Eigenvalue</b>	<b>Variance (%)</b>	<b>Cumulative Variance (%)</b>
Dimension 1	6.49	81.08	81.08
Dimension 2	0.70	8.71	89.79
Dimension 3	0.37	4.61	94.40
Dimension 4	0.16	2.00	96.40
Dimension 5	0.15	1.84	98.24
Dimension 6	0.07	0.85	99.10
Dimension 7	0.04	0.53	99.62
Dimension 8	0.03	0.38	100.00

Table B.3. Loadings of eight movement metrics from a principal component analysis (PCA) for 15 timber rattlesnakes (*Crotalus horridus*) in southeast Ohio during years when asymptomatic or symptomatic of snake fungal disease. We considered annual summaries of mean and median movement rates (MR), mean and max net squared displacement (NSD), cumulative step lengths (SL) and 50%, 95%, and 100% minimum convex polygon (MCP) home range areas. The first three principal components (PC) explained 94.4% of the variance. We considered variables with loadings close to -1 or 1 to be the most influential variables on a component.

<b>Metrics</b>	<b>PC1</b>	<b>PC2</b>	<b>PC3</b>
Mean MR	0.35	0.33	0.40
Median MR	0.29	0.77	
Max NSD	0.36	-0.30	0.40
Mean NSD	0.36	-0.41	0.27
Cumulative SL	0.37		
50% MCP	0.34		-0.73
95% MCP	0.38	-0.12	-0.23
100 % MCP	0.38	-0.13	

Table B.4. Coordinates of eight movement metrics from a principal component analysis (PCA) for 15 timber rattlesnakes (*Crotalus horridus*) in southeast Ohio during years when asymptomatic or symptomatic of snake fungal disease. We considered annual summaries of mean and median movement rates (MR), mean and max net squared displacement (NSD), cumulative step lengths (SL) and 50%, 95%, and 100% minimum convex polygon (MCP) home range areas. The first three principal components (PC) explained 94.4% of the variance.

<b>Metrics</b>	<b>PC1</b>	<b>PC2</b>	<b>PC3</b>
Mean MR	0.75	0.56	0.04
Median MR	0.52	0.76	-0.27
Max NSD	0.89	0.18	0.38
Mean NSD	0.93	-0.03	0.33
Cumulative SL	0.84	-0.07	-0.27
50% MCP	0.88	-0.37	-0.05
95% MCP	0.91	-0.31	-0.12
100 % MCP	0.92	-0.30	-0.16

Table B.5. Candidate Bayesian mixed effect Bernoulli models of site use by timber rattlesnakes (*Crotalus horridus*) during years unaffected or affected by snake fungal disease (SFD). Probability of site use by a snake infected with SFD was modeled as a function of thirteen geospatial landscape and forest structural variables (5-m resolution), with individual snakes as random effects. Each snake (n = 15) was considered asymptomatic or symptomatic of SFD infection for at least one year each. The most parsimonious model (in bold type) for each sex was determined using diagnostic plots and leave-one-out cross validation (LOO).

Candidate Models	LOO
<b>Non-Gravid Females</b>	n = 6
[G] Site Use ~ Beers + CHM + mTemp + Mid + NMDS1 + NMDS2 + NDMS3 + OVE + TDE + Slope + Age + Stream + UND + (1 Snake)	-4.1
[1] Site Use ~ CHM + mTemp + NMDS1 + NDMS3 + OVE + TDE + Slope + Age + Stream + UND + (1 Snake)	-0.5
<b>[2] Site Use ~ CHM + mTemp + NMDS1 + NDMS3 + Slope + Age + Stream + UND + (1 Snake)</b>	0
[3] Site Use ~ NMDS1 + NDMS3 + Age + Stream + (1 Snake)	-1.2
<b>Males</b>	n = 9
[G] Site Use ~ Beers + CHM + mTemp + Mid + NMDS1 + NMDS2 + NDMS3 + OVE + TDE + Slope + Age + Stream + UND + (1 Snake)	-6.8
[1] Site Use ~ Beers + Age + Stream + (1 Snake)	0
<b>[2] Site Use ~ Beers + Stream + (1 Snake)</b>	-0.1

Table B.6. Candidate Bayesian mixed effect models of external snake body temperatures taken with a digital infrared thermometer at sites (n = 870) used by timber rattlesnakes (*Crotalus horridus*) during years unaffected or affected by snake fungal disease (SFD). Each snake (n = 15) was considered asymptomatic or symptomatic of SFD infection for at least one year each. We modeled snake body temperature as a function of additive or interactive combinations of SFD status and season of observation. We defined spring as April–June, summer as July–August, and fall as September–October. We included random effects of individual snakes and month of observation. The most parsimonious model (in bold type) was determined using diagnostic plots and leave-one-out cross validation (LOO).

<b>Candidate Models</b>	<b>LOO</b>
<b>[1] Temp ~ SFD *Season + (1 Snake) + (1 Month)</b>	0
[2] Temp ~ SFD + Season + (1 Snake) + (1 Month)	-5.2

Table B.7. Candidate Bayesian mixed effect models of solar insolation at sites ( $n = 730$ ) used by timber rattlesnakes (*Crotalus horridus*) during years unaffected or affected by snake fungal disease (SFD). Each snake ( $n = 15$ ) was considered asymptomatic or symptomatic of SFD infection for at least one year each. We modeled solar insolation ( $\text{kWH/m}^2$ ), corrected by proportion canopy cover (CSI), as a function of additive or interactive combinations of SFD status and season of observation. We defined spring as April–June, summer as July–August, and fall as September–October. We included random effects of individual snakes and month of observation. The most parsimonious model (in bold type) was determined using diagnostic plots and leave-one-out cross validation (LOO).

<b>Candidate Models</b>	<b>LOO</b>
[1] $\sqrt{\text{CSI}} \sim \text{SFD} * \text{Season} + (1 \text{Snake}) + (1 \text{Month})$	-1.7
<b>[2] <math>\sqrt{\text{CSI}} \sim \text{SFD} + \text{Season} + (1 \text{Snake}) + (1 \text{Month})</math></b>	0
[3] $\sqrt{\text{CSI}} \sim \text{SFD} + (1 \text{Snake}) + (1 \text{Month})$	0

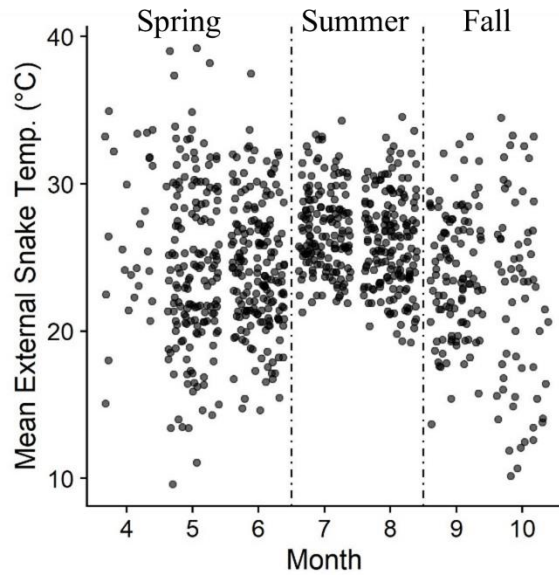


Figure B.1. External body temperatures ( $n = 870$ ) of 15 timber rattlesnakes (*Crotalus horridus*) in southeastern Ohio. We measured body temperature with a digital infrared thermometer. We classified seasons for temperature and solar radiation models based on the partitioning of snake body temperatures between April–June, July–August, and September–October.

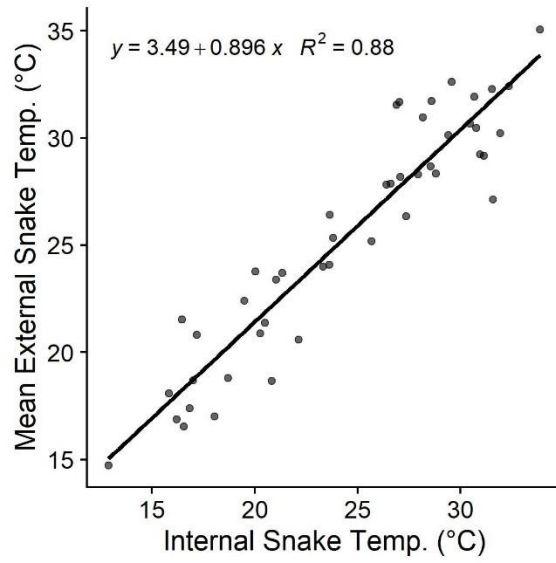


Figure B.2. Linear relationship between external snake body temperatures (n = 9 snakes; 46 observations) taken with a digital infrared thermometer and the matching internal snake body temperature recorded hourly with an implanted RFID tag.